Analysis of Photocatalysis for Precursor Removal and Formation Inhibition of Disinfection Byproducts

by

Erin Daugherty

A Thesis Presented in Partial Fulfillment
of the Requirements for the Degree
Master of Science

Approved July 2011 by the
Graduate Supervisory Committee:

Morteza Abbaszadegan, Chair
Brooke Mayer
Peter Fox

ARIZONA STATE UNIVERSITY

August 2011

ABSTRACT

Disinfection byproducts are the result of reactions between natural organic matter (NOM) and a disinfectant. The formation and speciation of DBP formation is largely dependent on the disinfectant used and the natural organic matter (NOM) concentration and composition. This study examined the use of photocatalysis with titanium dioxide for the oxidation and removal of DBP precursors (NOM) and the inhibition of DBP formation. Water sources were collected from various points in the treatment process, treated with photocatalysis, and chlorinated to analyze the implications on total trihalomethane (TTHM) and the five haloacetic acids (HAA5) formations. The three sub-objectives for this study included: the comparison of enhanced and standard coagulation to photocatalysis for the removal of DBP precursors; the analysis of photocatalysis and characterization of organic matter using size exclusion chromatography and fluorescence spectroscopy and excitation-emission matrices; and the analysis of photocatalysis before GAC filtration.

There were consistencies in the trends for each objective including reduced DBP precursors, measured as dissolved organic carbon DOC concentration and UV absorbance at 254 nm. Both of these parameters decreased with increased photocatalytic treatment and could be due in part to the adsorption to as well as the oxidation of NOM on the TiO_2 surface. This resulted in lower THM and HAA concentrations at Medium and High photocatalytic treatment levels.

However, at No UV exposure and Low photocatalytic treatment levels where oxidation reactions were inherently incomplete, there was an increase in THM and HAA formation potential, in most cases being significantly greater than those found in the raw water or Control samples.

The size exclusion chromatography (SEC) results suggest that photocatalysis preferentially degrades the higher molecular mass fraction of NOM releasing lower molecular mass (LMM) compounds that have not been completely oxidized. The molecular weight distributions could explain the THM and HAA formation potentials that decreased at the No UV exposure samples but increased at Low photocatalytic treatment levels. The use of photocatalysis before GAC adsorption appears to increase bed life of the contactors; however, higher photocatalytic treatment levels have been shown to completely mineralize NOM and would therefore not require additional GAC adsorption after photocatalysis.

DEDICATION

This thesis is dedicated to everyone who has helped me along the way including my wonderful fellow graduate students, friends, and family as well as the faculty, staff, and committee members. If it was not for their guidance and support I would have never made it. Thank you!

ACKNOWLEDGMENTS

This thesis would not have been possible without the help and involvement of many people. First and foremost I would like to acknowledge my committee members for all their help and guidance. I would also like to acknowledge Kiril Hristovski for his valuable feedback and support; Dr. Paul Westerhoff and his students for sharing their laboratory and knowledge; the amazing people over at the Scottsdale Water Campus including Susan Butler, Laura McCasland, Kathy Gettens, and Binga Talabi; Don Henderson and the guys at the Chaparral Water Treatment Plant; Aaron Dotson and David Ladner for their help with the spectra fluorescence analysis and graphing EEMs; Chao-An Chiu for his incredible help with GAC RSSCTs and DOC and SEC analysis; and Peter Goguen for his help with almost everything

TABLE OF CONTENTS

Page

Page

LIST OF TABLES

LIST OF FIGURES

Page

Page

Chapter 1

INTRODUCTION

MOTIVATION FOR STUDY

Disinfection is a vital part of the drinking water treatment process and has been practiced for centuries to protect human health and reduce the risk of water borne illness and disease. The most common disinfectant in use in the United States today is chorine due to its highly oxidizing nature and economic appeal (*1*).

The City of Phoenix, AZ currently uses chlorine for disinfection and targets a 1 to 2 mg/L residual for drinking water leaving the treatment plant. However, this concentration can be significantly reduced during transport within the distribution system due to organic matter and biofilms that can be present in the existing infrastructure and react readily with chlorine. In such cases, higher chlorine concentrations are added to avoid the depletion of the disinfectant residual. However, the complex reaction between an oxidizing chemical such as chlorine and existing natural organic matter (NOM) leads to the formation of disinfection byproducts (DBPs). Since the 1970's when the chloroform was first discovered in chlorinated waters, there has been much debate over the potential health impacts of disinfection by products (*2, 3,4,5*). Numerous studies have shown conflicting results, some of which claim that DBPs are carcinogenic while others claim that there is no evidence to support a direct and

concrete link between chlorinated waters and cancer, especially in the small doses found in drinking water (*6*).

Despite the dispute, the United States Environmental Protection Agency (USEPA) began regulating certain DBPs known as the trihalomethanes in 1979 with the Total Trihalomethane (TTHM) Rule that regulated TTHM concentrations in finished drinking water with a maximum contaminant level (MCL) of 100 µg/L (*7*). Later regulations such as the Stage 1 Disinfectant/Disinfection Byproducts (D/DBP) Rule which will be discussed in later sections also included the regulation and MCLs of the haloacetic acids (HAA), bromate, and chlorite. The recently promulgated Stage 2 Disinfectant/Disinfection Byproducts (D/DBP) Rule requires water treatment facilities to implement monitoring for THMs and HAAs and begin formulating a plan to meet new compliance methods and standards.

As a result, water treatment plants (WTPs) are investigating new process and updating their facilities to meet the new USEPA regulations. The Stage 1 D/DBP Rule listed one of the best available technologies for organic matter or DBP precursor removal as granular activated carbon (GAC) with an empty bed contact time of 10 min. Other documented treatment processes that have been utilized for DBP precursor removal and control of DBP formation have been enhanced coagulation or softening, membrane filtration, and advanced oxidation processes.

This study focused on the use of an advanced oxidation technology to oxidize organic matter to reduce DBP formation. Photocatalysis has

long been used for disinfection and treatment of wastewater and its oxidizing capabilities in drinking water treatment. This study examines the use of photocatalysis with titanium dioxide for the oxidation of DBP procures and the inhibition of DBP formation.

STUDY OBJECTIVES

The main objective of this study is to examine the use of photocatalysis for the inhibition of DBP formation through the oxidation and removal of DBP precursors also known as natural organic matter (NOM).

Water samples were taken from the following sources:

1. The Salt River (Phoenix, AZ)
2. After sedimentation (settled water) at the Scottsdale Water Campus (Scottsdale, AZ)
3. Before granular activated carbon (GAC) filtration at the Chaparral WTP (Scottsdale, AZ)
4. After granular activated carbon (GAC) filtration at the Chaparral WTP (Scottsdale, AZ)
5. At a distribution hot spot with high THM concentrations (Scottsdale, AZ)

The overall objective was to analyze the use of photocatalysis on all water sources for the removal and oxidation of DBP precursors and to

limit the formation of THM and HAA DBPs. The sub-objectives covered by each chapter in this report are as follows:

1. The Comparison of Coagulation and Photocatalysis for Disinfection Byproduct Precursor Removal
2. Photocatalysis and the Characterization of Organic Matter
3. Analysis of Photocatalysis Before GAC Adsorption

The first sub-objective was performed using the Salt River water, the second sub-objective was performed using the settled water, post-GAC filtration water, and the distribution hot spot water, and the third objective was performed using the pre-GAC filtration water. All five water sources have various NOM concentrations and compositions that will affect the formation of DBPs. In each objective the primary results will examine precursor removal and THM or HAA formation. The following section will describe the general methods, procedures, and instruments used in all experiments. Individual analysis methods and procedures will be addressed in the corresponding chapters under the Materials and Methods sections.

Chapter 2

LITERATURE REVIEW

Drinking water treatment is an ever-evolving process that is driven by regulatory organizations as well as public perception. The primary goal of water treatment is to protect consumer or public health by removing toxic chemicals, microbial pathogens, and aesthetic contaminants that impact color, odor, and taste of finished water. The application of an oxidizing chemical for disinfection can achieve one or more of these goals through the inactivation of microbial pathogens and the oxidation of organic material. Disinfection in the United States is most commonly achieved through chlorination at one or more points in the treatment process. Alternative disinfectants and oxidants can be used alone or with chlorine depending on the individual treatment facility, water quality parameters, and treatment goals.

In the 1970's chloroform was detected in chlorinated waters and so began the battle against disinfection byproducts (DBPs) – a fight that has been the subject of much controversy and dispute in the water treatment community. In addition, the issue of DBPs created a difficult tradeoff between microbial pathogen inactivation and the formation of potentially carcinogenic DBPs. In his essay entitled "Disinfection Byproducts – A View From North America," Richard J Karlin, Deputy Executive Director of the American Water Works Association (AWWA) Research Foundation in 1999, expressed his opinion that the American public had forgotten why

disinfection was necessary in the first place – to prevent the spread of potentially fatal waterborne diseases (*6*). Karlin is not alone in his thinking and there are others who question the proposed harmful effects of DBPs. The published literature regarding research on the issue is filled with conflicting results and loose correlations (*6*). Regardless of individual opinion, DBPs pose enough of a concern that they have been regulated by the USEPA since 1979.

RELEVANT REGULATIONS

Under the Safe Drinking Water Act of 1974, the USEPA was authorized to determine and establish safe drinking water regulations including the enforcement of regulatory standards, required monitoring, application of specific treatment processes, and the submittal of reports regarding compliances of required regulations by treatment facilities (*2*).

The Total Trihalomethane Rule. After the discovery of chloroform in chlorinated waters, the USEPA responded quickly, instituting the Total Trihalomethane (TTHM) Rule in 1979 (*3,7*). Under this rule the USEPA set an interim maximum contaminant level (MCL) of 100 µg/L for the sum of the four trihalomethanes including chloroform ($CHCl_3$), bromodichloromethane ($CHBrCl_2$), dibromochloromethane ($CHBr_2Cl$), and bromoform ($CHBr_3$). Compliance was based on running annual average concentrations of quarterly averages of all samples taken at various locations in the distribution system. This rule applied to any community

water system that served at least 10,000 people and added a disinfectant at any point within the treatment process (*8, 9*).

In 1983, the USEPA promulgated regulations stating the best, generally available treatment technologies for DBP control including the use of chloramines and chlorine dioxide as alternative disinfectants. Also listed were methods for THM precursor reduction including improving clarification, eliminating prechlorination, and using powder activated carbon (PAC) (*3*).

EPA Stage 1 Disinfectants and Disinfection Byproducts (D/DBP) Rule. Implemented in 1996, the Stage 1 D/DBP Rule modified the original TTHM Rule of 1979 by lowering the MCL for TTHMs and adding MCLs for the sum of the five haloacetic acids (HAA5), bromate, and chlorite, as summarized in Table 1 below (*7*).

Table 1

Stage 1 D/DBP Rule MCLs

Name	Chemical Formula	MCLG (mg/L)1	MCL (mg/L)1
TTHMs		-	0.08
Trichloromethane	$CHCl_3$	-	
Bromodichloromethane	$CHBrCl_2$	0	
Dibromochloromethane	$CHBr_2Cl$	0.06	
Bromoform	$CHBr_3$	0	
HAA5		-	0.06
Monochlororacetic Acid	$CH_2ClCOOH$	-	
Monobromoacetic Acid	$CH_2BrCOOH$	-	
Dichloroacetic Acid	$CHCl_2COOH$	0	
Dibromoacetic Acid	$CHBr_2COOH$	-	
Trichloroacetic Acid	CCl_3COOH	0.3	
Bromate	BrO_3-	0	0.01
Chlorite	ClO_2-	0.8	1

The rule also established maximum residual disinfectant level goals (MRDLGs) and maximum residual disinfectant levels (MRDLs) for chlorine, chloramines, and chlorine dioxide, as shown in Table 2 below (7).

Table 2

Stage 1D/DBP Rule Maximum Disinfectant Residual Levels

Disinfectant	MRDLGs (mg/L)	MRDLGs (mg/L)
chlorine	4	4
chloramines	4	4
chlorine dioxide	0.8	0.8

The rule applied to all community water systems including transient and non-transient non-community systems and those serving less than 10,000 people (*7*). Compliance was based on running annual averages (RAA) from all samples taken from all locations within the distribution system. Furthermore, the Stage 1 D/DBP Rule established the best available technologies for controlling residual levels of disinfectants and DBPs. For disinfectants the primary method of control was to manage treatment processes to reduce the disinfectant demand and reduce disinfectant dosages by controlling the disinfection process. For DBP control the best available technologies were enhanced coagulation or softening and/or GAC filtration with an empty bed contact time (EBCT) of 10 minutes and reactivation at least every 6 months (*7*). The required percentage removal of TOC as designated by the EPA is listed in Table 3 (*7*).

Table 3

Stage 1 D/DBP Rule Required Percent TOC Removal by Enhanced Coagulation and Softening

Source Water TOC (mg/L)	Source Water Alkalinity (mg/L as $CaCO_3$)		
	0 - 60	60 - 120	> 120
2.0 - 4.0	35	25	15
4.0 - 8.0	45	35	25
> 8.0	50	40	30

The Information Collection Rule. The Information Collection Rule (ICR) of 1998 was implemented by the USEPA and required data collection and monitoring of microbial pathogens, fecal contamination indicators, disinfectant dose, and disinfection byproducts such as THMs and HAAs (*7*). The rule applied to large public water systems serving over 100,000 people using surface water or water under the direct influence of surface water for 18 months (*10*). The primary goal of the effort was to assess potential health risks and public health decisions, and influence future regulations. The results from the ICR showed that while treatment systems may be in full compliance with DBP regulations, there were a large number of locations throughout the distribution system that had DBP concentrations that exceeded the MCLs (*8*). The issue was in the

averaging of distribution system samples and the variation of concentrations during certain times of the year, which led to the modification of the Stage 1 D/DBP Rule and establishment of the Stage 2 D/DBP Rule.

EPA Stage 2 Disinfectants and Disinfection Byproducts (D/DBP) Rule. The Stage 2 D/DBP Rule of 2006 does not change any of the MCLs set forth in the Stage 1 D/DBP Rule, however, due to the realization that the RAA was producing potentially misleading results and that compliance was being achieved despite the exceedingly high DBP concentrations at certain points within the distribution system, the compliance standards were modified (*11*). Instead of compliance being based on the RAA, it would now be based on locational running annual averages (LRAA) of sample locations within the distribution system. These new sampling locations were to represent areas that were either known or anticipated to have higher levels of DBP concentrations. In addition, treatment facilities were required to continuously monitor for DBP formation and develop strategies for control with the deadline for compliance being the beginning in April of 2012 for large treatment facilities and October of 2013 for the smaller treatment facilities (*11*).

DISINFECTANTS

As previously discussed, disinfection byproducts are the result of a disinfectant or oxidizing agent reacting with naturally occurring organic matter (NOM). The formation and speciation of DBPs is dependent on a

number of factors including the dose and type of oxidant or disinfectant used. Traditionally, some water treatment facilities practiced prechlorination at the beginning of their treatment train; however, after the realization that this practice was actually producing a significantly higher amount of DBPs, most treatment facilities either stopped prechlorination or moved the chlorine addition point further down the treatment train after sedimentation. This option, however, could not be applied to those treatment facilities that needed preoxidation as a means of iron, manganese, and taste and odor control. In these cases where preoxidation is required, alternative oxidants or disinfectants can be used. The following is a discussion of the more common alternative disinfectants in use today.

Chloramines. Chloramines are formed through the addition of ammonia to chlorinated waters. Hypochlorous acid and ammonia can react to form monochloramine, dichloramine, and trichloramine also known as nitrogen trichloramine. The sum of the three chloramine species' concentrations is commonly expressed as combined chlorine and is different than free chlorine, which is the total chlorine minus the combined chlorine *(1)*. The pH, temperature, and ratio of chlorine to ammonia will determine the relative amounts of the chloramines species formed and in turn the formation of DBPs.

Chloramines are weaker than free chlorine and as such they require a longer contact time for disinfection but they tend to last longer, which

makes them a good choice for secondary disinfection and large distribution systems in which a disinfectant residual is required *(1)*. There is a concern over the nitrification of ammonia which depletes the chloramine residual under higher temperatures and results in a low chlorine:ammonia ratio. Increasing the chlorine:ammonia ratio can help control ammonia nitrification (*3*).

Chlorine Dioxide. Chlorine dioxide is a stronger disinfectant than chlorine, making it better at inactivating viruses and bacteria over a broad pH range (*3*). At room temperature, chlorine dioxide is similar to chlorine in that it is a greenish-yellow gas but is unstable at high concentration and must be generated on-site by reacting sodium chlorite with chlorine or hypochlorous acid. However, the sodium chlorite must be completely converted to chlorine dioxide to avoid the presence of chlorite in the resulting product (*1*). Once formed, chlorine dioxide is stable and soluble in water, and is used to control taste and odor compounds as well as iron and manganese. The compound also provides a longer lasting residual and is a good candidate for preoxidation or secondary disinfection. Under the presence of higher pH values and elevated temperatures, however, it can dissociate into chlorite and chlorate. Reaction with ozone also produces chlorate. Chlorine dioxide dosages are typically less than chlorine dosages but the higher costs still limit their use to smaller treatment facilities *(1)*.

Ozone. Similar to chlorine dioxide, ozone gas must be generated on-site due to its instability; however, it is very reactive making it stronger than chlorine and able to inactivate *Giardia* and *Cryptosporidium* more efficiently (*3*). On the other hand its high reactivity with common drinking water constituents causes “auto-decomposition” in which ozone is initially decomposed by the hydroxide ion and causes a series of chain reactions to further decompose ozone and produce the hydroxyl radical (*1*). The hydroxyl radical is one of the strongest chemical oxidants and can react very rapidly with a plethora of inorganic and organic compounds. Due to its highly reactive nature, ozone does not produce a long lasting residual but does make an excellent candidate for preoxidation and primary disinfection.

Upon reaction, ozone partially oxidizes natural organic material (NOM) to lower molecular weight compounds including aldehydes and organic acids (*3*). In brominated waters, ozone can react with bromide to produce hypobromous acid, further reacting with the NOM to create brominated DBPs and biologically degradable organic compounds that could increase assimilable organic carbon (AOC), thereby fostering bacterial growth in distribution systems.

Ultraviolet Radiation. Ultraviolet (UV) radiation has long been used for its biocidal effects since it was discovered that microbial decay was associated with sunlight (*1*). Disinfection with UV has been used in wastewater and drinking water treatment facilities across the United

States. Unlike chemical oxidants, UV dosages are based on the emitted radiation from the lamps and are expressed in power per unit volume of fluid under UV exposure such as W/m^3 or as surface intensity such as W/m^2 *(1).* Although it is effective, there are many considerations associated with UV practice that need to be taken into account. The first is the presence of suspended particles such as proteins, chemical compounds, organic substances, and a variety of other suspended materials that could absorb the UV radiation and shield microorganisms. To avoid this issue, treatment must be performed prior to UV treatment to minimize the amount of suspended particles. Another consideration is adequate mixing to ensure that all microbes can be equally exposed to the UV radiation. Despite the operational and maintenance considerations, UV is a great primary disinfectant but not a secondary disinfectant due to its complete lack of residual. There is no known direct formation of DBPs resulting from UV exposure (*1*).

DISINFECTION BYPRODUCTS

The formation and speciation of DBPs is extremely variable and dependent on factors such as NOM composition and chemical properties, water quality parameters, disinfectant type and dose. The less commonly known DBPs will be covered later in this section; however, as this study revolves primarily around THM and HAA formation upon chlorination, the immediate focus will be on those compounds and chlorine as the disinfectant.

Chlorine Disinfection Reactions and Kinetics. Chlorine may be added as a disinfectant in one of three ways (*12*):

- As chlorine (Cl2) in the form of a compressed gas that is dissolved in water at application point which is 100% by weight available chlorine.

- As calcium hypochlorite ($Ca(OCl)_2$) as a dry solid which is 99.2% by weight available chlorine.

- As a sodium hypochlorite (NaOCl) solution which is 95.8% by weight available chlorine.

The amount of chlorine in chlorine gas or hypochlorite salts, such as those listed above, is referred to as available chlorine. Since one mole of hypochlorite is electrochemically equivalent to one mole of elemental chlorine, it can be determined that calcium hypochlorite contains 2 moles and sodium hypochlorite contains 1 mole of chlorine, giving the weight percentages listed above (*12*). However, it is important to note that using sodium hypochlorite could result in the formation of chlorate leading to the formation of the DBP chlorite. The sum of chlorine (Cl2), hypochlorous acid (HOCl), and the hyporchlorite ion (OCl-) concentrations are referred to as free available chlorine and are each a result of chlorine addition to water. The distribution of free chlorine between hypochlorous acid and the hypochlorite ions is a function of temperature and pH, where hypochlorous acid is predominant at low pH and the hypochlorite ion is predominant at

higher pH values (*12*). These reactions are important considerations since the amount of DBPs formed during disinfection is a direct result of the concentration of disinfectant used.

As an oxidizing chemical and disinfectant, chlorine is known for its reactive properties especially its affect on biological matter such as cell membranes, nucleic material and cellular proteins (*1*). These same oxidizing abilities also allow chlorine to react with non-living, NOM by attacking the carbon-carbon double bonds and creating increasingly oxidized organic byproducts until they become simply structured organic fragments. Some of these simplified organics include but are not limited to the C1-C3 acids, diacids, aldehydes and ketones that create halogenated byproducts and are known as organic halide by-products. The byproducts can be measure as total organic halide (TOX) or dissolved organic halides (DOX) and since NOM has very low initial TOX concentrations, these measured compounds are DBPs.

Disinfection Byproduct Precursors. Although much focus has been placed on NOM being the precursors for DBPs, free chlorine can react with both inorganic and organic compounds to form DBPs. The presence of bromine and nitrites also impact the type of DBPs formed. In water treatment the term “organic compounds” can refer to any of the three sources of organics: natural organic matter (NOM), domestic and commercial activities (synthetic organic compounds or SOCs), and those created during water treatment processes and reactions (*13*). However,

for this study the main focus is the formation of DBPs (THMs and HAAs in particular) as a result of chlorine reacting with NOM, so DBP precursors in this context is considered to be NOM as measured by dissolved organic carbon (DOC) as it has become common practice to use total organic carbon (TOC), DOC, and UV_{254} measurements as surrogates for organic content.

The NOM compounds make up the majority of organic compounds found in drinking water and are formed from biological activity including secretions from higher organisms, decay of organic matter including animals, plants and algae, metabolites from microorganisms, aliphatic and aromatic hydrocarbons. They are comprised of basic organic compounds such as hydrophilic acids, amino acids, proteins, hydrocarbons, lipids, and humic and fulvic acids (*10, 13*). The humic acids, fulvic acids, and humin make up the hydrophobic acids that are rich in aromatic carbon, conjugated double bonds, and phenolic structures (*14*).The hydrophilic substances include carbohydrates, sugar, and amino acids that contain aliphatic carbon and nitrogenous compounds.

The composition of NOM can change seasonally and will vary depending on the geographical location and surrounding environment. In general, NOM molecules are very soluble and can be found in extremely high concentrations without precipitating. Molecules are also negatively charged with anionic functional groups and have a relatively broad range of molecular weights (MW). However, the range of MWs differs in the

literature with some sources saying that the range is from 500 to 10,000 Da while others state it is from 500 to 30,000 Da (*15,16*). Natural organic matter has a predominantly elemental composition of carbon (45 – 60 %), oxygen (35 – 40 %), hydrogen (4 – 5 %), and nitrogen (1 %)(*10*).

Due to the complex combinations of compounds that comprise NOM, it is very difficult to precisely characterize NOM chemistry and composition. Composition and classification of NOM into certain fractions has been commonly practiced over the years using a variety of techniques including (*17*):

1. Fractionation based on chemical structure and function groups into:
    - Fulvic acids
    - Humic acids
    - Transphilic acids, bases, and neutrals
    - Hydrophobic acids, bases, and neutrals
    - Hydrophilic acids, bases, and neutrals
2. Size Exclusion Chromatography (SEC) that provides molecular weight distributions into three regions:
    - Polysaccharides, proteins, and colloids
    - Humic substances
    - Low MW organic acids
3. Excitation Emission Matrix (EEM) resulting from fluorescence spectroscopy – displays fluorescence intensity in a 3D spectrum
4. Dissolved Organic Nitrogen (DON) measurements

The specific ultraviolet absorbance or SUVA (UV_{254}/DOC) values can also be used to classify NOM. High SUVA values indicates primarily hydrophobic and high molecular weight (MW) compounds while lower SUVA values indicate primarily hydrophilic compounds with low molecular charge density and low MW (*14*). Although all organic matter is the main precursor to the formation of DBPs, research has shown that both the hydrophobic fraction with high aromatic carbon content and high MW and the hydrophilic fraction with high aromatic carbon content play a significant role in DBP formation (*14*).

Disinfection Byproducts. Although TTHMs, HAA5, chlorite, and bromate are currently the only USEPA regulated DBPs, there are still many DBPs, both inorganic and organic that can be created during the oxidation/disinfection process. The emphasis on THMs and HAAs results not only from their common and sometimes abundant presence in drinking water, but also because they are relatively easy to detect and quantify. However, this does not mean that other DBPs do not form nor do they pose any less potential health threat. The relatively uncommon DBPs formed include the: haloacetaldehydes, formaldehyde, haloketones, haloacetonitriles, chloropicrin, cyanogens chloride, chlorophenols, 3-chloro-4-(dichloromethyl)-5hydroxy-2(5H)-furanone also known as (MX), and N-nitrosodimethylamine (NDMA) recently discovered as a byproduct of chloramination (*13*). The previously listed DBPs, although not as common, are gaining interest in the water quality field due to their

potentially adverse health effects. However, for this study only THMs and HAAs were considered because emphasis is on disinfection with chlorine and because they are regulated by the USEPA.

Total Trihalomethanes*.* Trihalomethanes are formed when one or more of the hydrogen atoms on the methane molecule (CH4) is replaced by a halogen atom most commonly chlorine or bromine. There are four common THMs that are regulated, as shown in Table 2-1. The formation of THMs depends on the contact time between chlorine and organic matter, measured as DOC. Concentrations of THM formation can be measured directly or standard methods have been established that measure the THM formation potential (THMFP). The THMFP measures THM concentrations under a set of controlled conditions including pH, contact time, temperature, and residua chlorine concentrations (*18*).There are a variety of standard methods that are used for measuring THMFP however, this paper will focus of the THMFP Standard Method 5710B and 6232 and the Simulated Distribution System Trihalomethanes (SDS-THM) Standard Method 5710C. The THMFP and SDS-THM were modified and used to measure the formation of THMs after chlorination doses that were chosen to mimic the condition founds within the distribution system.

The THMFP is the difference between the final and initial concentrations of TTHMs but has also been equated to the final TTHM concentration and needs to be clearly defined when stating the results (*19*). The THMFP is also a maximum potential formation measurement

since a higher chlorine dose is used. In this procedure, samples are buffered to a pH of 7 ± 0.2, dosed with a calculated amount of chlorine designed to achieve a 3 to 5 mg Cl_2/L residual, and stored at 25 ± 2ºC for seven days. The resulting TTHM concentration formed is then the THMFP or it is calculated depending on the definition mentioned above (*19*).

The SDS-THM method is designed to mimic the conditions of the local distribution system including pH, temperature, disinfectant dose and residual, and reaction time. The definition of SDS-THMs is the concentration of TTHMs that has been "disinfected comparably to finished drinking water and under the same conditions and time as the water distribution system," (*19*). The concentrations of TTHMs formed will be considerably less than those for the THMFP since a lower residual (< 1 mg Cl_2/L) is targeted and a lower dose is used. More detailed descriptions of both methods can be found in the Standard Methods book *(19).*

Haloacetic Acids. Haloacetic acids are formed when halogen atoms (most commonly chlorine or bromine) replace one or more of the hydrogen atoms on the acetic acid molecule (CH_3COOH. This can form up to nine haloacetic acids depending on the type and quantity of the replacing halogen atom. The nine HAAs can be split into three groups with different biological and chemical properties (*3*).

1. Monohaloacetic acids – one halogen
    i. Monochloroacetic acid
    ii. Monobromoacetic acid

2. Dihaloacetic acids – two halogens
    i. Dichloroacetic acid
    ii. Bromochloroacetic acid
    iii. Dibromoacetic acid
3. Trihaloacetic acids – three halogens
    i. Trichloroacetic acid
    ii. Bromodichloroacetic acid
    iii. Chlorodibromoacetic acid
    iv. Tribromoacetic acid

Despite the existence of nine HAAs, only five are regulated by the USEPA as shown in Table 1. As with the THMs, there is a Standard Method 5710D for the testing of HAA formation that can be found in the Standard Methods book (*19)*. For both THMs and HAAs, the methods used for formation analysis are discussed in Section 1.3.

STRATEGIES FOR THE CONTROL OF DISINFECTION BYPRODUCTS

The most common practice for controlling the formation of DBPs is to reduce the amount of DBP precursors or organics within the treatment facility. Such treatment processes as listed by the USEPA, include enhanced softening or coagulation and GAC 10 filtration which is simply GAC filtration with and EBCT of 10 minutes (*7*). Other processes that have been used to control DPB formation include membrane filtration, convention treatment modifications, and DBP removal through advanced oxidation processes, and GAC adsorption *(14).* However since this study

revolves around EPA regulations on DBP formation, only enhanced coagulation, GAC filtration and the proposed photocatalysis will be discussed in this section

Enhanced Coagulation. Coagulation adds a chemical during rapid mixing to destabilize charged suspended particles and allow for preliminary aggregation followed by flocculation that encourages further aggregation into flocs and settling prior to filtration. Coagulation captures suspended particles that will not settle as a result of negligible settling velocity and are colloidal solids that are held in suspension by electrostatic, negatively charged forces (*10*). The three technical steps in the process are: coagulant formation, particle destabilization, and interparticle collisions (*20*). Common coagulants used today are (*10*):

1. Inorganic Metallic Coagulants

    - Aluminum and Ferric Ions – each of which dissociate into trivalent ions and then hydrate going through a series of hydrolytic reactions to form soluble mononuclear and polynuclear species that can interact with particles in water. These include aluminum sulfate or “Alum”, ferric sulfate, sodium aluminate, and ferric and aluminum chloride. Alum is a class of chemical compounds that contains aluminum sulfate (another term for alum) [$Al(SO_4)_2.12H_2O$] and can have other metallic elements attached such as potassium alum.

2. Prehydrolyzed Metal Salts

    - Resulted from the unpredictability associated with the formation of alum and iron salt species. Prehydrolyzed salts are produced by mixing the various ferric and alum salts with water and hydroxide. These are commercially known as PACl for the prehydrolyzed alum salts and have the general chemical formula of $Al_a(OH)_b(Cl)_c(SO4)_d$.

3. Organic Polymers

    - Also known as polyelectrolytes, organic polymers have distinct physicochemical properties due to their polymer chain structure of repeating chemical compounds or units that have functional groups which provide an electrical charge to the structure. These charges can be anionic or nonionic to form bridges between particles.

The addition of a coagulant causes destabilization of particles' surface charges. These surface charges are what attract and repel particles, including the repulsive electric double layer forces and the attractive London-van der Waals forces (*20*). Destabilization mechanisms of these forces include compression of the electric double layer that allows particles with similar surface charges to get *close to one another by*

reducing the energy required to move particles into contact; surface charge neutralization by reducing the particles' net surface charge and also minimizing energy required to move particles into contact; and bridging between particles and/or adsorption through polymer addition. After particle destabilization the flocculation process can begin (*20*).

Enhanced coagulation involves the same principles and practices outlined above; however, changes are made to further encourage the removal of NOM by increasing the coagulant dose and/or decreasing the pH. The design of the enhanced coagulation process must involve the consideration of coagulant type and dose, pH, mixing speeds and time, and the addition of any coagulant aids. The use of ferric and alum salts are common, but ferric salts have the potential to cause corrosion within the treatment facility and introduce heavy metals (*3*). In such cases, acid addition, such as sulfuric acid, is an easy way to lower pH, reduce coagulant dose, and achieve better TOC removal.

Granular Activated Carbon. Activated carbon can be created using a variety of carbon-based raw materials including wood, peat, coal, and lignite (*5*). This raw material is then converted to char in a process called carbonization and then activated through oxidation in order to created the internal pore structures. Once used, granular activated carbon (GAC) can be reactivated and reused after the removal of any adsorbates that have left a residue on the GAC surface. Although this process allows for the reuse of the GAC there are some disadvantages that include the loss of

mass and change in pore size distribution that add to the costs of using GAC (*5*).

Granular activated carbon is used for the adsorption and subsequent removal of dissolved and suspended particles in solution. Today, GAC is commonly used for the removal of color, taste, and odor causing compounds, synthetic organic compounds (SOCs), DBP precursors or NOM, and even heavy metals. The adsorption of materials onto GAC surfaces (adsorbent) is the result of mass transfer processes that involves the surface chemistry of the interacting particles. There are four generalized steps a particle must follow to be adsorbed (*5*):

1. Bulk solution transport:
    a. Adsorbate must be transported towards the absorbent particle surface from bulk fluid through diffusion (if negligible water movement) or mixing (if there is turbulent flow).
2. External film transport resistance:
    a. Once adsorbate reaches the stationary boundary layer of water surrounding the particles surface, it must be transported across this layer by molecular diffusion.
3. Internal pore transport:
    a. Adsorbate must then be transported to adsorbents available pore space to ensure adsorption.

4. Adsorption:

    a. After an available site is occupied by the adsorbate, bonds are formed between the adsorbate and adsorbent and may include in some cases a chemical reaction.

In GAC contactors, understanding the adsorption process is critical and necessary to evaluate breakthrough curves and performance. There are three types of commonly used GAC contactors: gravity feed contactors, pressure contactors, and upflow or fluidized bed contactors, any of which can be operated in parallel or in series (*10*). The concentration profile for GAC contactors changes with time with accumulation of adsorbate occurring near the inlet during the initial filtration. As time of filtration increases and the GAC becomes more saturated, the concentration profiles moves in the direction of the flow, slowly saturating the entire column. As this occurs, effluent water quality also decreases since less pore space is available for adsorption and the adsorbate is flushed out with of the column. The plot of effluent concentration versus either time or the volume of water processed is called the breakthrough curve and is used to find the time at which the breakthrough concentration or maximum allowable effluent concentration is reached, as shown in the Figure 1 below (*10*).

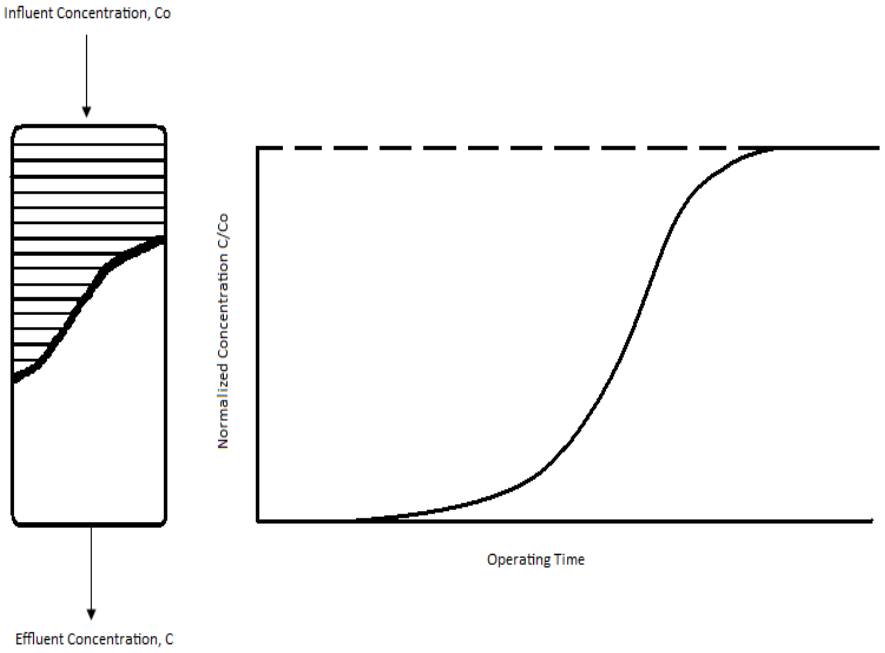

Figure 1: Schematic of Breakthrough Curves for GAC Columns (Adapted from (*10*).

To help evaluate GAC contactor performance, rapid small scale column tests (RSSCTs) were introduced that allowed experiments to be conducted in less time than pilot plant studies, use smaller amounts of water, and not require extensive isotherm or kinetic studies (*10*).The RSSCT is based on dimensionless groups that represent the transfer mechanisms of the adsorbate in the large and small scaled systems. These dimensionless groups for the large and small scaled systems are then set equal to each other to maintain similarity between the two. The individual GAC particles are also ground down to a small size using a mortar and pestle and standard sized sieves. The scaling procedure and equations derived from the dispersed-flow pore and surface diffusion

model (DFPSDM) will not be discussed in this section of the report but have been extensively covered in the work by Crittenden et al.(*10*).

Photocatalysis and Titanium Dioxide. Photolysis is the process of light-induced oxidation and reduction of compounds through their absorbance of photons and the resulting energy release. Photocatalysis is based on the same principle but utilizes a catalyst, primarily a semiconductor - in this case nano-sized titanium dioxide - which can react with surrounding compounds and molecules to produce free radicals including the hydroxyl radical. Titanium dioxide is a commonly used and favorable catalyst due to its high photocatalytic activity, purity, particle size, and surface properties (*21*). Relevant variables for photocatalysis include, catalyst concentration, activating UV wavelength and intensity, pH and water matrix parameters (*14*).

The process of photo-activating titanium dioxide is shown below in Figure 2. The first step is activation by exposure to UV light. Titanium dioxide can be activated through exposure to UV light with wavelengths in the 200 to 400 nm range (*10, 22*). In step 2, after the absorbance of light energy, an excited electron in the outer valence band moves to the conduction band. In order to do this the electron must first have enough energy to bridge the band gap. This jump from the valence band to the conduction band by the electron leaves a hole, or vacancy, in the valence band as shown in step 3, while the electron now occupies space on the conduction band as shown in step 4. When water reacts with the vacancy

on the valence band, hydroxyl radicals (HO•) can be produced, and the electron on the conduction band can reduce hydrogen ions and oxygen depending on the pH to produce superoxide radicals (O2-•), as shown below, or hydrogen gas (H_2).

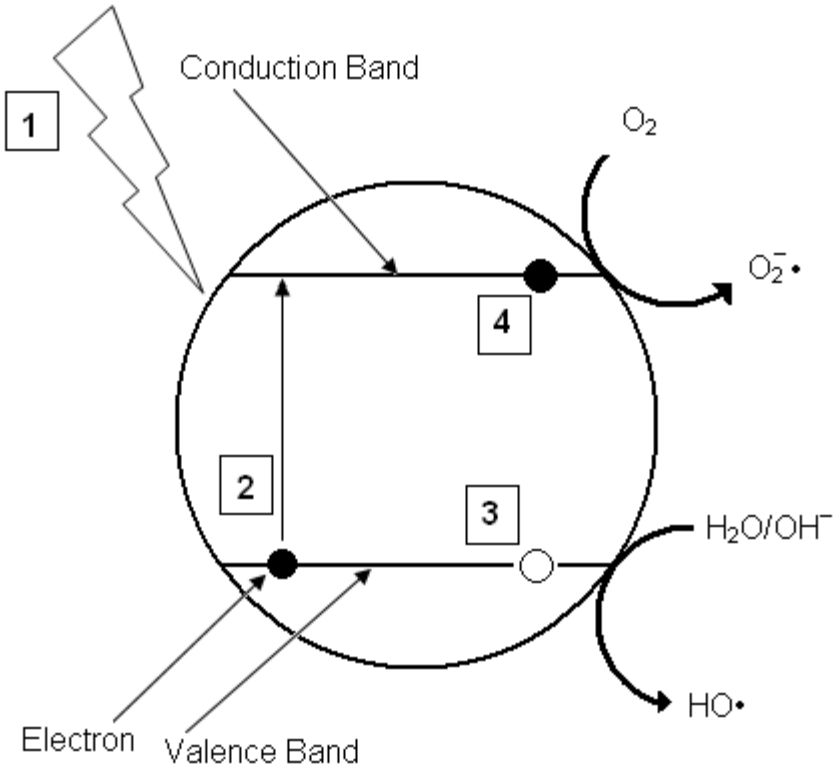

Figure 2: Photoactivation of Titanium Dioxide Particle (*10*)

This production of hydroxyl radicals at ambient temperatures and atmospheric pressure is what makes advanced oxidation processes (AOPs) such as photocatalysis so favorable. The hydroxyl radical, as previously discussed, is one of the most powerful chemical oxidants and is effective at oxidizing an array of organic contaminants including NOM.

However, hydroxyl radicals have an extremely fast reaction rate constant with values ranging from 10^4 to 10^{10} (L/mol*s) (*10*). Due to their fast and nonselective reactions, the hydroxyl radicals can be quickly scavenged by any background inorganic or organic matter, making the influences of NOM, pH, carbonate, and bicarbonate important factors. The reactions between the hydroxyl radicals and organic compounds involve the extraction of hydrogen atoms and additional reactions with double bonds which are much faster than the extraction of hydrogen atom. However, these reactions produce organic radicals that can be subsequently oxidized, forming peroxy- organic radicals ($ROO^{\bullet}$). The general trend for AOP byproducts for organic contaminants has been observed as follows (*10*):

Organic pollutant → aldehydes → carboxylic acids → carbon dioxide and mineral acids

Chapter 3

GENERAL MATERIALS AND METHODS

As previously mentioned the scope of this study involves the examination of photocatalysis on various water samples collected throughout the water treatment process train for the removal of DBP precursors and the inhibition of THMs and HAAs. The primary focus of each sub-objective is the removal of DBP precursors as measured by dissolved organic carbon (DOC) and UV_{254} absorbency, and the formation of THMs and HAA after photocatalytic treatment and chlorination targeting a 1 mg/L residual.

WATER SAMPLE COLLECTION, PRESERVATION, AND STORAGE

As mentioned in Section 1.2, water samples were taken from 5 different locations and were all tested using the PhotoCAT machine manufactured by Purifics® (London, ON, Canada). The volume capacity of the PhotoCAT® machine was 16 liters (L) or a little more than four gallons. For all water sources with the exception of the Pre-GAC Adsorption source, a minimum sample volume of five gallons was collected to ensure extra sample water if needed. Water samples were collected in plastic containers or buckets that were washed and triple rinsed with Alconox. In some case of Pre- and Post-GAC Adsorption, the containers and buckets needed to be disinfected with chlorine and then quenched with sodium thiosulfate, scrubbed and triple rinsed before use. In most cases water samples were treated with the PhotoCAT® within one or two days of

collection. Samples were stored in their collection containers at approximately 72℉ prior to treatment.

PHOTOCATALYSIS USING PURIFIC'S PHOTOCAT® MACHINE

The Purfic's PhotoCAT® Lab machine used for photocatalysis was operated in a batch configuration in which 16 L samples were transferred into the machine along with nano-particle titanium dioxide (TiO_2) and continuously recycled throughout the experiment. The PhotoCAT® consists of a 16 L capacity accumulator tanks that stores the majority of the sample; eight low-pressure, mercury UV lamps in series; a submicron pore sized ceramic filter that produces TiO_2 free effluent; and an air compressor that not only provided air to the system but produced an air hammer to release any TiO_2 remaining on the surface of the ceramic filter so that it could be recycled. Although the machine was equipped with eight UV lamps, experiments were conducted with only five lamps since three were out of service for the duration of all experiments. Prior to each experiment the PhotoCAT® was flushed with City of Tempe tap water and run to purge the various components of the machine. A final run and flush with de-ionized water was also performed before the start of any experiment. As mentioned before the raw water and TiO_2 were put into the PhotoCAT® at the same time and the TiO_2 was recycled in a slurry suspension. The TiO_2 used was the reagent-grade Degussa P25 that consists of two types of crystal forms: approximately 70-80% anatase and 20-30% rutile TiO_2, and has a surface area of 50 m^2/g (*23*). The targeted

concentration of TiO_2 used was based on the optimal dose determined in the preceding study of 1 g/L resulting in approximately 16 grams of titanium dioxide for each experiment (*25*).

Five samples were analyzed for each water source, including an untreated control water sample and were treated to four different treatment levels using the PhotoCAT® Lab at targeted specified energy consumption levels of 0 kWh/m^3, 5 kWh/m^3, 80 kWh/m^3, and 160 kWh/m^3. These treatment levels are hereafter referred to as No UV, Low, Medium, and High photocatalytic treatment levels. The No UV samples were those samples collected after the UV and TiO_2 were run through the machine without any UV exposure to provide a measure of filter performance. Operation times associated with each treatment level were calculated based on flow rate, available water volume, and energy consumption and are as follows: No UV - 0 minutes, Low - 10 minutes, Medium – 2.5 hours, High – 4.5 hours. These values are an approximation and were based on the total sample volume and number of lamps in operation. Samples were collected from the PhotoCAT® after filtration in 1 L amber bottles. Prior to use, the amber bottles were acid washed and ashed at 550℃ to ensure organic removal.

ANALYTICAL METHODS AND MEASUREMENTS

For each of the water sources the same treatment procedures were performed. Each sample was treated with photocatalysis to various levels based on energy consumption. Samples were collected at each treatment

level to use for general water quality measurements and a chlorine demand and DBP formation potential test. Prior to any chlorination general water quality measurements and more sophisticated analysis were performed. General measurements included such water quality parameters as dissolved organic carbon (DOC), UV_{254} absorbency, pH, alkalinity, turbidity, and ion concentrations for chloride, bromide, sulfate, and nitrate. The DOC and UV_{254} measurements were indicators of organic content while the other measurements provided insight into how the overall water quality was changing. More sophisticated analysis included size exclusion chromatography and fluorescence spectroscopy excitation-emission matrices in an effort to characterize organic matter which will be discussed in later chapters.

The analytical measurements were the exact same as those performed in the related study performed by Gerrity et al. (*25*). These measurements were the same for all water sources and included pH, turbidity, alkalinity, UV_{254} absorbency, DOC, total dissolved nitrogen (TDN), and ion chromatography (IC) including nitrate, sulfate, chloride, and bromide ion concentrations. The pH was measured using a pH meter manufactured by Mettler (Columbus, OH). Turbidity was measured using the 2100P Turbidimeter manufactured by Hach (Loveland, CO). Total Alkalinity was determined using sulfuric acid titration cartridges in a digital titrator (Hach model 16900) and bromocresol green-methyl red indicator powder packets. The UV_{254} absorbance measurements were measured using a

Hach DR 5000 machine. For these measurements, each double sided quartz cuvette was soaked in a 10% by volume hydrochloric (HCl) acid solution and rinsed with nano-pure water before reading. Between samples the cuvette was triple rinse with nano-pure water as well. For DOC/TDN and IC measurements, raw water and coagulation samples were filtered prior to analysis using a 0.45 um Whatman (Middlesex, UK) GF/C glass microfiber filters to remove particulate organic matter. For DOC/TDN, samples were analyzed using the 5050A Total Organic Carbon Analyzer by Shimadzu (Kyoto, Japan). Before analysis however, DOC/TDN samples were acidified using a 1 M HCl solution. The IC samples were analyzed using the DX-120 ion chromatograph manufactured by Dionex (Sunnyvale, CA). The eluent for the IC machine was prepared by de-gassing 2 L of nano-pure water with helium gas for 10 minutes and then mixed with 1.2 mL of 0.5 M $NaHCO_3$ and 10.8 mL of 0.5 M Na_2CO_3. Six standard solutions in the anticipated sample range for chloride, nitrate, bromide, and sulfate were prepared and analyzed prior to sample analysis. The same standard curves were used for each analysis for consistency.

CHLORINATION EXPERIMENT

After general measurements were made a chlorination test was performed to test for DBP formation. This test is a modified version of the standard simulated distribution system (SDS-THM) test described in more detail in the literature review under the Trihalomethane section. Before

chlorination a 24-hour chlorine demand test was performed on each water sample. To do this, each water sample was split into three separate acid-washed and ashed amber bottles and was dosed with chlorine to target a 1, 3, and 5 mg/L concentration. The concentrations were then measured after 24 hours using the Hach D4/4000U spectrophotometer and total chlorine reagent powder packets. The information collected was then used to construct a regression curve used determine the appropriate dose for each sample to target a 1 mg/L residual after 24 hours since a targeted disinfectant residual of 2 mg/L is required within the distribution system for Phoenix, AZ. Prior to chlorination samples were incubated at 28℃ for 24 hours to simulate environmental conditions within the Phoenix, AZ distribution system. Afterwards, each sample was dosed with their respective chlorine amount. Total chlorine measurements were taken every 15 minutes up to two (2) hours, then every two hours up to six (6) hours, and then a final measurement at 24 hours. More samples were taken within the first two hours since the reactions between organic matter and chlorine occur relatively quickly and the majority of DBPs are thought to form during this initial phase. The THM and HAA samples were taken simultaneously as the chlorine readings at various times depending on the experiment. The THM samples were taken for each experiment while the HAA samples were taken for each water source with the exception of the Salt River water. The THM samples were preserved by adding HCl while HAA bottles were preserved with crystallized ammonium chloride. Before

analysis the untreated control samples were filtered using glass fiber filters (0.45 µm).This removes particulates that could be hard on the machines. However, due to the ceramic filter the samples treated using the PhotoCAT® Lab did not need to be filtered with the glass fiber filters. All samples were then analyzed by the City of Scottsdale's Water Campus using modified USEPA Methods 552 (HAAs) and 524.2 (THMs) . For the HAA analysis, samples were placed in ABI Qtrap® 250 mL amber glass bottles and preserved with 50 mg of ammonium chloride. An Applied Bios systems Triple Quadrupole MS (ABI Qtrap) system was used for the analysis. For the THM analysis, samples were placed in 40 mL volatile organic analysis (VOA) vials and preserved with ascorbic and hydrochloric acid. An OI Analytical 4560 Concentrator was used with an HP 6890 Plus GC System and an HP 5973 Mass Selective Detector (Mass Spectrometer) for the analysis.

Results for each experiment were then analyzed for the removal of organics or DBP precursors and THM and HAA formation. All measurements made in each experiment can be found in the Appendix tables. The Literature Review Chapter provides more general background knowledge regarding photocatalytic oxidation and DBP formation.

Chapter 4

COMPARISON OF PHOTOCATALYSIS, COAGULATION, AND ENHANCED COAGULATION FOR THE REMOVAL OF DISINFECTION BYPRODUCT PRECURSORS

INTRODUCTION

Photocatalysis has been used for disinfection purposes in both drinking and waste water treatment. However, as concern over disinfection byproducts (DBPs) and their potentially carcinogenic characteristics increased, water treatment facilities were forced to investigate new ways of controlling DBP formation. According to the United States Environmental Protection Agency (USEPA), one of the best available technologies (BATs) for removing DBP precursors is enhanced coagulation or softening (*7*). The precursor or natural organic matter (NOM) removal requirements for these treatment processes are listed in Table 3.

The process of standard coagulation is the same for enhanced coagulation in which a coagulant is added to destabilize particles and allow for the interaction between particles so they can aggregate and settle out of solution. These processes are explained in more detail in Chapter 2. In order to meet TOC removal requirements using enhanced coagulation, a higher coagulant dose and/or acid addition to lower the pH is commonly used. Acid addition is an efficient way to achieve a lower pH and destabilize particles by forming higher valance species and reduces

repulsive forces by approaching the isoelectric point. Acid addition also decreases the amount of coagulant used. Another benefit of using acid addition rather than increasing the coagulant dose is the elimination of excess sludge production and disposal (*24*).

Photocatalysis is one of many advanced oxidation processes (AOPs) that is has been investigated to replace enhanced coagulation due to its oxidizing capabilities and no sludge production. As discussed in Chapter 2, photocatalysis uses ultraviolet radiation to activate titanium dioxide in order to produce free radicals that participate in oxidation/reduction reactions and facilitate degradation of NOM. For this study, photocatalysis is compared to standard and enhanced coagulation for the removal of DBP precursors and control of DBP formation.

MATERIALS AND METHODS

This individual study is a continuation of the research performed by Gerrity et al. (*25*), and, as such, all laboratory equipment and methods used were done in the same manner to ensure consistency. Water samples for this experiment were taken from the Salt River outside of Phoenix, AZ. Samples included an untreated or Control sample and those that were treated with photocatalysis to four different levels of treatment, standard coagulation, and enhanced coagulation. After the samples were treated, general measurements were made and then a chlorination and DBP formation test was performed as discussed in Chapter 3 General Materials and Methods.

Standard and Enhanced Coagulation. The coagulation experiments were performed using the standard bench-scale jar-test apparatus (PB-700 Phipps & Bird, Richmond, VA). Four clean jars were filled with 1.5 L of untreated Salt River water and ferric chloride was added as the coagulant at a predetermined optimal dose of 40 mg/L (*25*). Two of the jars were run with no pH adjustment while the other two were adjusted to a pH of 6 by adding hydrochloric acid to allow for duplicate samples. Immediately after coagulant addition, the jars were rapidly mixed at 100 rpm for 1 minute. For the flocculation stage, the jars were mixed for 10 minutes each at 40 and 20 rpm and then allowed to settle with no mixing for 30 minutes.

Photocatalysis. Pilot-scale photocatalysis was performed using the Photo-Cat Lab® from Purifics® (London, ON, Canada). Reagent-grade Degussa P25 TiO_2 was used in this experiment at an optimal dose of 1 g/L, as found from the previous study (*25*). Treated samples were taken from the machine at energy consumption values of 0 kWh/m^3 (no UV exposure just filtration), 5 kWh/m^3, 80 kWh/m^3, and 160 kWh/m^3, which correlated to No UV, Low, Medium, and High treatment levels respectively. For a more detailed description of the methods for photocatalysis see Chapter 3.

General Experimental Measurements. After treatment, two liter samples were taken to allow for general water quality measurements and a chlorine demand and DBP formation potential tests. The general

measurements taken in this study included pH, alkalinity, turbidity, total dissolved nitrogen (TDN), dissolved organic carbon (DOC), and UV_{254} absorbance as described in Chapter 3. In addition, the specific UV absorbance, or SUVA, was calculated for each sample. SUVA is defined as the ratio of UV absorption at 254 nm to the DOC concentration in mg/L. The SUVA can be used to estimate the formation potential of DBPs and also provides insight as to the treatability of water. Water with SUVA values less than 2 L/mg*m are considered difficult to treat, while those with SUVA values greater than 2 L/mg*m are more easily treatable waters but have more potential to form DBPs (*3*).

Chlorination and DBP Formation. To test for the formation of DBPs a modified standard formation potential and simulated distribution system (SDS) test was performed as described in Chapter 2. Prior to chlorination, a 24-hour chlorine demand test was performed on each sample to determine the appropriate chlorine dose to target a 1 mg/L residual after 24 hours. This 24 hour time period was chosen to comply with the Standard SDS method and simulate the estimated residence time of the sample in the distribution system. After chlorination, total chlorine measurements were taken every 15 minutes up until 2 hours, every 2 hours up until 4 hours, 8 hours, and a final reading at 24 hours. Samples were taken for THM concentrations at 15 minutes, 2 hours, and 24 hours after chlorination and sent to the City of Scottsdale's Water Campus for analysis. The THM samples were refrigerated and hydrochloric acid (HCl)

was added to preserve the samples and to ensure no further THM formation would occur. The samples were also collected to eliminate any headspace to prevent volatilization and loss of THMs from the sample.

RESULTS AND DISCUSSION

General Measurements. Trends from the resulting data show that for each of the water samples the pH was fairly constant with the exception of the enhanced coagulation which was adjusted to a target pH of 6. The results also showed that water quality was improved with increased levels of photocatalysis and enhanced coagulation had more improvement than standard coagulation, as shown in Table 4 below.

Table 4

General Measurements for SRP Samples

	pH	Turbidity (NTU)	DOC (mg/L)	UV_{254} (cm^{-1})	SUVA (L/mg-m)	TDN (mg-N/L)
Control	8.02	2.86	4.85	0.086	1.78	0.32
No UV (0 kWh/m3)	7.99	0.4	3.37	0.052	1.543	0.3
Low (5 kWh/m3)	8.04	0.3	3.38	0.025	0.73	0.33
Medium (80 kWh/m3)	8.27	0.44	0.74	0	0	0.43
High (160 kWh/m3)	8.26	0.38	0.64	0	0	0.47
Coagulation	7.11	1.04	5.51	0.058	1.047	0.3
Enhanced Coagulation	5.67	0.48	3.98	0.045	1.131	0.21

Turbidity was significantly reduced by 86% by simply running the water through the Photo-Cat® ceramic filter and then remained fairly

consistent during subsequent photocatalysis. For standard and enhanced coagulation turbidity was reduced by 64% and 83% respectively as compared to the Control sample. For the DOC results, the No UV and Low treatment levels reduced DOC by approximately 30%, which could be the result of the ceramic filter or adsorption of NOM onto the titanium dioxide surface. The Medium and High treatment levels had an 85% and 87% reduction respectively. These results are similar to those found in the literature that report photocatalysis as an effective means of NOM destruction (*14, 22, 24-27*). There is also evidence to support that hydrophobic, higher molecular mass (HMM) compounds preferentially adsorb to the surface of TiO_2 since they have more reactive functional groups than the lower molecular mass compounds (*14, 24, 26, 27*). This could explain the physical removal of DOC from the Control to the No UV samples since the TiO_2 and anything adsorbed to its surface was removed by the submicron filter.

After standard coagulation DOC actually increased by 14% while enhanced coagulation resulted in an 18% decrease. These results are interesting since standard and enhanced coagulation are designed to remove organic material, especially the hydrophobic fraction that has HMM compounds and is more aromatic in structure (*14, 28*). However this leaves behind the hydrophilic, lower molecular mass (LMM) compounds that are more difficult to treat and/or remove.

For the UV_{254} results, the No UV and Low treatment levels showed a 40% and 70% DOC reduction respectively, while the Medium and High treatment levels showed possibly complete or near complete oxidation with 100% reduction. The DOC and UV_{254} measurements are an indication of organic content of the samples. These results show that for increased photocatalysis organic matter is being removed through oxidation. Studies have shown that given enough time for oxidation during photocatalysis, organic matter can be completely oxidized or mineralized, which appears to be what is happening in the Medium and High treatment levels (*14*).

Not only do these measurements represent organic content but DBP precursors as well. A reduction in these measurements is an indication that DBP precursors are being removed and the formation potential of DBPs is being reduced. The drop in turbidity, DOC, and UV_{254} from the Control Sample to the No UV sample occurs in the absence of UV light exposure. This suggests that although there may be some oxidation occurring, there may also be a physical removal process happening as well as discussed above with NOM adsorption onto titanium dioxide.

The SUVA values also decreased with increased photocatalytic treatment indicating increased difficulty in treatment and a decrease in potential DBP formation as indicated by the reduction in DBP precursors. Decreased SUVA values are also an indication of the reduction in

aromaticity of the organic matter by the breakdown of HMM aromatic rings during photocatalytic oxidation (*14*).

For the TDN measurements photocatalysis appeared to increase concentrations while enhanced coagulation seemed to decrease concentrations. In the case of the No UV and Low treatment levels TDN nitrogen levels were about the same while the Medium and High treatment levels experienced a 34% and 47% increase respectively. This could be the result of the oxidation of organic nitrogen to inorganic nitrogen with increased photocatalysis levels. The standard and enhanced coagulation results, however, showed about the same TDN concentration and a 35% decrease respectively.

Chlorination and DBP Formation. The resulting total THM formation potentials (TTHMFP), defined here as the TTHM formation after a 24 hour chlorination period, as well as the chlorine residuals for each treatment level are listed below in Table 5.

The results in Table 5show Medium and High photocatalytic treatment levels had individual TTHMFP concentrations were very low ; however, TTHMFP spiked at the Low treatment levels with concentrations slightly higher than those found in the control sample. In addition, over the 24 hour chlorination experiment there was a peak in THM concentration at 2 hours after chlorination as well. The table also shows the chlorine demands and residuals for each treatment level and indicated that for the

higher photocatalytic treatment levels there was slightly less of a chlorine demand than the No UV, Low, and coagulation samples.

Table 5

TTHM Concentrations for SRP Samples

				TTHMFP (ug/L)		
	Initial Cl_2 (mg/L)	24 hr Residual Cl_2 (mg/L)	24 hr Cl_2 Demand (mg/L)	15 min	2 hr	24 hr
Control	3.5	0.73	2.77	21	35	21
None (0 kWh/m3)	2.5	0.73	1.77	19	27	14
Low (5 kWh/m3)	3.6	0.8	2.8	25	40	26
Medium (80 kWh/m3)	2.5	1.01	1.49	ND	7	4
High (160 kWh/m3)	1.8	0.82	0.98	ND	2	2
Coagulation	2.1	0.35	1.75	14	13	6
Enhanced Coagulation	1.5	0.19	2.77	4	5	4

The following Figures 3 and 4 help to compare TTHMFP with DOC concentration. In these figures, the expected increase in TTHMFP with increased DOC concentrations can be seen in the results for the photocatalysis treated samples. However, the graphs also show the interesting result of the low photocatalytic treatment level that had higher DOC and UV_{254} values than the Control and No UV treatment levels but produced a significantly larger TTHFP.

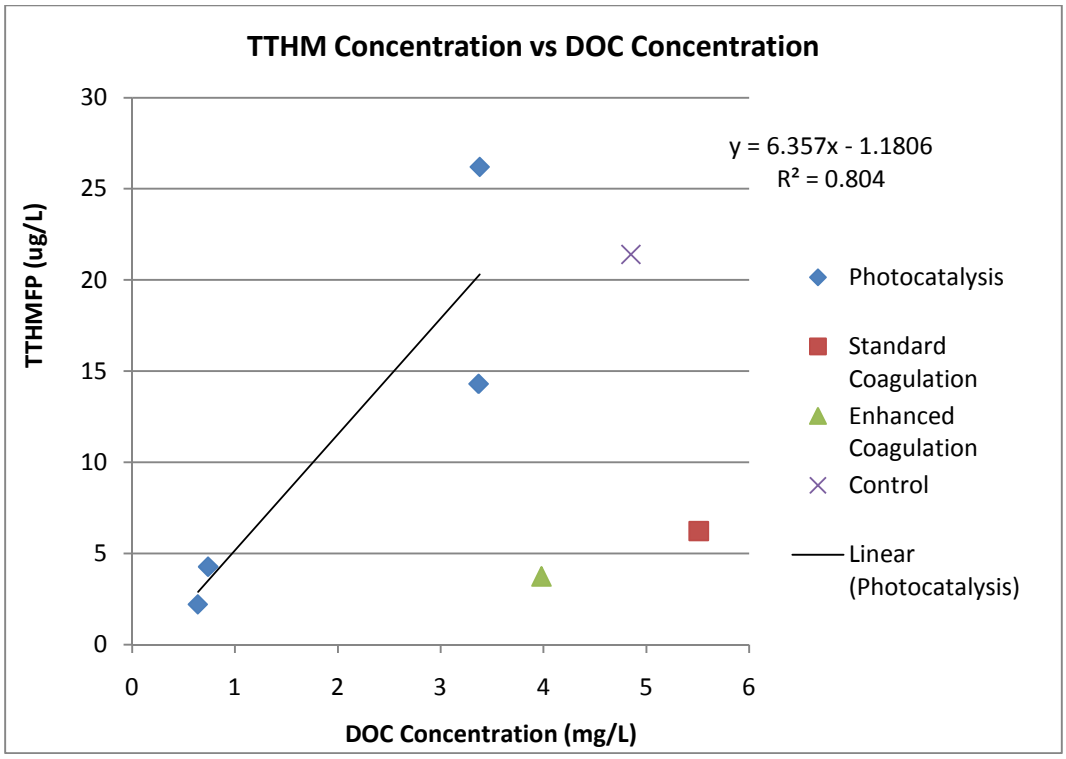

Figure 3: TTHMFP vs. DOC concentration for various treatment levels

The relationship between TTHMFP and the coagulation processes can also be seen in the graphs. These data points show that while the DOC concentrations were greater than those for all the samples treated with photocatalysis, the TTHMFP was significantly lower and closely resembled those of the Medium and High photocatalytic treatment levels.

To help analyze TTHM formation, a plot of the specific TTHMFP (STTHMFP) for each treatment level was developed as shown in Figure 4. The STTHMFP is the TTHMFP normalized on a DOC basis and gives the amount of TTHMs formed per mg of DOC.

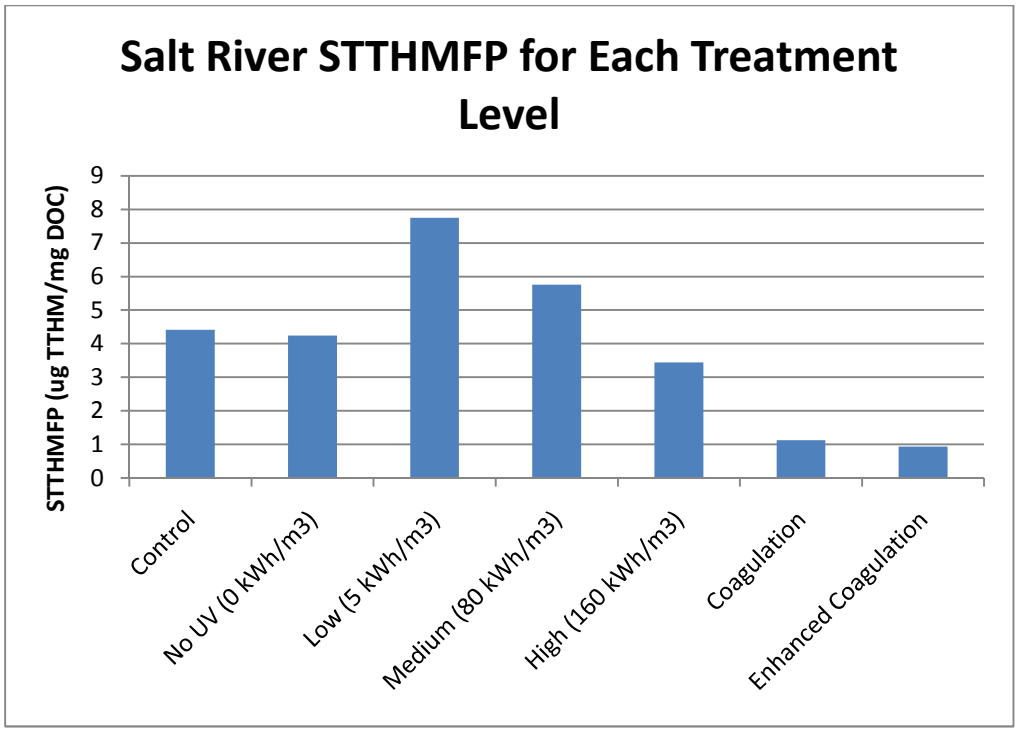

Figure 4: The Salt River specific TTMFP for each treatment level

The Low treatment level had the highest STTHMFP as also indicated by the spike in TTHM concentration found in Table 5. The spike in TTHMFP could be the result of incomplete oxidation of organic material that had adsorbed or was close to the TiO_2 surface during the No UV sampling. Work by Philippe et al., showed that for certain hydrophilic compounds chloroform concentration formation potentials actually increased after short retention times in a photocatalytic reactor (*27*). There have also been reports such as the work by Liu et al., which has stated that incomplete oxidation resulting in a shift towards LMM compounds can lead to increased DBPFP (*14*). Other sources have confirmed that in addition to the HMM humic acids, the LMM compounds may be

responsible for DBP formation as well but are only oxidized after the HMM compounds (*14, 28*).

Both coagulation treatments had the lowest STTHMFP despite their higher DOC concentrations than the samples treated with photocatalysis. Since this relationship is based on the ratio of TTHMFP to DOC concentration, the low STTHMFP is most likely due to the significantly lower TTHMFP concentrations. These results show that for organic content removal, photocatalysis is capable of completely mineralizing NOM at higher treatment level. In addition enhanced coagulation performed better than standard coagulation in terms of organic removal, but was still significantly higher than the photocatalysis samples. However, the enhanced coagulation formed less THMs than the photocatalysis samples. Therefore, treatment processes should be chosen based on treatment goals and influent water quality.

Chapter 5

ORGANIC MATTER CHARACTERIZATION AFTER PHOTOCATALYSIS AND THE IMPACT ON DISINFECTION BYPRODUCT FORMATION

INTRODUCTION

Disinfection byproducts (DBPs) are formed when a disinfectant reacts with organic matter. Formation and speciation of DBPs are highly dependent on a number of factors, including the disinfectant, dose of disinfect, amount of organic matter present, type of organic matter present, other compounds in the water, and other water quality parameters. For example, the trihalomethanes and haloacetic acids are the two types of organic DBPs regulated by the USEPA; however, there are more that are currently unregulated. These other DBPs include the haloacetonitriles that are formed from chlorine; aldehydes that can be formed from chlorine or ozone; aldoketoacids and carboxylic acids that are formed from ozone; oxyhalides that are formed by chlorine dioxide; and nitrosamines and cyanogens halides that are formed by chloramines (*10*). Some of these unregulated DBPs are potentially more hazardous and pose an ever greater health risk, especially brominated DBPs (*13*).

Speciation and concentration of DBPs formed during the disinfection process is a direct result of the composition and amount of organic matter available for oxidation. Many studies have been conducted to characterize organic matter and subsequent DBP formation in order to analyze, model and predict how DBPs will form during disinfection

processes. As a result, some common methods of characterization and classification were developed. These include the methods mentioned in Section 2.3.2 but primarily focus on separating organic matter into molecular size ranges through the use of membrane filters or high-performance liquid chromatography (HPLC).

For this experiment the characterization methods of high-performance size exclusion chromatography (HPSEC) and fluorescence spectroscopy excitation-emission matrices (EEMs) will be the primary focus and were used to analyze samples after photocatalysis and compared to the trihalomethane (THM) and haloacetic acid (HAA) formation resulting from each treatment level.

MATERIALS AND METHODS

Water samples for this experiment were collected from three different points within the treatment facility and distribution system, including after sedimentation, after granular activated carbon (GAC) adsorption, and at a “hot spot” within the distribution system where DBP concentrations were considerably high. The variety of sampling locations in the treatment process, allows for the analysis of photocatalysis implementation into existing treatment process. Photocatalysis will be examined for places it would be most effective in the treatment processes as well as the most feasible based on energy consumption. In addition, these sample locations were chosen because of their inherently different NOM compositions and concentrations resulting from previous treatment

processes. This will allow for the analysis and comparison of DBP formation resulting from water sources containing NOM with varying concentrations and compositions. After photocatalysis, samples were taken for general measurements and characterization analysis. Additional samples were then used for chlorination and THM and HAA formation analysis.

For this experiment all water sources were treated using the Photo-Cat Lab® from Purifics® (London, ON, Canada). The same methods described in Chapter 3 for the treatment using the PhotoCAT®, general measurements and chlorination for DBP formation are used for this experiment as well. However, in these experiments THM and HAA samples were taken at 15 min, 1 hour, 2 hours, 6 hours and 24 hours. These samples were preserved and analyzed by the Scottsdale Water Campus.

Organic Matter Composition and Characteristic Analysis. In an effort to characterize the organic content of the samples, high-performance size exclusion chromatography (HPSEC) and fluorescence spectroscopy excitation-emission matrices (EEM) analyses were performed.

HP Size Exclusion Chromatography. The purpose of size exclusion chromatography is to separate molecules in a sample solution and create a molecular weight distribution of molecular compounds present. In essence, a sample is passed through the column and the

organic solutes enter the pores of the stationary media by molecular diffusion. Larger molecular weight molecules will pass through more quickly compared to the smaller molecular weight particles that are slowed do to their diffusion into the pores.

The molecular weight distribution is based on size and the time at which they exit the column. Using a mathematical relationship between elements of known molecular size and time, the amount (as measured by DOC response) and molecular weight of the unknown molecules in the sample can be determined. High performance liquid chromatography (HPLC) was performed with a Waters Alliance 2695 Separations Module (Milford, MA) with a TSK-50S column and Toyopearl HW-50S resin (Japan). The HPLC was connected to an on-line modified Sievers 800 Turbo TOC Analyzer (GE Analytical Instruments, Boulder, CO). The eluent was a phosphate buffer (0.0024M NaH_2PO_4 + 0.0016 M Na_2HPO_4 + 0.025 M Na_2SO_4, pH = 6.8) with a conductivity of 4.57 mS, ionic strength of 0.1 M, and a flow rate of 1 mL/min. Prior to analysis, 5 mL of the samples were to be filtered with glass fiber filters (0.45 µm) and conductivity was adjusted to 4.57 mS using a 40-times concentrated eluent solution. The injection volume of the samples was 1 mL with a total analysis time of 100 min. To convert he retention time to molecular weight, seven polyethylene glycol (PEG) standards were used for calibration.

Fluorescence Spectroscopy Excitation-Emission Matrices (EEM). For the fluorescence spectroscopy and an excitation-emission

matrix (EEM) analysis were used to analyze samples. The samples were placed in a four-sided quartz cuvette that was acid washed prior to use. No adjustments were made for DOC or ionic strength for any of the samples. During analysis, a range of wavelengths were then passed through the sample to excite the electrons in the molecules, causing them to emit light of lower energy and higher wavelengths. These emitted wavelengths along with the fluorescent intensities were then recorded. The excitation wavelengths ranged from 200 to 400 nm and the emission wavelengths ranged from 280 to 550 nm. Blanks using nano-pure water were also analyzed so that the background fluorescence could be subtracted from the sample results. Data output from the machine was analyzed using a Matlab program developed by David Ladner, a post-doctorate at and was primarily used for graphing purposes to qualitatively analyze compositional shifts in samples.

Data responses were classified according to the methods described in Chen et al. (*29*). In this method the EEM graph was delineated into five regions based on the fluorescence of specific compounds, dissolved organic matter (DOM) fractions, and marine or fresh waters as shown in Figure 5 (*29*). The five representative EEM regions were as follows: Region One – Aromatic Protein I; Region Two – Aromatic Protein II; Region Three – Fulvic Acid-Like; Region Four – Soluble Microbial Byproduct-Like; and Region Five – Humic Acid-Like.

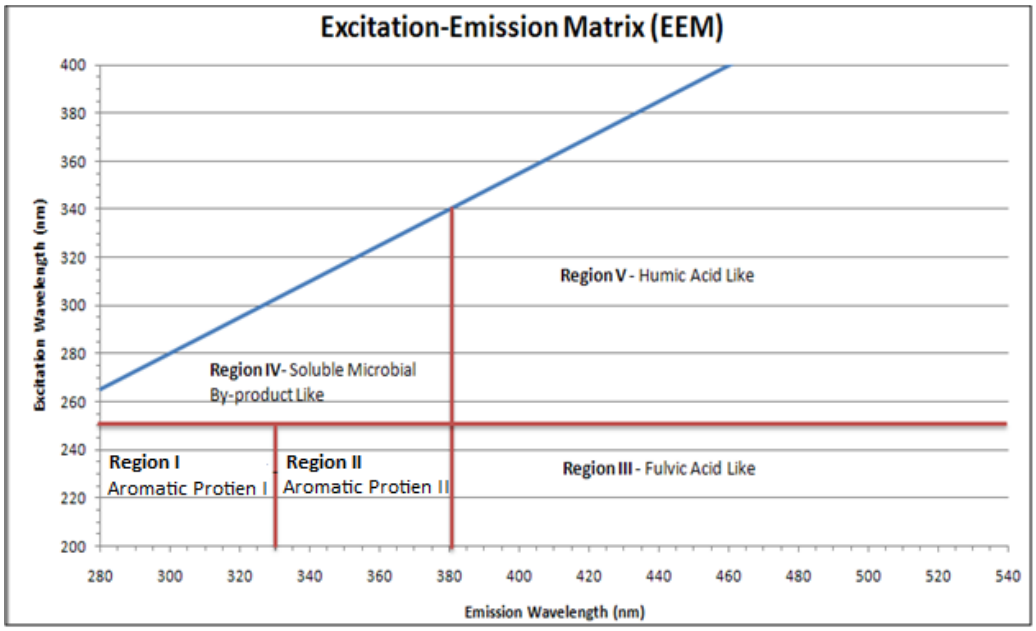

Figure 5: EEM regions (adapted from (*29*))

To aid in the comparison of the sample EEMs for this study, a qualitative method of representation was developed to assign a magnitude of response in each of the five regions. Magnitudes of response could be designated as Low (L), Medium (M), or High (H) based on the numerical responses. Consistent designation for each region was used for each water source by applying a fluorescence response range to each level, as shown below.

Response Magnitude	**Associated Value**
High (H)	80 +
Medium (M)	40 – 80
Low (L)	10 – 40
Zero (0)	No Response

RESULTS AND DISCUSSION

Since organic content can vary drastically among samples and can impact DBP formation, all three water sources were analyzed for their organic content as well as DBP formation. The primary focus will be amount of NOM present as measured by DOC and UV_{254}, composition and characterization, and THM and HAA formation potential.

General Measurements. The primary general measurements made for the settled water samples including UV_{254} absorbency, dissolved organic carbon (DOC), and total dissolved nitrogen (TDN) are shown in Figures 6 and 7. As mentioned DOC and UV_{254} are measurements of organic content in samples. Looking at the figures below, the most apparent trend is the variation in organic content of the three water sources used for this experiment. Even during photocatalytic oxidation, there are still slight variations in organic content. The control sample results show that the Settled Water and the Distribution Hot Spot samples had higher DOC values than those for the Post-GAC values. However, looking at the UV_{254} values, the Distribution Hot Spot had smaller values than the other two samples. For all three water sources the DOC concentrations reduced significantly from the Control to the No UV treatment level and the Low to Medium photocatalytic treatment level as a result of increased oxidation. The DOC percent removal for the Settled Water, Post-GAC, and Distribution Hot Spot at the No UV treatment levels

were 14%, 26%, and 48%, respectively, while those for the Medium treatment level were 83%, 89%, and 80% respectively.

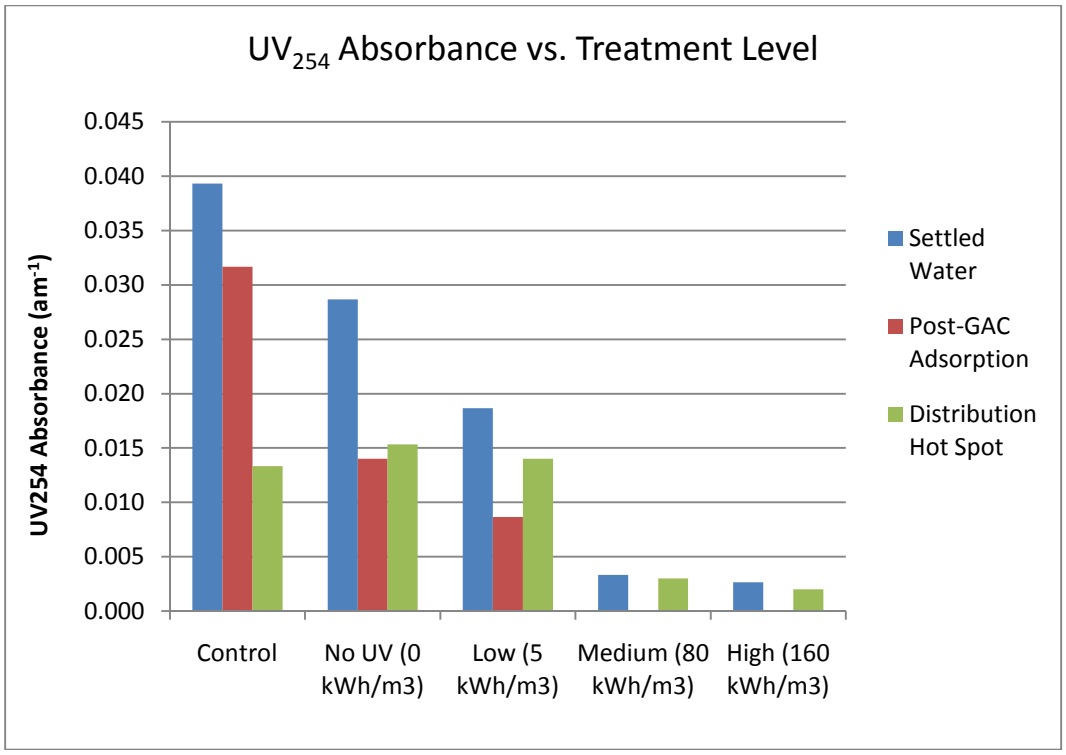

Figure 6: UV_{254} absorbance vs. treatment level for Settled Water, Post-GAC Adsorption, and Distribution Hot Spot

As mentioned in Chapter 4 the initial decrease in organic content as measured by DOC and UV_{254} is more likely due to adsorption of NOM onto the titanium dioxide, while during photocatalysis treatment NOM is being chemically oxidized by radical species in addition to adsorption on the TiO_2 surface.

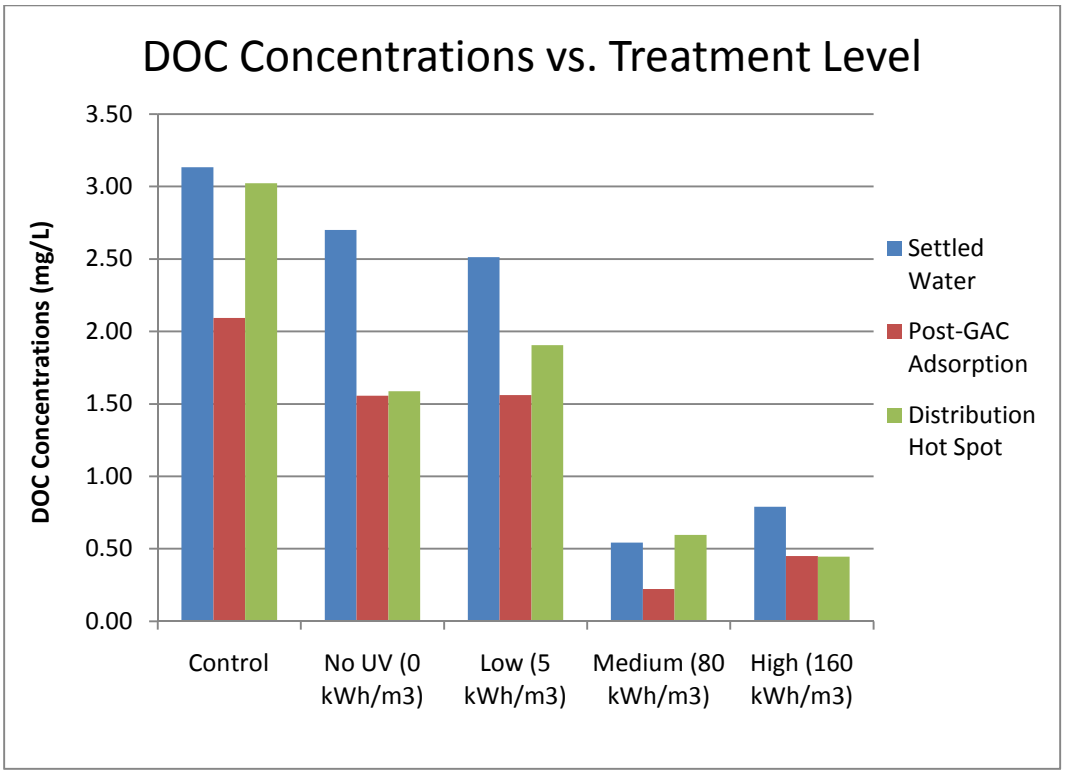

Figure 7: DOC concentration vs. treatment level for Settled Water, Post-GAC Adsorption, and Distribution Hot Spot

The TDN levels were fairly consistent for each of the water sources during photocatalysis, as shown in Figure 8. The ranges of concentrations for the Settled Water, Post-GAC, and Distribution Hot Spot were 0.47 - 0.57, 0.16 - 0.21, and 0.52 - 0.81 mg/L respectfully. Trends showed there was a small increase with increased photocatalytic treatment level, but this may be the result of variations in the machine's output readings. There is a definite trend, however, of the Settled Water and Distribution Hot Spot samples having larger TDN concentrations than the Post-GAC Adsorption samples. This may be a result of higher initial concentrations of organic nitrogen that is oxidized during photocatalysis.

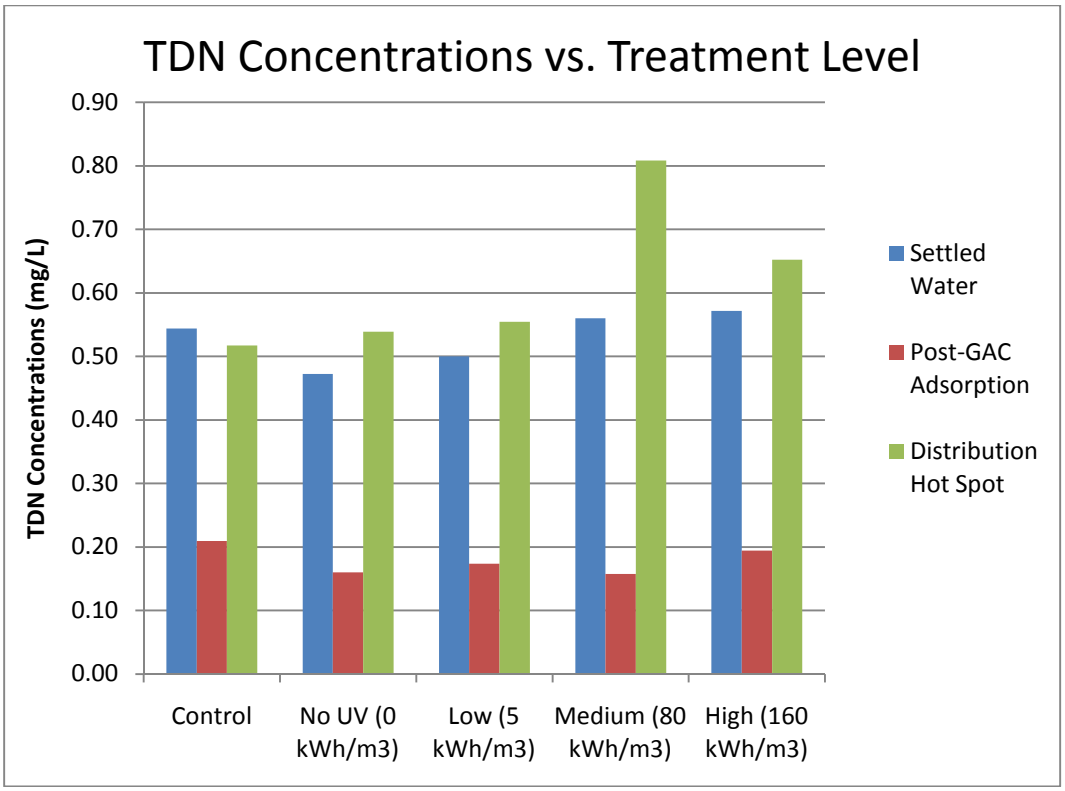

Figure 8: TDN concentration vs. treatment level for Settled Water, Post-GAC Adsorption, and Distribution Hot Spot

Size Exclusion Chromatography.

Settled Water. As previously stated, size exclusion chromatography results provide a molecular weight distribution of the sample and give insight into the classes of organic compounds that are present based on molecular weight ranges and corresponding DOC responses. For the Settled water, there was a peak in the 500-3,000 Da range for the Control, No UV, and Low treatment levels with the magnitude of these DOC peaks decreasing from 0.6 to 0.45 with increased treatment as indicated by the arrow in Figure 9.

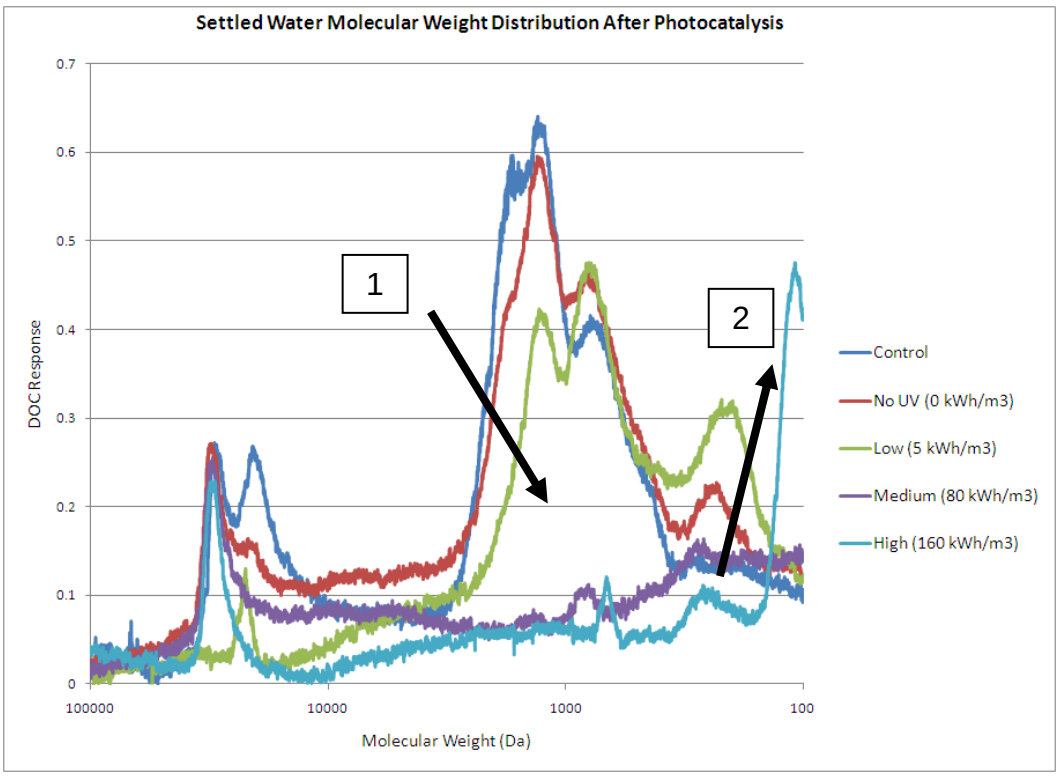

Figure 9: Settled Water Molecular Weight Distribution after Photocatalysis

These peaks were reduced at the Medium and High photocatalytic treatment levels as indicated by the relatively flat line. At these treatment levels there is a shift towards increasingly lower molecular mass (LMM) compounds as indicated by the second arrow on the graph. In this LMM range there is also an individual peak for the Low treatment level around 200-300 Da. On the other end of the graphs all treatment levels saw a DOC peak in the 20,000 to 50,000 Da range, which consists of higher molecular mass (HMM) molecules. The percentages of the total areas under the individual curves based on specified molecular weight ranges are summarized in Table 6.

Table 6

Percentage of Total Areas for Molecular Weight Distribution Ranges for Settled Water

	Control	No UV (0kWh/m3)	Low (5kWh/m3)	Medium (80kWh/m3)	High (160kWh/m3)
50,000-100,000	4.8%	5.0%	2.7%	4.1%	5.0%
30,000-50,000	5.0%	6.5%	2.0%	5.6%	3.8%
10,000-30,000	12.1%	9.9%	2.9%	7.5%	3.4%
5000-10,000	1.4%	2.0%	1.0%	1.4%	0.4%
1,000-5,000	3.3%	3.2%	2.0%	0.9%	0.7%
500-1,000	0.6%	0.7%	0.7%	0.2%	0.1%
100-500	0.2%	0.3%	0.3%	0.2%	0.1%

As indicated in Table 6, all samples had a relatively large fraction of its molecular weights (MW) in the 10,000 to 30,000 Da range. During photocatalytic treatment there was an overall significant decrease in all MW ranges for the Low treatment level in almost all ranges except the 100 to 500 and 500 to 1,000 Da ranges, which saw slight increases. For the other treatment levels there appears to be fluctuations in each range. However, the areas decreased for all MW ranges with High photocatalytic treatment with the majority still remaining in the 10,000 to 50,000 range. These numbers reflect the trends seen in Figure 9.

Post-GAC Adsorption. The Post-GAC results were somewhat similar to the Settled Water results for the MW distribution. For the Control, No UV, and Low treatment levels there was a DOC peak in the 500 to 3,000 Da range that decreased in magnitude from 0.7 to 0.4 with

increased treatment while simultaneously shifting to the right towards LMMs as shown by the arrow on the graph.

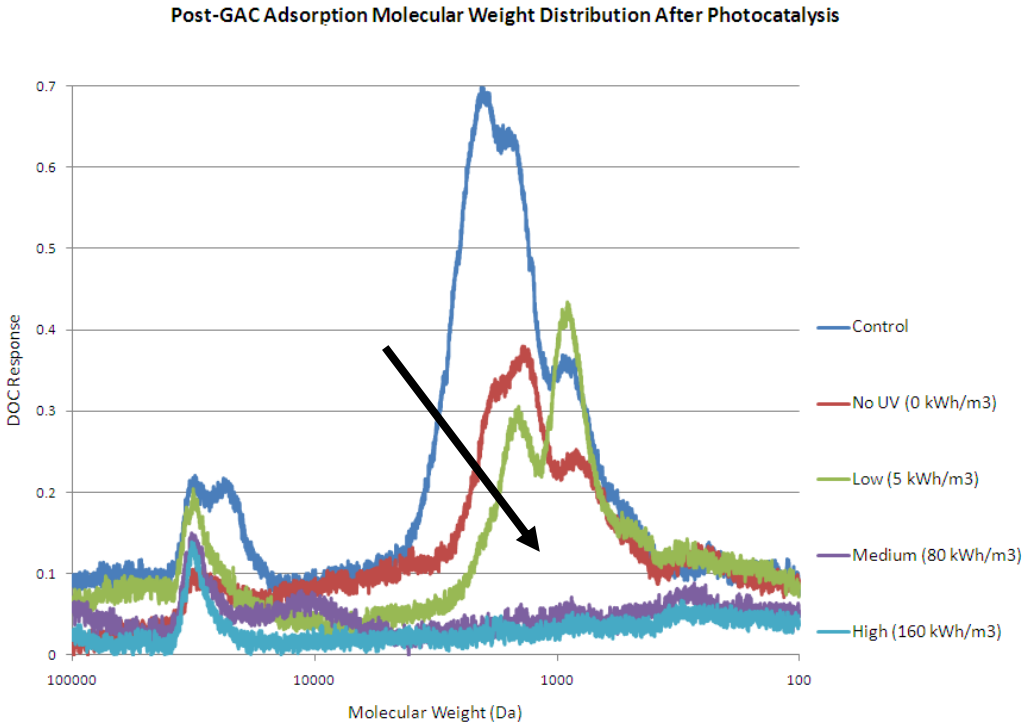

Figure 10: Post-GAC Adsorption Molecular Weight Distribution after Photocatalysis

However, the Low photocatalytic treatment sample did have an individual peak around the 1,000 Da mark. These peaks were absent in the Medium and High photocatalytic treatment samples as indicated by the relatively flat lines which appear to increase slightly towards the LMMs. As with the Settled Water there was a peak for all samples at the 30,000 mark, whose magnitudes appear to decrease with increased photocatalytic treatment. These results are illustrated in Figure 10 above.

The percentages of total areas under the MW distribution curves for specified MW ranges of each sample are summarized in Table 7.

Table 7

Percentage of Total Areas for Molecular Weight Distribution Ranges for Post-GAC Adsorption

	Control	No UV (0 kWh/m3)	Low (5 kWh/m3)	Medium (80 kWh/m3)	High (160 kWh/m3)
50,000-100,000	14.4%	3.3%	11.0%	6.3%	2.6%
30,000-50,000	7.6%	3.0%	6.5%	3.5%	2.5%
10,000-30,000	9.0%	4.8%	5.0%	3.9%	2.0%
5000-10,000	1.5%	1.4%	0.6%	0.7%	0.3%
1,000-5,000	4.2%	2.2%	1.3%	0.4%	0.3%
500-1,000	0.4%	0.3%	0.4%	0.1%	0.1%
100-500	0.1%	0.1%	0.1%	0.1%	0.1%

Unlike the Settled Water control sample, the Post-GAC control sample had a large portion of its MWs in the higher 50,000 to 100,000 Da range. However, the percentages for all ranges decreased with increased photocatalysis and saw less fluctuation than the Settled Water samples. At the Low treatment levels there was an interesting increase in the HMM (> 30,000) and LMM (< 1,000) as shown in the graph , while at the same time a slight decrease in the moderate molecular mass (MMM) ranges of 1,000 to 5,000 and 5,000 to 10,000 Da that can also be seen on the graph.

Distribution Hot Spot. The MW distribution results from the SEC for the Distribution Hot Spot were different than those for the previous two water sources. The most noticeable difference is the decrease in the DOC response magnitude and the less noticeable shift to smaller molecular weights as shown in Figure 11.

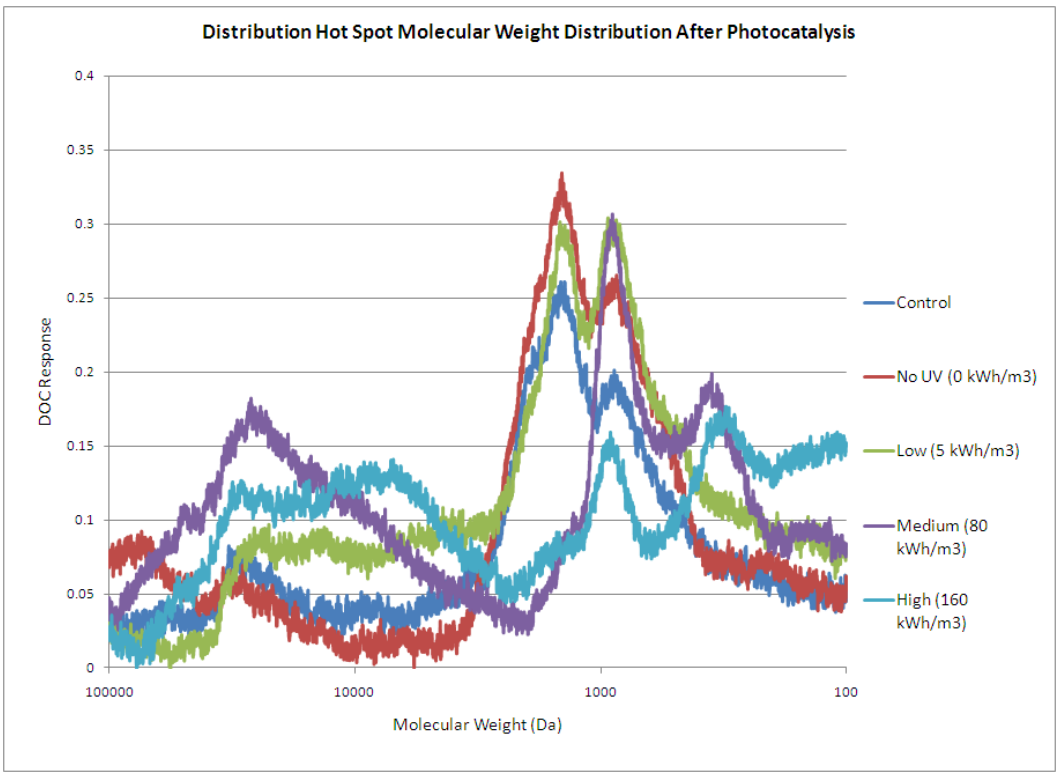

Figure 11: Distribution Hot Spot Molecular Weight Distribution after Photocatalysis

There is still a peak for the Control, No UV, and Low treatment levels in the 500 to 3,000 range; however, the magnitude is much less at 0.3 and there is not a noticeable decrease and shift with increased treatment. In fact, the Medium treatment level also has an individual DOC spike along with the Low treatment level spike at the 1,000 Da mark. The curve for the High treatment level appears to be increasing with decreasing molecular mass.

To help analyze the results Table 8 summarizes the actual areas under the individual curves based on specified MW ranges.

Table 8

Percentage of Total Areas for Molecular Weight Distribution Ranges for Distribution Hot Spot

	Control	No UV (0kWh/m3)	Low (5kWh/m3)	Medium (80kWh/m3)	High (160kWh/m3)
50,000-100,000	5.2%	12.4%	2.9%	10.1%	3.9%
30,000-50,000	2.9%	3.4%	1.9%	7.9%	5.1%
10,000-30,000	3.6%	2.5%	5.5%	9.9%	7.7%
5000-10,000	0.6%	0.3%	1.4%	1.5%	2.1%
1,000-5,000	1.5%	1.5%	1.8%	0.7%	1.1%
500-1,000	0.3%	0.4%	0.4%	0.4%	0.2%
100-500	0.1%	0.1%	0.2%	0.2%	0.2%

According to Table 8, there is a large fraction of the MW that falls above 30,000 Da. However, the Low treatment level saw an increase in area for MW less than 10,000 Da, and had the largest areas in the 500 to 1,000 and 1,000 to 5,000 Da ranges. Unlike the previous two sources, there was no definitive decrease in areas with increased or High photocatalytic treatment.

The results from the SEC analysis support the results of previous studies published in the literature. According to multiple sources, photocatalysis with titanium dioxide preferentially removes the hydrophobic, HMM, compounds that are more humic like (*26, 27, 30*). These selective oxidation reactions involving the HMM compounds are primarily based on the compound's ability to adsorb to the surface of the titanium dioxide where the reactions take place. Titanium dioxide is positively charged at pH values greater than 6.3 and is more efficient at

removing the larger, negatively charged compounds than the anionic hydrophilic and neutral compounds (*27*). This has been demonstrated in the results with the shift from the HMM compounds to the LMM compounds or those less than 1,000 Da which occurs at the Low photocatalytic treatment level. After initial photocatalysis the HMM compounds are incompletely oxidized to form the hydrophilic, LMM byproducts (200 to 1,000 Da) causing an increase in this size fraction. This fraction, while less reactive with chlorine than the HMM, can still cause an increase in DBPFP (*14, 26*).

Excitation Emission Matrices. As indicated in Table 4-4 below the EEM results showed that as photocatalytic treatment increased the organic content shifted from the higher regions to lower regions while the general intensities decreased for each region. This represents a shift to smaller aromatic proteins with smaller MW as confirmed by the SEC results. Complete images for all EEMs can be found in the Appendix of this report.

Settled Water. For the Settled Water samples, the EEM results in Table 9 show that there was a significant decrease in the humic acid fraction as well as a moderate decrease for the soluble microbial by-product like HMM compounds after Low photocatalytic treatment.

Table 9

EEM Analysis for Settled Water

	I	II	III	IV	V
	Aromatic Proteins I	Aromatic Proteins II	Fulvic Acid Like	Soluble Microbial By-product Like	Humic Acid Like
Control	H	H	H	H	H
No UV (0 kWh/m3)	H	H	H	H	H
Low (5 kWh/m3)	H	H	H	M	L
Medium (80 kWh/m3)	H	H	M	M	L
High (160 kWh/m3)	M	M	L	L	L

The LMM compounds including the fulvic acid aromatic proteins' fluorescence responses eventually decreased with high photocatalytic treatment, but only after the apparent oxidation of the HMM compounds.

Post GAC Filtration Water. The EEM results for the Post-GAC filtration water had different results than the Settled Water due to the different organic matter composition of the control sample, which had a higher LMM, content as shown by the responses in the lower regions rather than higher responses in all regions, as shown in Figure 10. After filtration through the machine, represented by the No UV sample, the response decreased for all regions followed by a significant increase for the Low photocatalytic treatment level in the lower regions I through III that represent the aromatic proteins and fulvic acids.

Table 10

EEM Analysis for Post-GAC Adsorption

	I	II	III	IV	V
	Aromatic Proteins I	Aromatic Proteins II	Fulvic Acid Like	Soluble Microbial By-product Like	Humic Acid Like
Control	L	H	H	L	M
No UV (0 kWh/m3)	L	L	M	L	L
Low (5 kWh/m3)	H	H	H	H	L
Medium (80 kWh/m3)	L	L	0	L	0
High (160 kWh/m3)	0	0	0	0	0

The Medium and High photocatalytic treatment levels saw significant decreases in response magnitude with values approaching zero in all regions. This zero response could represent complete mineralization or nearly complete mineralization of organic content in samples.

Distribution Hot Spot Water. The EEM results for the Distribution Hot Spot showed a decrease across all regions but there was also a definite shift to the lower regions that would represent selective oxidation, as seen in the Settled Water Results, as indicated in Table 11.

Table 11

EEM Analysis for Distribution Hot Spot

	I	II	III	IV	V
	Aromatic Proteins I	Aromatic Proteins II	Fulvic Acid Like	Soluble Microbial By-product Like	Humic Acid Like
Control	L	M	H	L	M
No UV (0 kWh/m3)	L	L	M	L	L
Low (5 kWh/m3)	0	0	L	0	L
Medium (80 kWh/m3)	0	0	0	0	0
High (160 kWh/m3)	0	0	0	0	0

The EEM results show what was discussed in the SEC results section, which is that photocatalysis appears to selectively degrade the HMM compounds such as the humic acids. This can be seen in the initial decrease in region V for all samples.

Disinfection Byproduct Formation. The TTHM and HAA5 concentrations after 24-hour chlorination test, defined here as the TTHMFP and HAA5FP, as function of treatment level are shown in Figures 12 and 13 below. The TTHMFP for each water source saw an increase for the No UV and Low photocatalytic treatment levels while the Medium and High treatment levels were significantly lower, except for the case of the Distribution Hot Spot samples. Another important factor to note is that the TTHMFP and HAA5FP for the Distribution Hot Spot Control sample were taken at the time of sampling as a measure of

existing DBPs. These values were not subtracted out of the TTHMFP and HAA5FP since it was assumed that after treatment with photocatalysis these concentrations would be reduced to negligible levels. This is due the volatile nature of THMs, and that during the photocatalytic processes the turbulent water flow and air hammer, as well as any oxidation processes could have significantly reduced existing THM concentrations.

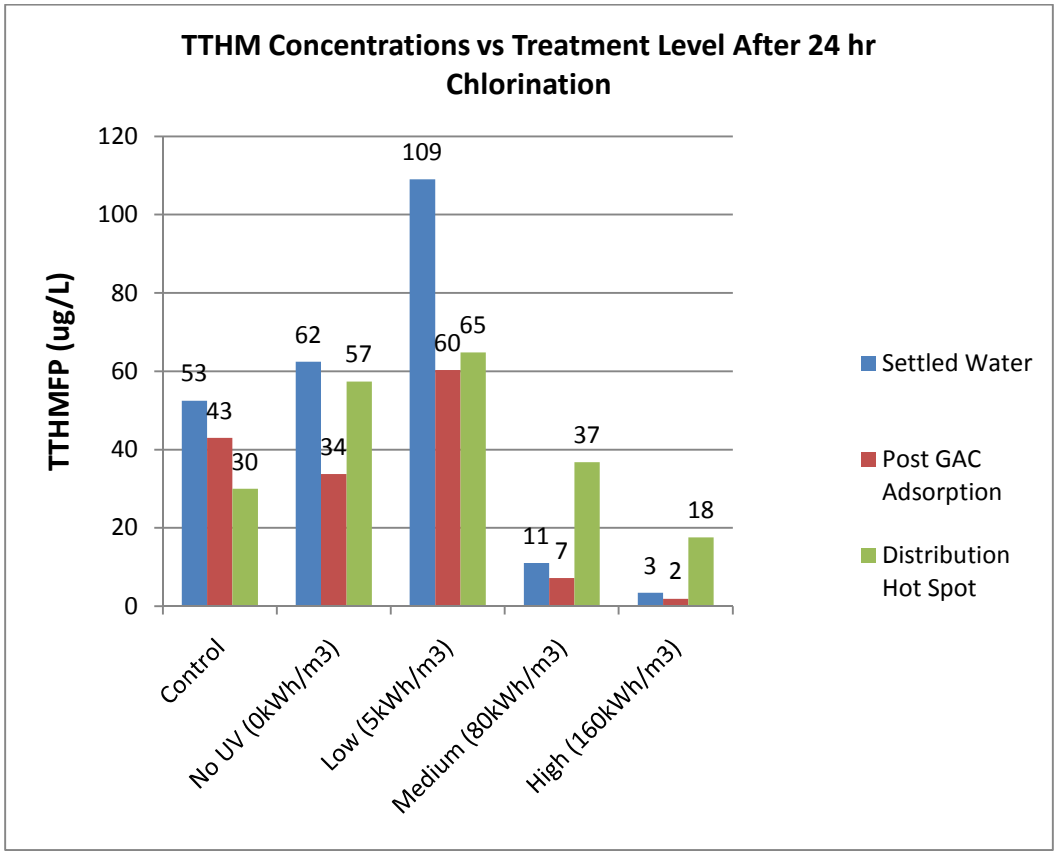

Figure 12: TTHMFP vs. Treatment Level after 24 Hour Chlorination

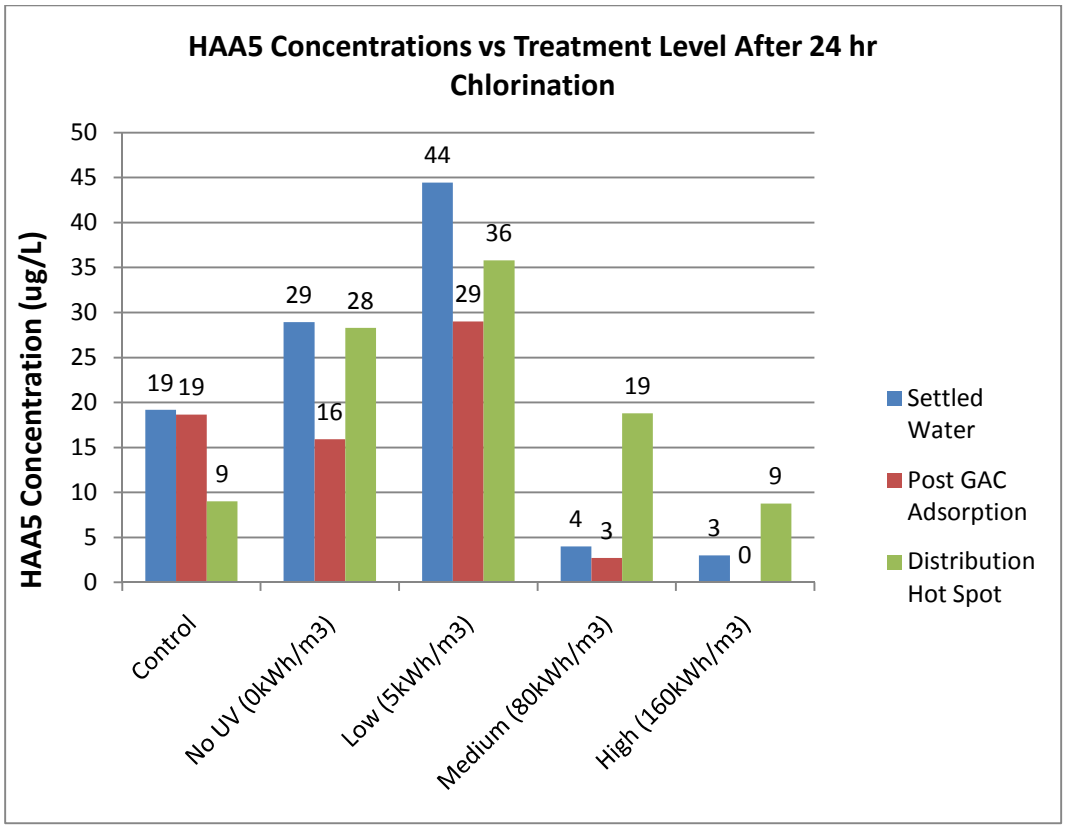

Figure 13: HAA5FP vs. treatment level after 24 hour chlorination

Similar to the TTHMFP, the HAA5FP saw an increase in the No UV and Low treatment levels while the Medium and High saw a significant reduction for the Settled Water and Post-GAC Filtration samples. In the case of the Distribution Hot Spot however, even after the High photocatalytic treatment levels the HAA5FP was equal to that of the Control sample.

The TTHMFP and HAA5FP were both normalized to their respective DOC concentrations to give the Specific TTHMFP and HAA5FP abbreviated as STTHMFP and SHAA5FP, as shown below in Figures 14 and 15.

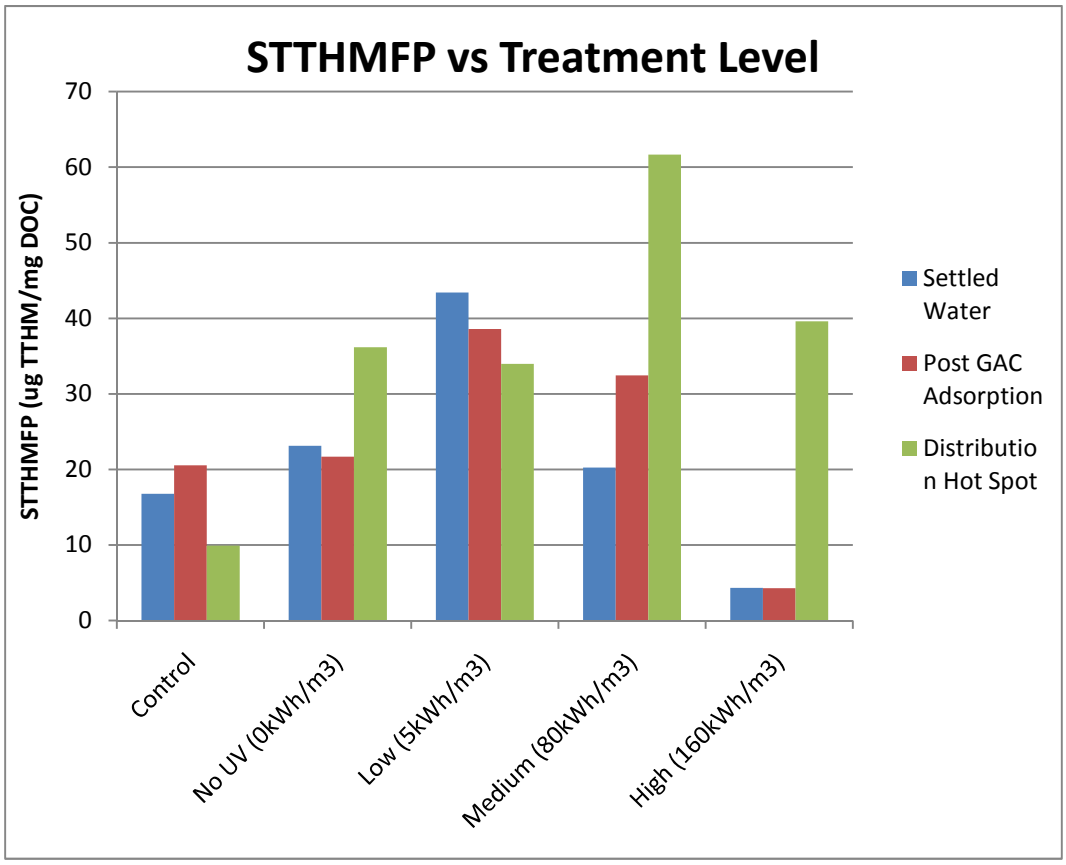

Figure 14: STTHMFP vs. treatment level after 24 hour chlorination

From Figure 14, it can be seen that there is an increase in STTHMFP with increased photocatalysis. These values are an indication of the potential for THM formation to occur. In this case there is a spike in the Low treatment level for the STTHMFP suggesting that this level will produce a larger amount of THMs. The large STTHMFP's for the Medium and High treatment levels is more a result of low (< 1 mg/L) DOC concentrations than high TTHMFP values. The same holds true for the SHAA5FP and the Distribution Hot Spot samples as shown below in Figure 15.

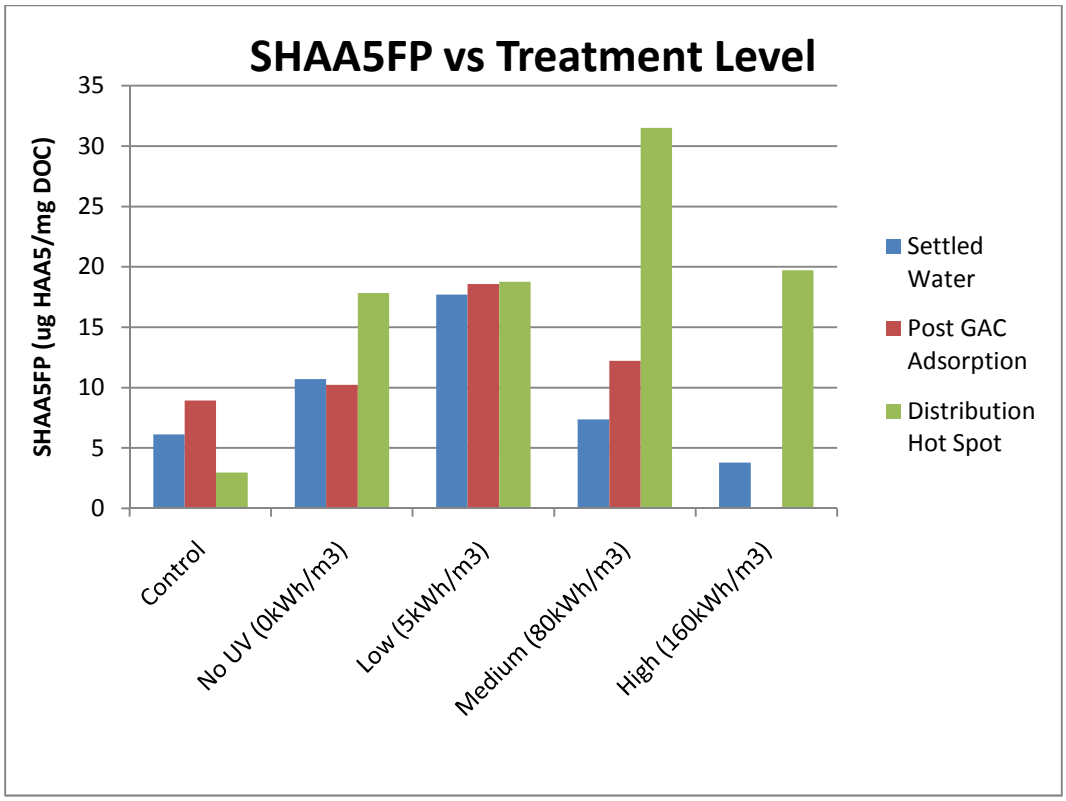

Figure 15: SHAA5FP vs. treatment level after 24 hour chlorination

When comparing the TTHMFP and HAA5FP to the SEC and EEM results there are some correlations that can be made but the large fluctuations between samples and source waters in the SEC results makes it hard to draw any concrete conclusions. However, it is evident that there is a spike in both TTHMFP and HAA5FP at the Low photocatalytic treatment level. To explain this using the SEC results, trends that were unique to this treatment level alone. While there were some variations, there seemed to be some consistency among the water sources that indicated at the Low treatment level there was a subtle increase in the LMM compounds in the 100 to 1,000 Da range. In some

cases, as for the Settled Water, this increase in the 100 to 1,000 Da range was also present for the No UV treatment level which corresponded to an increase in TTHMFP. In addition, the EEM results were compared with the TTHMFP and HAA5FP for any correlations. The EEM graphs showed that for the No UV and Low treatment levels the magnitude of response was High for regions I, II, and III representing the aromatic proteins and the fulvic acids. However, in the case of the Distribution Hot Spot at the Low treatment level, the magnitude of response was Low for regions III and V which represented the fulvic and humic like substances.

Both the TTMFP and HAA5FP experienced an increase at the Low Photocatalytic treatment level. As previously discussed, this could be the result of the large amount of incompletely oxidized LMM byproducts formed during the oxidation of the HMM compounds that adsorbed to the titanium dioxide surface. These LMM are slower to react with chlorine than the HMM, they can be just as big of a factor for DBP formation, especially in the absence of the HMM compounds in which they can potentially increase DBPFP (*14, 26, 31*).

Chapter 6

ANALYSIS OF PHOTOCATALYSIS BEFORE GRANUAL ACTIVATED CARBON ADSORPTION

INTRODUCTION

As stated in the USEPA's Stage 1 D/DBP Rule, treatment with granular activated carbon (GAC) filtration using an empty bed contact time (EBCT) of 10 min is one of the best available technologies for the removal of organics or disinfectant byproducts (DBPs) precursors.

However, seasonal shifts in organic content of source water can cause large problems for water treatment plants (WTPs) utilizing GAC contactors. This is the case for the City of Scottsdale, AZ Chaparral WTP that experiences significant increases in organic content during the summer months. The increased organic content is not being adequately removed by their conventional treatment process. As a result, the GAC contactors become saturated and need to be reactivated much more frequently than originally anticipated. This saturation of the GAC leads to decreased water quality and increased operation and maintenance costs.

In an effort to examine how photocatalysis could improve treatment processes, it was proposed that the study analyze the effect of implementing photocatalysis prior to the GAC contactors using the Chaparral WTP as a case study. The hypothesis of the study was that the photocatalysis would break down the HMM compounds allowing them to better adsorb to the GAC and improve the bed life of the contactors. To

model the full-sized GAC contactors at the plant, rapid small scale column testing (RSSCT) was used to analyze the contactors performance.

Small scale column testing has been used since the early 1980s to evaluate and estimate the performance of large contactors (5). In the mid 1980s, rapid small scale column testing was developed to predict the breakthrough behavior of full scaled contactors or larger columns based on the result of the scaled-down, smaller columns. The basic principle behind RSSCTs was discussed in Section 2.4 under Granular Activated Carbon. This experiment will treat water samples to practical levels of photocatalysis and run them through the small scaled columns to predict the breakthrough behavior and the corresponding DBP formation after chlorination.

MATERIALS AND METHODS

Water samples of 50 gallons were collecting from the City of Scottsdale, AZ Chaparral WTP using five 55 gallon plastic drums. Prior to sampling, the drums were washed and disinfected with chlorine. To ensure no residual, the chlorine solution was quenched with sodium thiosulfate and rinsed with de-ionized (DI) water. Due to the plant's operating schedule, samples had to be collected in advance in November of 2010 even though testing did not begin until mid-December 2010. Water quality measurements of DOC and UV_{254} were taken at the time of sampling and before experimentation began to quantify water quality degredation. To minimize water sample deterioration, mixing and aeration

was implemented using a commercially available submersible pump with plastic tubing and an air bubbler. The DOC measurement at the time of sampling was 2.02 mg/L and the average DOC measurement at the time of the experiment was 3.72 mg/L meaning there was a decrease in water quality as measured by an increase in DOC concentration of 1.70 mg/L. The 3.72 mg/L concentration was higher than the initial concentration but, still less than the 5 to 6 mg/L that the plant typically experiences during the summer months, and was therefore considered to have no significant impact on the experiment.

Photocatalytic Treatment with Purifics' PhotoCAT Lab. The 50-gallon water samples would be used for three treatment levels of photocatalysis using the Photo-Cat Lab® from Purifics® (London, ON, Canada) and then fed into the RSSCT GAC columns for filtration. Samples were treated to three different levels with photocatalysis including No UV, Low and Medium based on energy consumption of the machine as described in detail in Section 1.3. For this study the High photocatalysis treatment level was not included due to its high energy requirements. At this level it would be too costly to WTPs and because of the high level of oxidation at that treatment level there would be no need for GAC adsorption afterwards. Although it is still slightly energy intensive, the highest treatment from photocatalysis was the Medium treatment level.

Only two RSSCT columns could be operated at once, so the Control and No UV treatment levels were process first and stored in

separate, disinfected plastic drums. The drums were continuously mixed with a submersible pump and plastic tubing. After treatment with photocatalysis, the 50 gallon samples were passed through the two RSSCT columns starting with the Control and No UV samples followed by the Low and Medium samples.

Rapid Small Scale Column Testing (RSSCT) with GAC. In 2005, a study was performed by Paul Westerhoff and John Crittenden entitled "RSSCT Analysis for Scottsdale GAC Procurement" (32). The objective of the study was to analyze various types of GAC from different manufacturers for total organic carbon (TOC) and UV_{254} breakthrough data to enable the city to choose a GAC supplier for the treatment plant.

Table 12

Design and Operating Parameters for Full-Scale Contactor and RSSCT

Design Parameter	Units	Full-Scale	RSSCT
Particle Radius	cm	0.0513	0.0049
EBCT (Empty Bed Contact Time)	minutes	20	1.91
Loading Rate	gpm/ft^2 (m/hr)	4.3 (12)	3.0 (7.35)
GAC Contactor			
Length	ft	25	
Width	ft	50	
Surface Area	ft^2	1250	
RSSCT			
Column Diameter	cm		1.1
Bed Depth		10 ft	23.4 cm

As a source of consistency and comparison since the same water source was used, the RSSCT columns and operational parameters were conducted as described in the study. The primary design parameters adapted from the study are listed in Table 12 above (32).The GAC used for the RSSCTs and the Chaparral contactors was Filtrasorb 400, made from selected grades of bituminous coal, and manufactured by Calgon (Pittsburg, PA). To obtain the scaled down GAC particle diameter of 0.0049 cm, the GAC was initially pulverized and then grinded using a ceramic mortar and pestle. The GAC was then wet-sieved to obtain standard mesh 140 X170 sized particles. Grinded GAC had to be thoroughly rinsed with DI water to prevent clogging of the column and contamination. The columns were constructed based on the design in the previously mentioned study, as shown below (32).

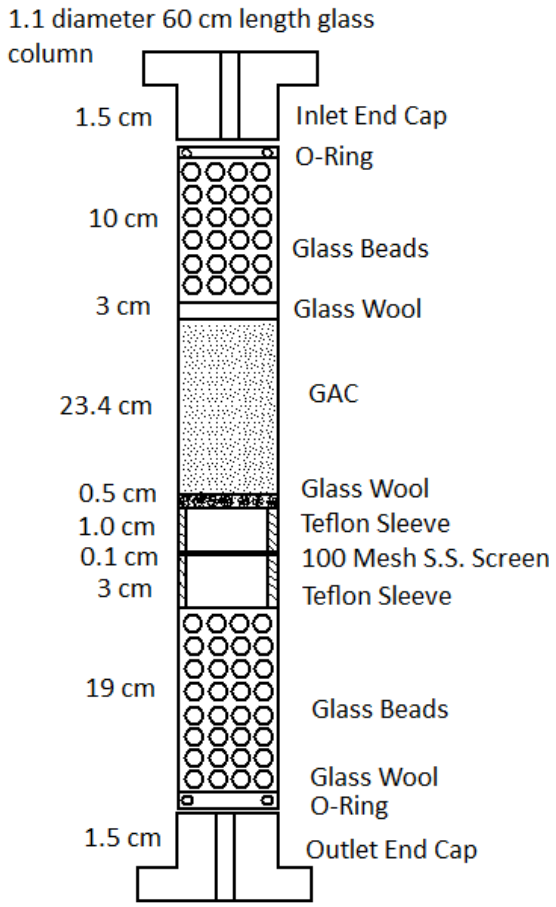

Figure 16: Schematic of GAC RSSCTs

Columns were assembled in completely saturated and pressurized conditions. During column packing the GAC was forced to settle and tapped to release any air that was trapped between particles and minimize pressure variations during operation.

Once the columns were set up and water was treated with photocatalysis, the samples were fed to the columns using peristaltic pumps. Samples for each treatment level were taken to represent various level of treatment using GAC adsorption. The times the samples were

taken were based on the normalized breakthrough curve for the UV_{254} absorbance as shown in Figure 17.

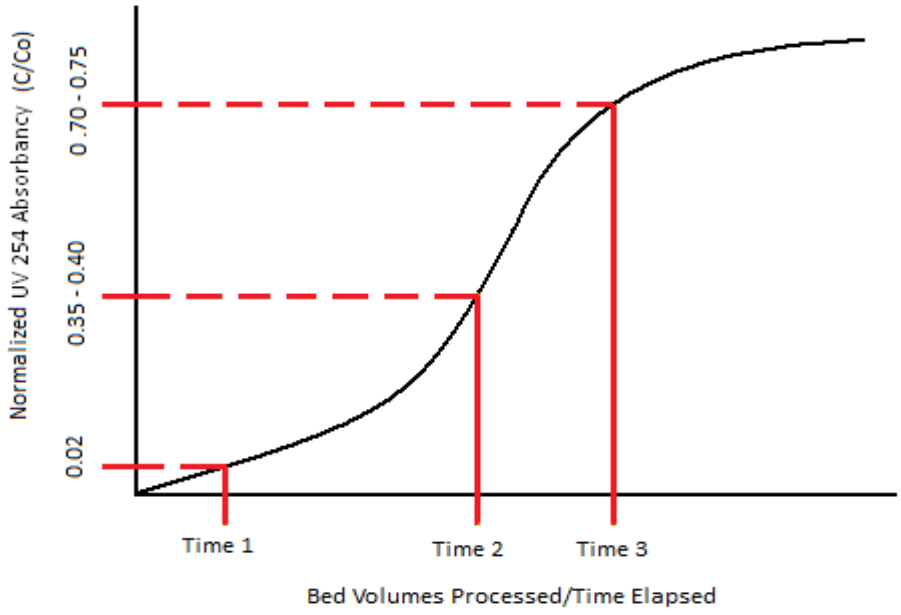

Figure 17: Breakthrough curves showing sample times after GAC adsorption

The times samples were taken after GAC adsorption began occurred when the ratio of UV_{254} to initial UV_{254} was approximately 2% (Time 1), 35-40% (Time 2), and 70-75% (Time 3). These results would allow for the comparison of DBP formation at different times of elapsed GAC adsorption. During the operation of the RSSCTs, samples for UV_{254} and DOC measurements were taken approximately every 6 to 8 hours. At the time of sampling, the flow rate was also checked, adjusted if necessary, and recorded to minimize variability in the flow and water volume processed.

RESULTS AND DISCUSSION

General Measurements. The primary, general measurements taken for each photocatalytic treatment level after the three GAC adsorption times are shown in Figures 18 and 19. Trends are similar to previous results, with DOC and UV_{254} values decreasing with increased photocatalytic oxidation and TDN concentrations increasing slightly.

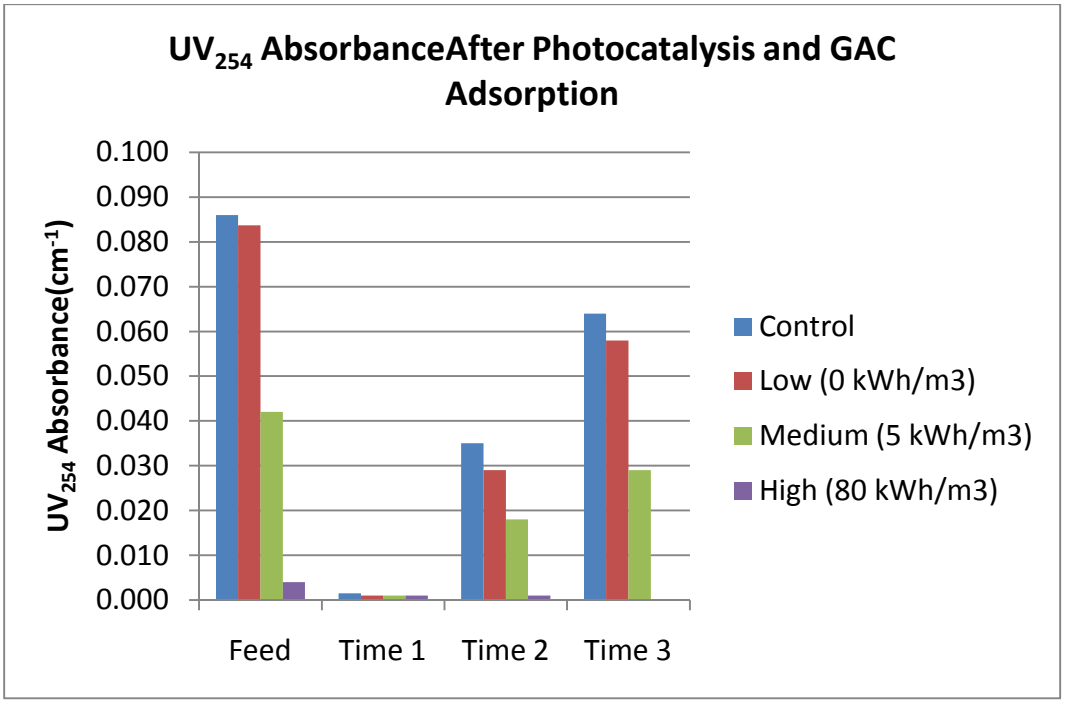

Figure 18: UV_{254} Absorbance after Photocatalysis and GAC Adsorption

The results for the UV_{254} values show that after initial GAC adsorption, there was a 98% removal rate for the Control, No UV, and Low treatment levels. The percent removal for the Medium treatment level was significantly lower at 75% due to the very small and almost negligible UV_{254} measurement of the feed water. As shown in the following results,

the Medium treatment level produced almost negligible DOC, UV_{254}, DBP formation that the primary focus will be on the Control, No UV, and Low treatment levels. At Time 2, removal decreased to about 60% for UV_{254} reduction, and by Time 3 the removal was about 30%, indicating a decline in effluent water quality and saturation of GAC.

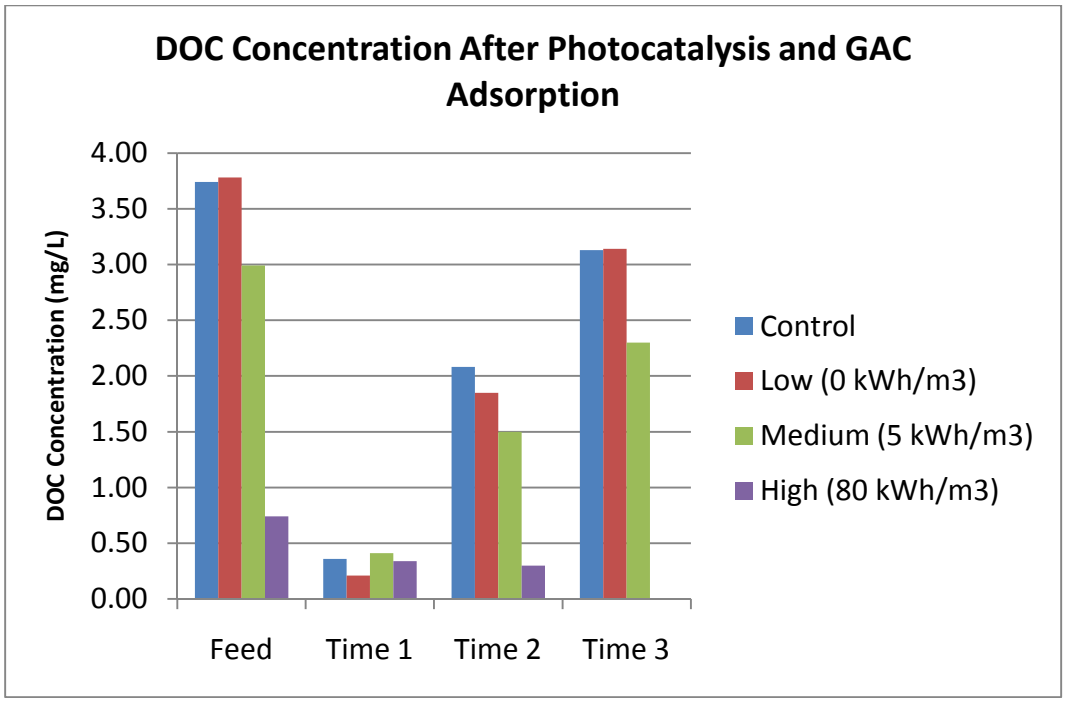

Figure 19: DOC Concentration after Photocatalysis and GAC Adsorption

The DOC had a similar trend as that found for the UV_{254} measurements. After GAC adsorption, at Time 1 removal rates were about 90%, 50% at Time 2, and 20% at Time 3, as shown in Figure 19 above. The TDN concentrations for increased photocatalysis actually increased but was somewhat removed through GAC adsorption as shown in Figure 20.

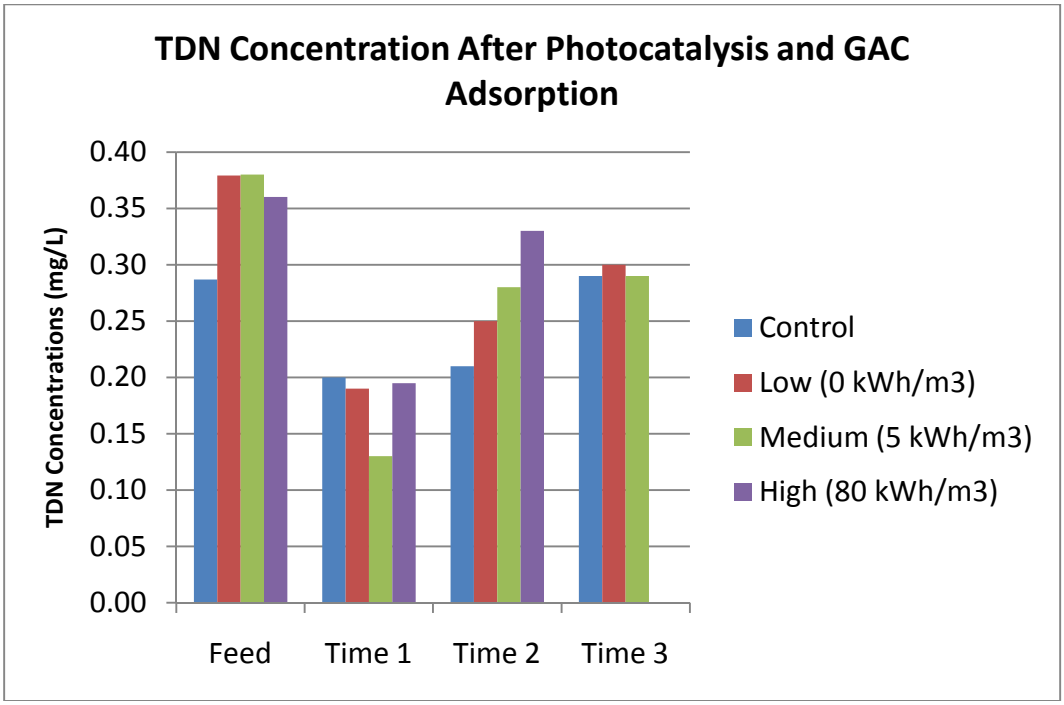

Figure 20: TDN Concentration after Photocatalysis and GAC Adsorption

The removal rate for TDN varied for each treatment level but in general was about 30 - 65% at Time 1, 25 - 35% at Time 2, and about 20% at Time 3. However, at Time 3, the control sample actually reached breakthrough with no removal.

Rapid Small Scale Column Test. After running the RSSCT, the UV_{254} and DOC data were plotted as a function of the bed volumes processed by the columns, which also correlates to the elapsed adsorption time. Both raw and normalized data were plotted to illustrate the results and breakthrough curves of the columns, as shown in Figures 21-24.

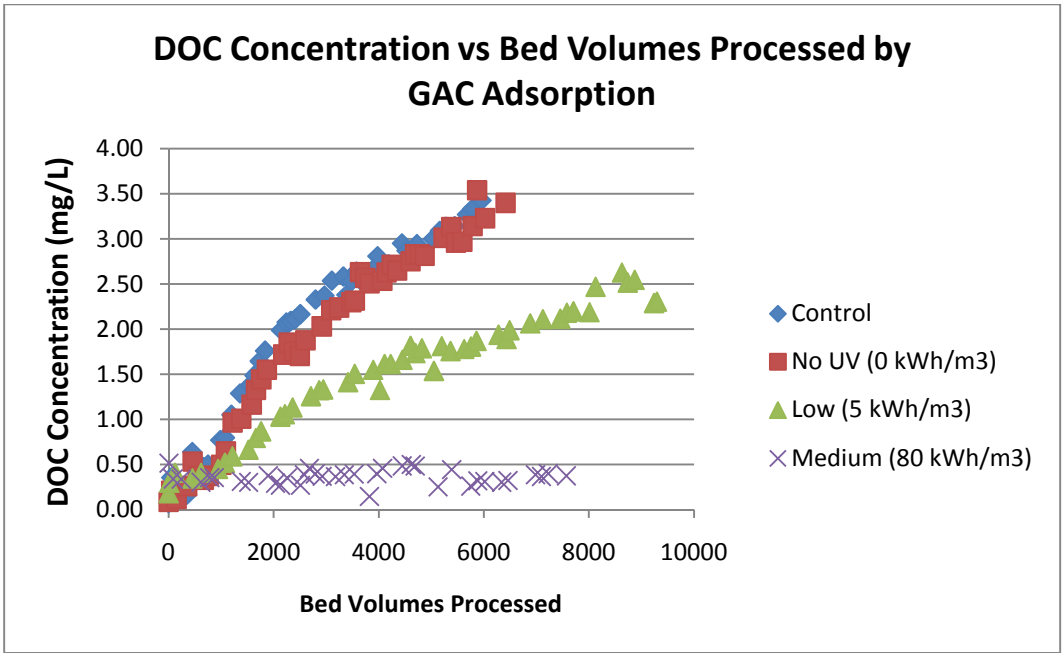

Figure 21: DOC Concentration vs. Bed Volumes Processed by GAC Filtration. Influent concentrations can be found in Figure 19.

The graph above illustrates what that for increased photocatalytic oxidation there was a decrease in DOC concentrations, with negligible concentrations at the Medium treatment level.

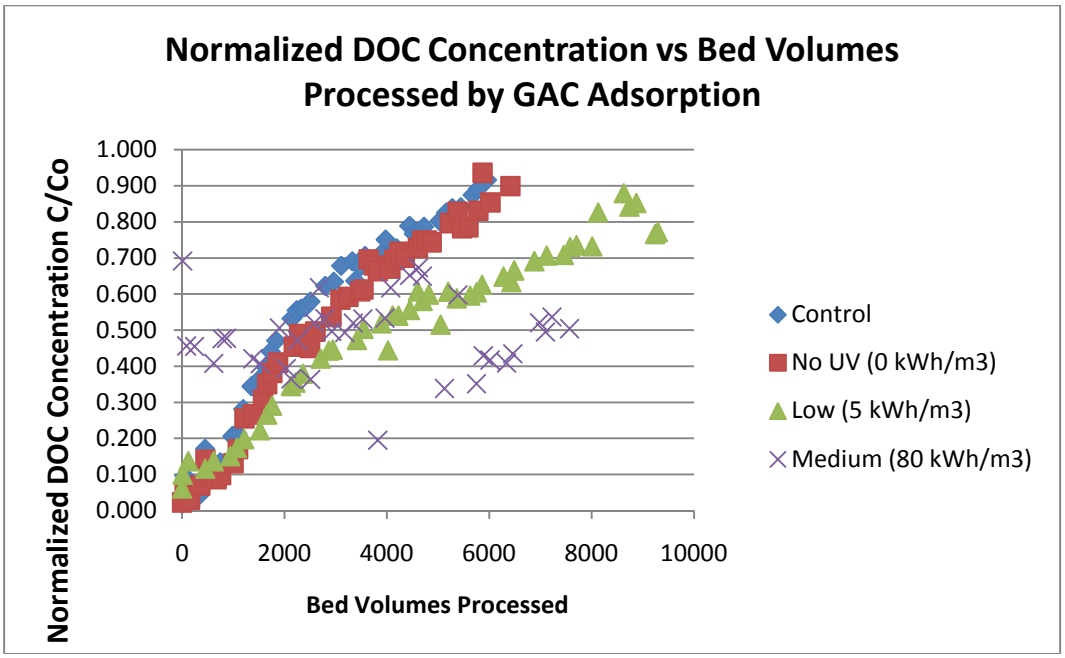

Figure 22: Normalized DOC Concentration vs. Bed Volumes Processed by GAC Filtration.

The normalized graph above plots the ratio of the effluent concentration to influent concentration and examines the breakthrough behavior of each column. As shown, the Control, No UV, and Low treatment levels reach approximately 90% breakthrough by the end of the test. However, the times at which they reached 90% increased with increased photocatalytic oxidation suggesting an increase in bed life.

The UV_{254} results were again similar to the DOC results in that values decreased with increased photocatalytic oxidation and the Medium treatment levels had negligible measurements for effluent quality. This is to be expected since there is such a high level of treatment in conjunction with GAC adsorption and there should be no or a very limited amount of

organics passing through the columns. These results also indicate increased bed life.

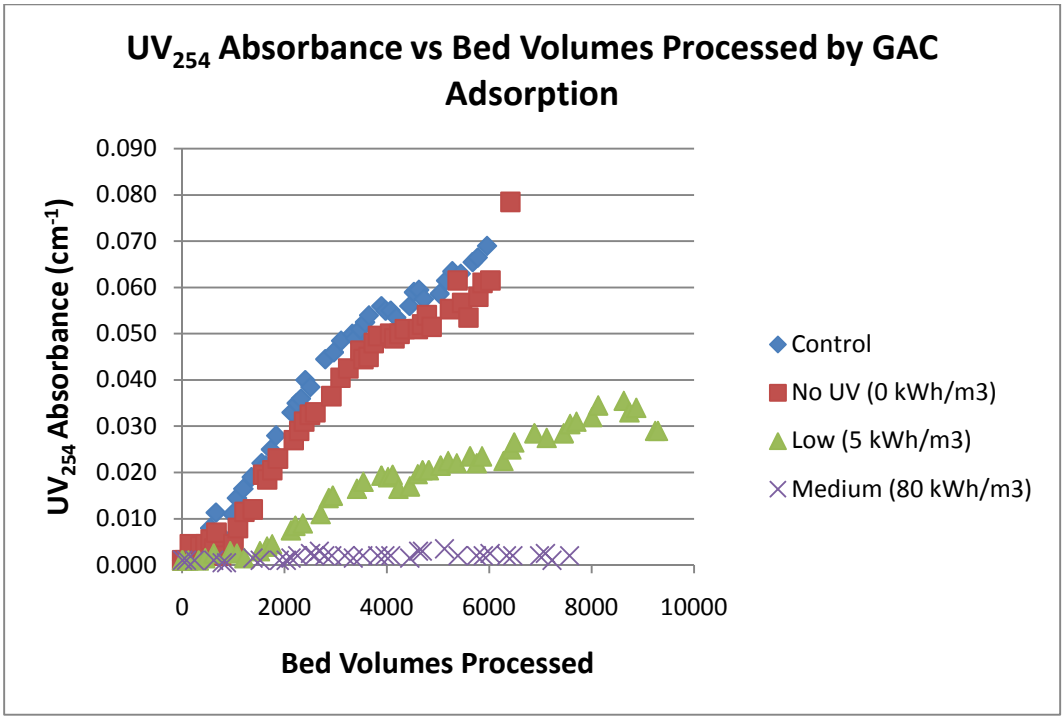

Figure 23: UV_{254} Absorbance vs. Bed Volumes Processed by GAC Filtration. Influent concentrations can be found in Figure 18.

The normalized UV_{254} graph showed that the Control, No UV, and Low treatment levels experienced approximately 80% breakthrough by the end of the tests. As with the DOC results, the Medium treatment level measurements were below detection level of the instruments used, and led to the variable concentrations ratios as shown. For example the data points are more scattered indicating a variation in data that could be the result of very small measurements or the variation in measurements of the machine.

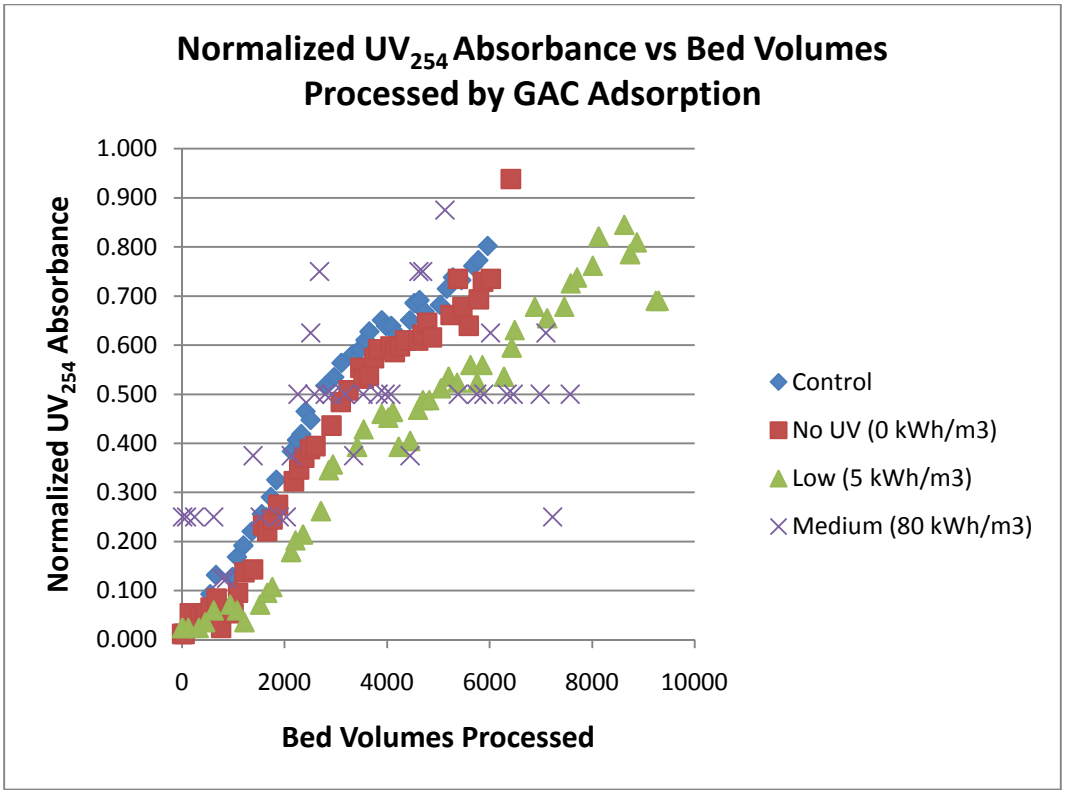

Figure 24: Normalized UV_{254} Absorbance vs. Bed Volumes Processed by GAC Filtration

The plots for total dissolved nitrogen (TDN) concentration as a function of bed volumes processed are shown in Figures 25 and 26. The first graph shows that TDN concentrations increased with increased photocatalytic oxidation and appeared to level out over time as they approached influent concentrations as shown in the normalized graph as well. The normalized graph show that the Control and Medium Treatment level samples reached breakthrough at about 4000 bed volumes when influent concentrations were equal to effluent concentrations. The No UV and Low treatment levels approach break through but only achieve about 90 - 95% during testing.

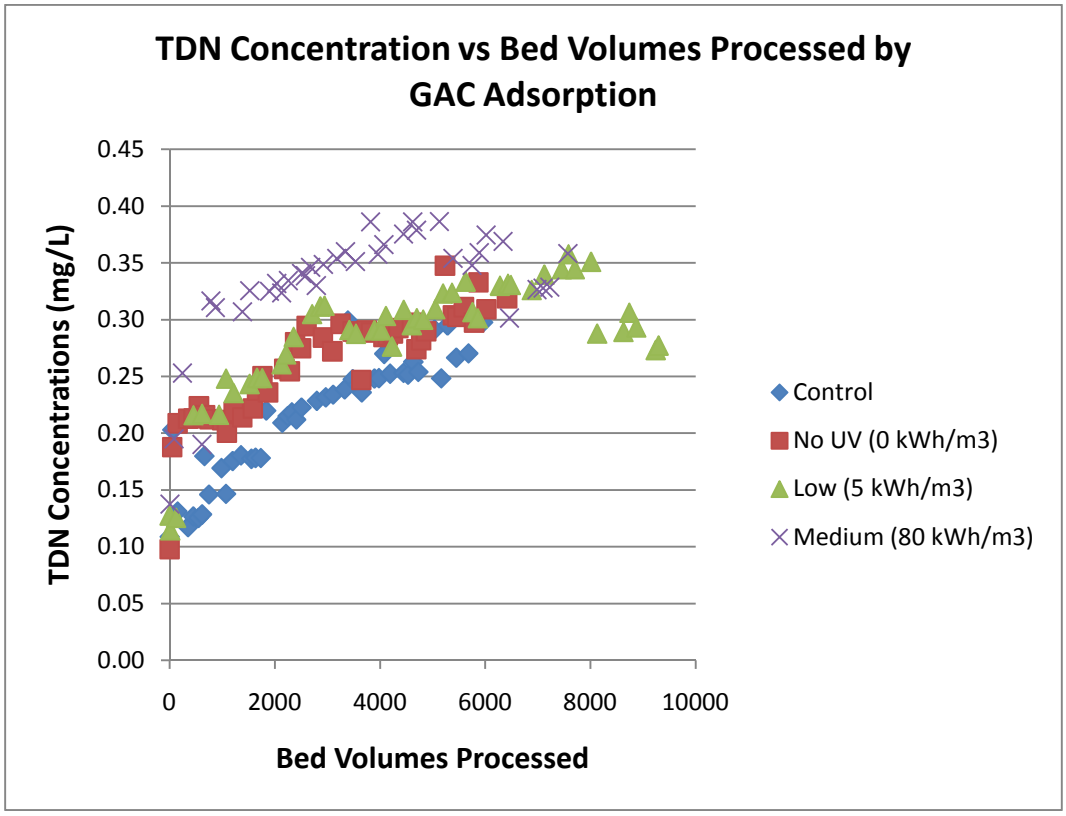

Figure 25: TDN Concentration vs. Bed Volumes Processed by GAC Filtration. Influent concentrations can be found in Figure 20.

The normalized graph show that the Control and Medium Treatment level samples reached breakthrough at about 4000 bed volumes when influent concentrations were equal to effluent concentrations. The No UV and Low treatment levels approach break through but only achieve about 90 - 95% during testing. The normalized results help show the breakthrough points of samples while the raw data points allow for the visualization of actual concentrations.

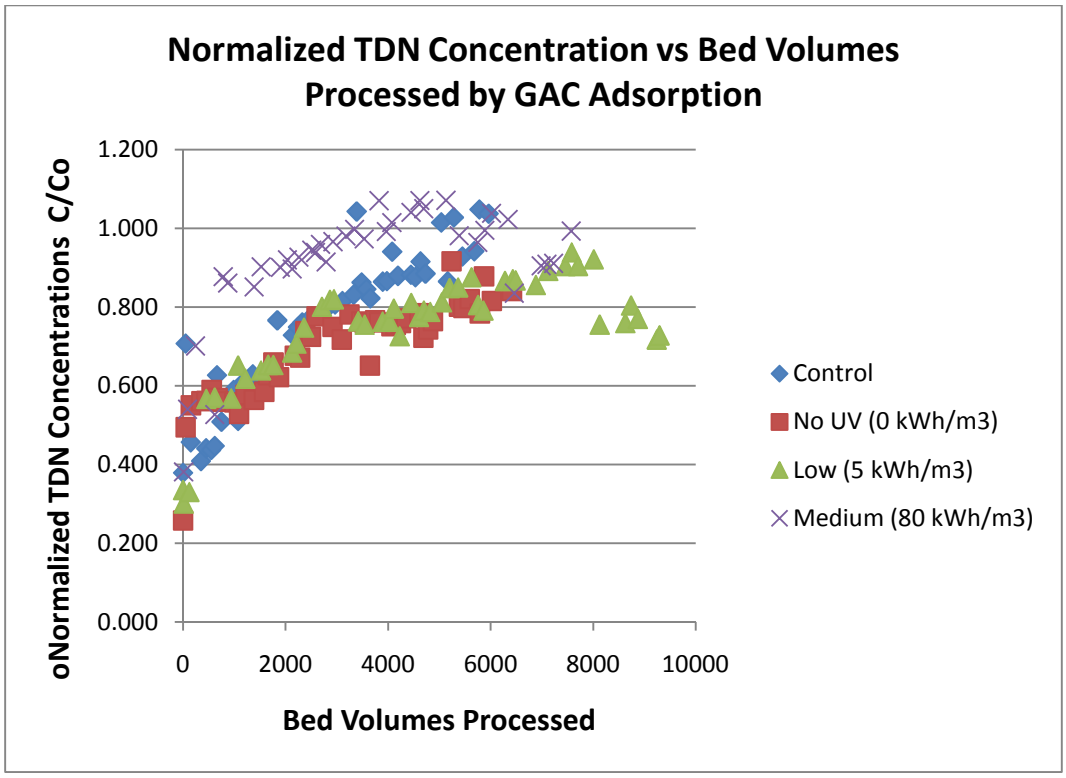

Figure 26: Normalized TDN Concentration vs. Bed Volumes Processed by GAC Filtration

Disinfection Byproduct Formation. In addition to seeing the removal of organic material through decreased UV_{254} absorbance and DOC concentration, there was also significant reduction in TTHMFP with the Medium photocatalytic treatment level being near the detection limit as shown in Figure 27. The graph also shows a spike in TTHMFP at the Low catalytic treatment level, as in previous results. The TTHMFP also increased with increased GAC adsorption time due to the higher organic content (UV_{254} and DOC concentrations) in the effluent as shown in the general measurements' results section.

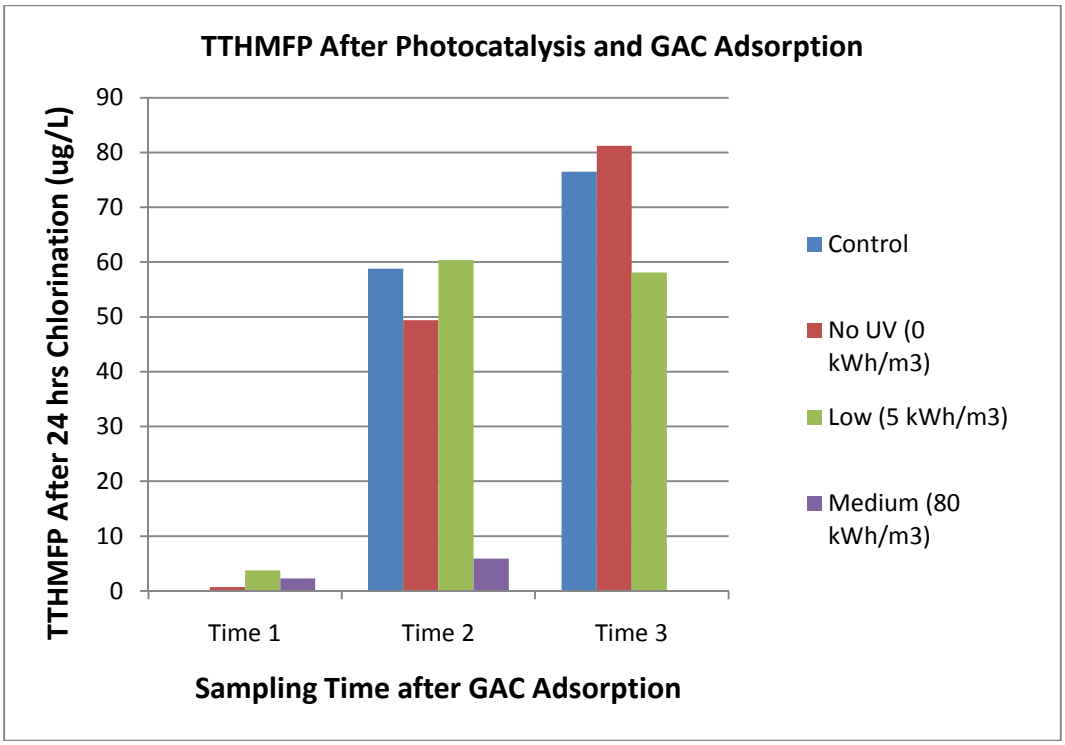

Figure 27: TTHMFP after Photocatalysis and GAC Adsorption

The HAA5FP results showed a clear increase at the Low treatment levels and a spike at the No UV treatment levels, while the Medium photocatalytic treatment level produced negligible HAA5 concentrations as shown in Figure 28. After sampling for TTHMFP, it become apparent that there was not enough sample volume left to measure HAA5FP for the Control and No UV Time 1 samples which is why there is no data for these samples on the graph.

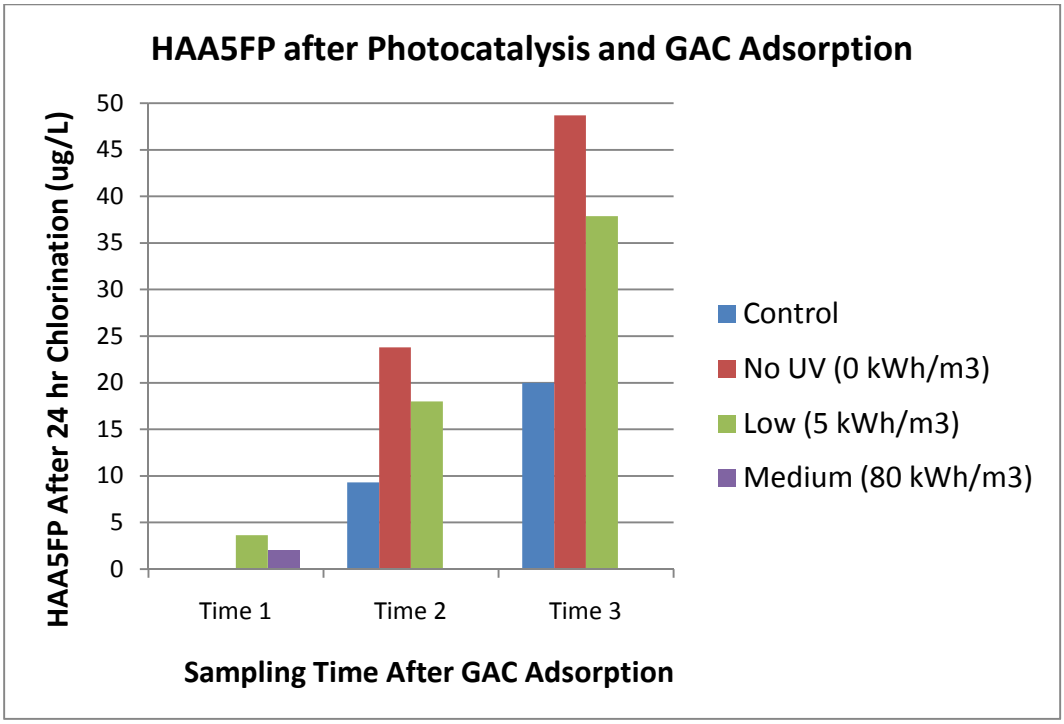

Figure 28: HAA5FP after Photocatalysis and GAC Adsorption

Both the TTHMFP and HAA5FP were normalized on a DOC basis to get the specific formation potentials STTHMFP and SHAA5FP as shown in Figures 29 and 30. The graphs show that the STTHMFP and SHAA5FP were greatest for the Low photocatalytic treatment level at Time 2 in particular.

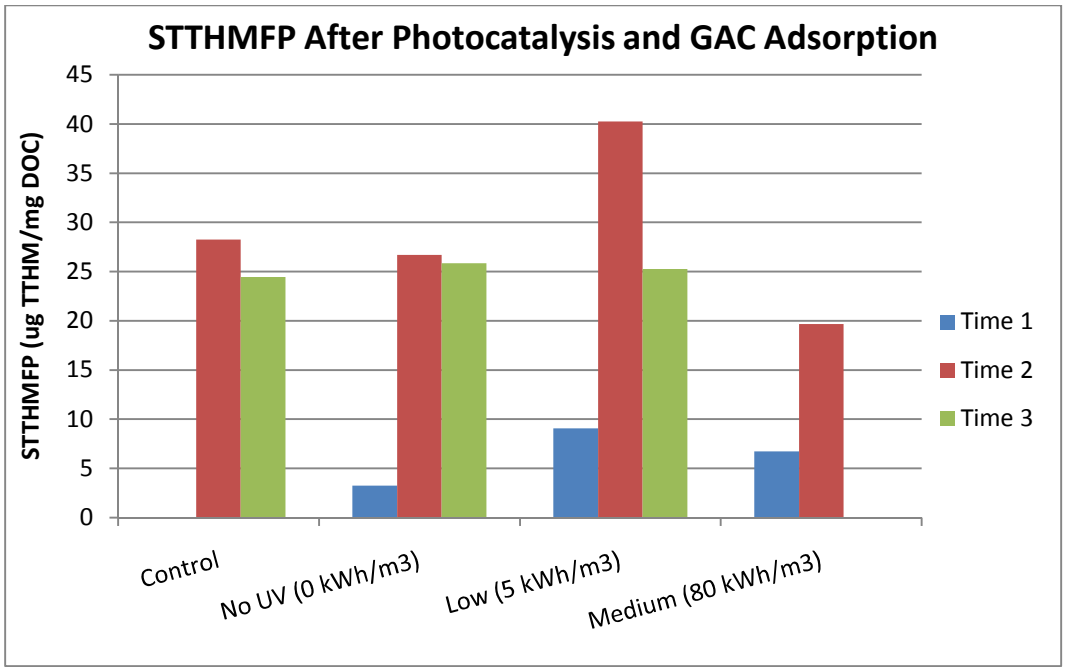

Figure 29: STTHMFP after Photocatalysis and GAC Adsorption

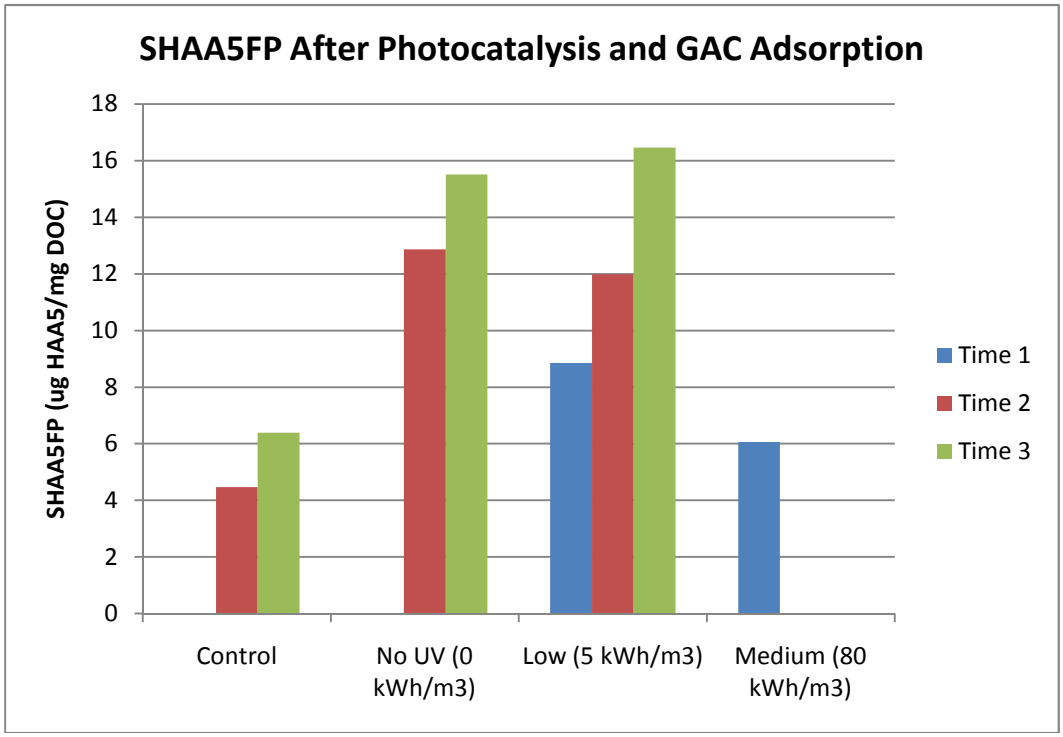

Figure 30: SHAA5FP after Photocatalysis and GAC Adsorption

Disinfection Byproduct Formation Correlations. Figures 31 and 32 illustrate the correlations between TTHM and HAA5 formation with DOC concentration and UV_{254} absorbance after 24 hours of chlorine exposure. In general TTHM concentrations increased with increased DOC concentrations with the exception of the Low photocatalytic treatment sample, which had higher TTHM concentrations despite the lower DOC concentrations than the other treatment levels.

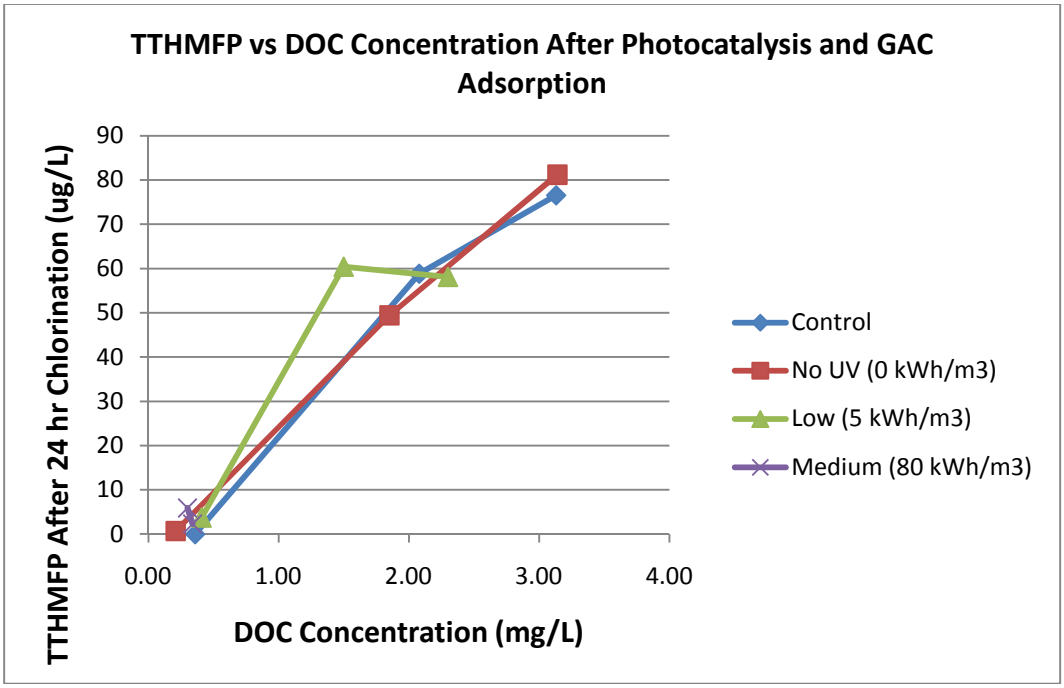

Figure 31: TTHMFP vs. DOC Concentration after Photocatalysis and GAC Adsorption

The trends shown for the UV_{254} absorbance were similar to the DOC results. In general TTHM concentrations increased with increased UV_{254} values with the exception of the Low treatment level which had higher TTHM concentrations at lower UV_{254} values.

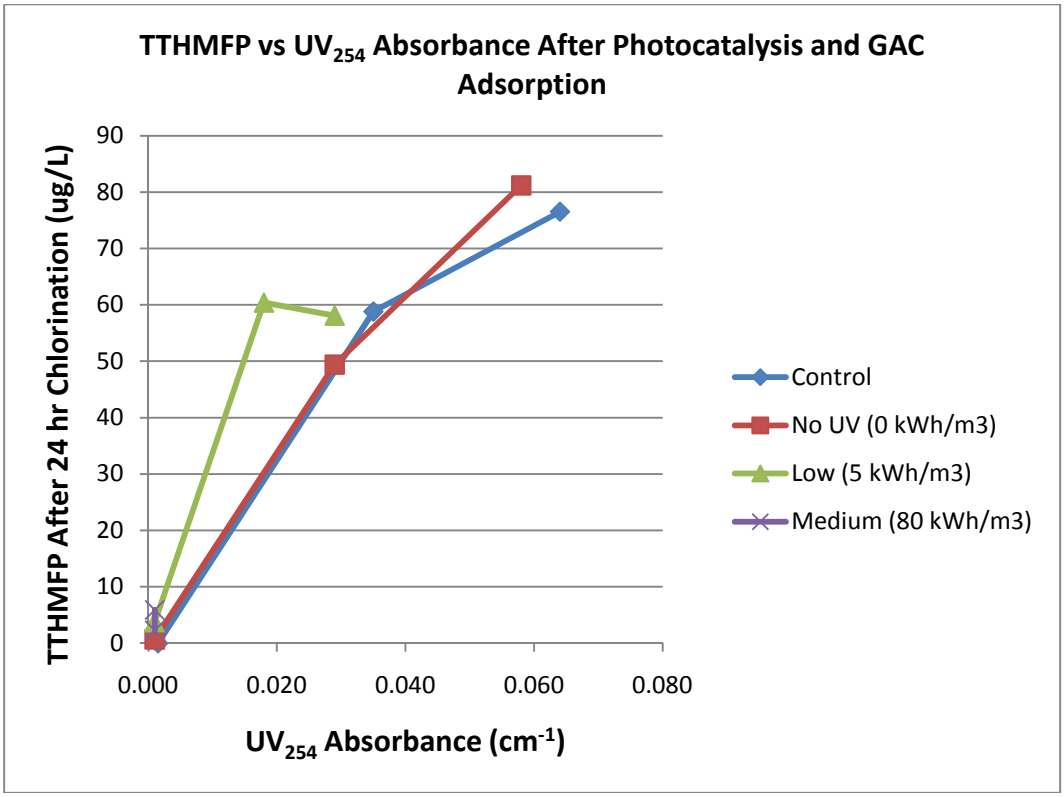

Figure 32: TTHMFP vs. UV_{254} Absorbance after Photocatalysis and GAC Adsorption

The resulting correlations for the HAA5 formations as a function of DOC and UV_{254} were interesting and somewhat similar to those found with the TTHMs as shown in the Figures 33 and 34. However, the spike in HAA5 concentration occurred during the No UV treatment level rather than the Low treatment level sample.

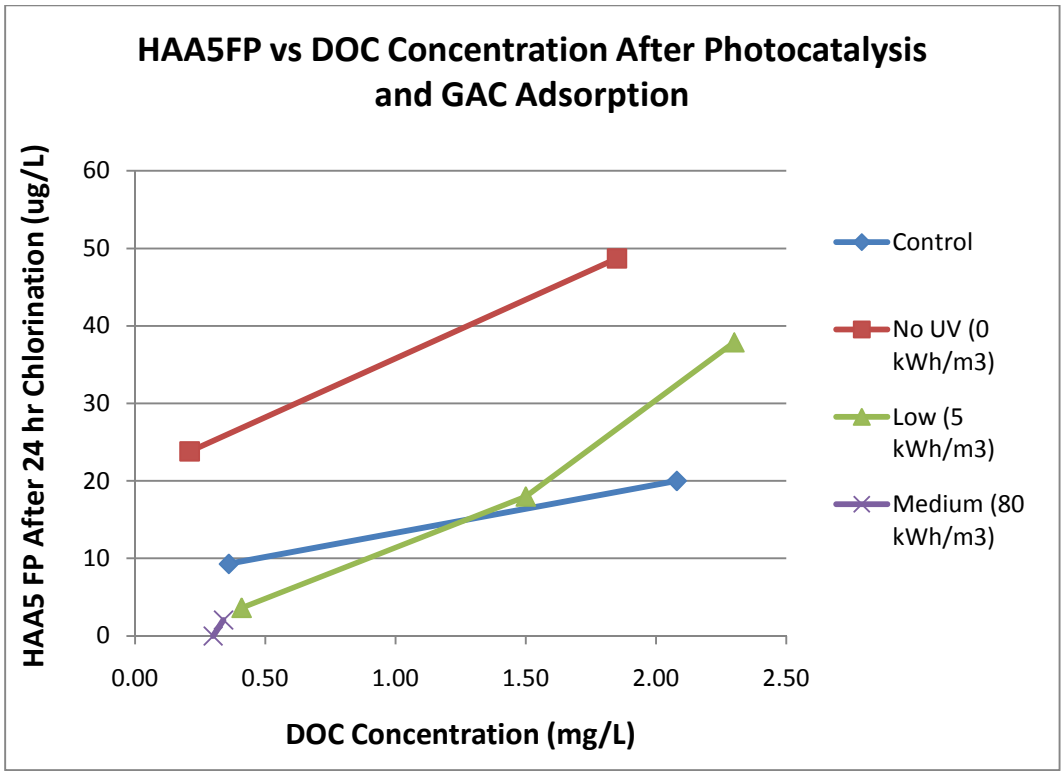

Figure 33: HAA5FP vs. DOC Concentration after Photocatalysis and GAC Adsorption

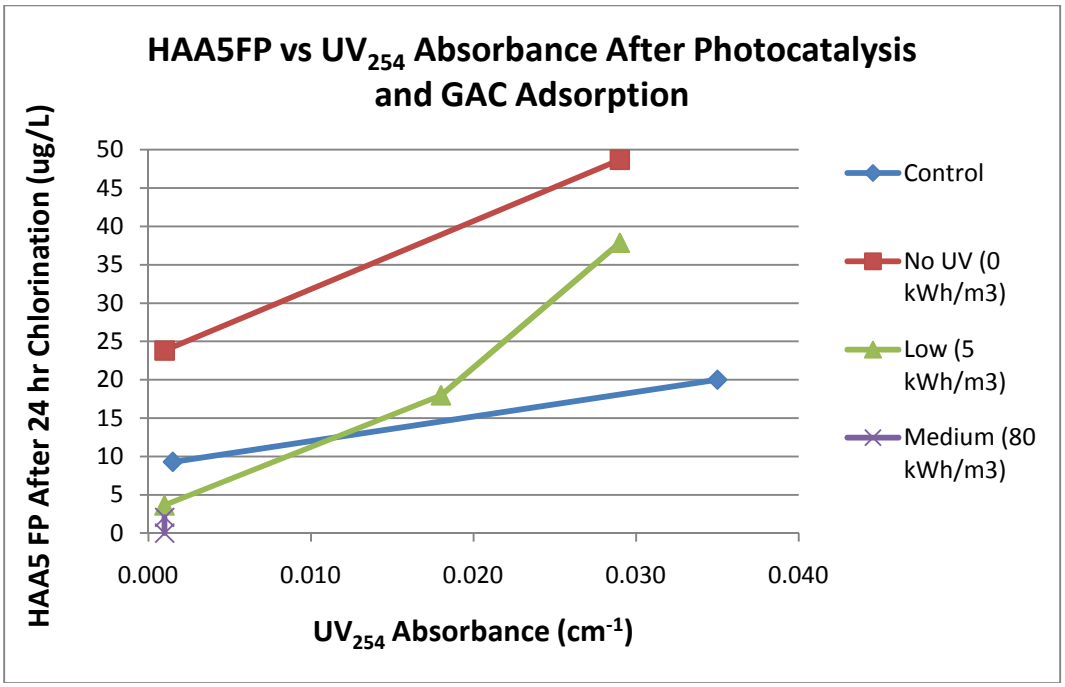

Figure 34: HAA5FP vs. UV_{254} Absorbance after Photocatalysis and GAC Adsorption

As shown in the RSSCT plots the DOC and UV_{254} values although decreasing with increased photocatalytic treatment, increase with increased filtration time as expected. However, the initial improvement in water quality at Time 1 gives the indication that GAC is significantly improving the water quality through physical adsorption. The process through which GAC preferentially adsorbs organic matter is based on the Van der Waals forces of attraction and repulsion and cause more non-polar and larger compounds to be more readily adsorbed to activated carbon (*10*). Photocatalysis is known to selectively degrade HMM compounds resulting in a shift towards LMM compounds as mentioned in Chapter 4. However, GAC also selectively adsorbs the HMM, hydrophobic compounds before the LMM compounds due to the surface charge

interactions. However, these HMM compounds are initially oxidized during photocatalysis, so it should be expected that that the moderate to low MM compounds are being removed with the GAC. As saturation begins to occur, these moderate to low MM compounds are passed through the column and could result in the spike in DBP formation. At the same time the No UV treatment that has experienced minimal oxidation still has some of the HMM compounds that could have saturated the GAC more quickly and allowed a higher portion of the HMM compounds to pass through the column. This can be seen in Figures 21 and 23 with the No UV sample closely following the trends of the Control sample. As shown in Chapter 4, the presence of LMM compounds could result in the spike at the No UV treatment level if there is a slightly higher ration of LMM:HMM compounds.

Chapter 7

CONCLUSIONS AND CONSIDERATIONS

The results from the three objectives appear to align with the findings published in the literature. Trends show that photocatalysis does efficiently oxidize organic matter resulting in decreased DBPFP given a sufficient amount of time for the reactions to take place. In sufficient oxidation time (low photocatalytic treatment) was shown to actually increase DBPFP, which suggests incomplete oxidation of organic matter. Reductions in organic matter from the Control to the No UV samples indicate the adsorption onto the surface of titanium dioxide. These molecules have been identified in the literature as being HMM, hydrophobic and humic substances that are readily oxidized during photocatalysis and chlorination due to their location of the titanium dioxide surface and chemical properties. Their breakdown into smaller LMM, hydrophilic compounds makes them more resistant to oxidation. It has been suggested that these LMM compounds are just as important as the humic HMM compounds during DBP formation. As the results in Chapter 4 showed, there was an increase in DBPFP during the Low photocatalytic treatment levels when there was an increase in the LMM ranges. As far as implementation into previous treatment processes, photocatalysis does improve the water quality and prevents the formation of DBPs, as was the case for the Post-GAC adsorption samples. Photocatalytic oxidation prior to GAC adsorption also proved to increase the bed life of the GAC

contactors. Using photocatalysis has also been shown to significantly reduce the THM and HAA formations at high treatment levels, with the exception of the distribution hot spot samples that were only slightly reduced from the untreated samples. Therefore careful consideration should be used since higher photocatalytic treatment levels eliminate the need for subsequent GAC adsorption and are more expensive, whereas lower photocatalytic treatment levels although less energy and cost intensive provide incomplete oxidation, resulting in increased DBPFP.

To help interpret the data and further investigate some of the results of this study, future consideration should be made. The first consideration would be to include more water quality measurements including Nitrogen content such as nitrate/nitrite/ammonium, bromide concentrations and assimilable organic carbon (AOC). The nitrogen and bromide measurements could provide more insight into what other potential DBPs are being formed. The AOC provides a measure of the amount of available substrate for microbial utilization is being produced. This is important since the initial proposed use of photocatalysis was for the implementation at distribution hot spots. However, if photocatalysis is actually producing compounds that are more biodegradable, it would actually encourage biological growth within the distribution system resulting in higher chlorine demands and increase DBP formation.

REFERENCES

1. Singer, P.C. and Reckhow, D.A. Chemical Oxidation, In *Water Quality and Treatment: A Handbook of Community Water Supplies,* Fifth ed.; Letterman, R.D., Ed.; McGraw-Hill: 1999; p 12.1.

2. Pontius, F.W. and Clark, S.W. Drinking Water Quality Standards, Regulations, and Goals, In *Water Quality and Treatment: A Handbook of Community Water Supplies,* Fifth ed.; Letterman, R.D., Ed.; McGraw-Hill: 1999; p 1.1.

3. Xie, Y.F. *Disinfection Byproducts in Drinking Water: Formation, Analysis, and Control.* CRC Press LLC.: Boca Raton, FL, 2004.

4. Bull, R.J. Health Effects of Drinking Water Disinfectants and Disinfection Byproducts. *Envrion Sci Technol* **1982,** *16 (10), 554A-559A.*

5. Snoeyink, V.L. and Summer, R.S. Adsorption of Organic Compounds, In *Water Quality and Treatment: A Handbook of Community Water Supplies,* Fifth ed.; Letterman, R.D., Ed.; McGraw-Hill: 1999;p 13.1.

6. Karlin, R.J. Disinfection Byproducts – A View From North America, In *Disinfection Byproducts in Drinking Water: Current Issues,* First ed.; Fielding, M. and Farimond, M., Eds.; Royal Society of Chemistry: 1999.

7. USEPA National Primary Drinking Water Regulations: Disinfectants and Disinfection Byproducts; Final Rule. *Federal Register* **1998,** *63,* 69390.

8. Westerhoff, P. Chemistry and Treatment of Disinfection Byproducts in Drinking water. *Southwest Hydrology* **November/December 2006,** 20.

9. USEPA. Drinking Water Priority Rulemaking: Microbial and Disinfection Byporduct Rules. **June 2001.**

10. MWH. *Water Treatment: Principles and Design.* John Wiley and Sons, Inc.: Hoboken, New Jersey, 2005.

11. USEPA National Primary Drinking Water Regulations: Stage 2 Disinfectants and Disinfection Byproducts Rule. *Federal Register* **2006,** *71,* 388.

12. Haas, C.N. Disinfection, In *Water Quality and Treatment: A Handbook of Community Water Supplies,* Fifth ed.; Letterman, R.D., Ed.; McGraw-Hill: 1999; p 14.1.

13. Cohn, P.D.; Cox, M.; Berger, P.S. Health and Aesthetic Aspects of Water Quality, In *Water Quality and Treatment: A Handbook of Community Water Supplies,* Fifth ed.; Letterman, R.D., Ed.; McGraw-Hill: 1999. p 2.1.

14. Matilainen, A. and Sillanpaa, M. Removal of natural organic matter from drinking water by advanced oxidation processes. *Chemosphere* **2010,** *80,* 351.

15. Amy, G.L.; Sierka, R.A.; Bedessem, J.; Price, D.; Tan, L. Molecular Size Distributions of Dissolved Organic Matter. *Journal AWWA* **June 1992,** 67.

16. Pelekani, C.; Newcombe, G.; Snoeyink, V.L.; Hepplewhite, C.; Assemi, S.; Beckett, R. Characterization of natural organic matter using high performance size exclusion chromatography. *Envrion Sci Technol* **1999,** *33,* 2807.

17. Karanfil, T.; Krasner, S.W.; Westerhoff, P.; Xie, Y. Recent Advances in Disinfection By-product Formation, Occurrence, Control, Health Effects, and Regulations, In *Disinfection Byproducts in Drinking Water: Occurrence, Formation, Health Effects and Control,* Anonymous ; Oxford University Press, USA: 2008.

18. Crepeau, K.L.; Fram, M.S.; Bush, N. Method of analysis by the U.S. Geological Survey California District Sacramento Laboratory - Determination of Trihalomethane Formation Potential, Method Validation, and Quality Control Practices. **2004,** *U.S. Geological Survey Scientific Investigations Report 2004–5003.*

19. Eaton, A.D.; Clescen, L.S.; Rice, E.W.; Greenburg, A.E. Standard Methods for the Examination of Water and Wastewater. American Public Health Association, AWWA, WEF: **2005.**

20. Letterman, R.D.; Amirtharajah, A.; O'Melia, C.R. Coagulation and Flocculation, In *Water Quality and Treatment: A Handbook of Community Water Supplies,* Fifth ed.; Letterman, R.D., Ed.; McGraw-Hill: 1999;p 6.1.

21. Murray, C.A. and Parsons, S.A. Preliminary laboratory investigation of disinfection by-product precursor removal using an advanced oxidation process. *Water and Environment Journal* **2006,** *20,* 123.

22. Hand, D.W.; Perram, D.L.; Crittenden, J.C. Destruction of DBP precursors with catalytic oxidation. *Journal AWWA* **June 1995,** 84.

23. Thiruvenkatachari, R.; Vigneswaran, S.; Moon, I.S. A review on UV/TiO2 photocatalytic oxidation process. *Korean J. Chem. Eng.* **2008,** *25,* 64.

24. Murray, C.A.; Goslan, E.H.; Parsons, S.A. TiO2/UV: Single stage drinking water treatment for NOM removal? *J. Environ. Eng. Sci.* **2007,** *6,* 311.

25. Gerrity, D.; Mayer, B.; Ryu, H.; Crittenden, J.; Abbaszadegan, M. A comparison of pilot-scale photocatalysis and enhanced coagulation for disinfection byproduct mitigation. *Water Res* **2009,** *43,* 1597 - 1610.
`

26. Liu, S.; Lim, M.; Fabris, R.; Chow, C.; Drikas, M.; Amal, R. TiO2 photocatalysis of natural organic matter in surface water: Impact on trihalomethane and haloacetic acid formation potential. *Envrion Sci Technol* **2008,** *42,* 6218.

27. Philippe, K.K.; Hans, C.; MacAdam, C.; Jefferson, B.; Hart, J.; Parsons, S.A. Photocatalytic oxidation of natural organic matter surrogates and the impact on trihalomethane formation potential. *Chemosphere* **2010,** *81,* 1509.

28. Cheng, Y.L.; Wong, R.J.; Lin, J.C.; Huang, C.; Lee, D.J.; Lai, J.Y. Pre-treatment of natural organic matters containing raw water using coagulation. *Separation Science and Technology* **2010,** *45,* 911.

29. Chen, W.; Westerhoff, P.; Leenheer, J.A.; Booksh, K. Fluorescence excitation-emission matrix region integration to quantify spectra for dissolved organic matter. *Envrion Sci Technol* **2003,** *37,* 5701.

30. Tercreo Espinoza, L.A. and Frimmel, F.H. A simple simulation of the degradation of natural organic matter in homogeneous and heterogeneous advanced oxidation processes. *Water Res.* **2009,** *43,* 3902.

31. Imai, A.; Matsushige, K.; Nagai, T. Trihalomethane formation potential of dissolve organic matter in a shallow eutrophic lake. *Water Res.* **2003,** *37,* 4284.

32. Westerhoff, P. and Crittenden, J.C. RSSCT Analysis for Scottsdale GAC Procurement. **2005,**

APPENDIX A

GENERAL MEASUREMENTS

Table A-1

pH

					Pre-GAC			
	Salt River Water	Settled Water	Post - GAC Adsorption	Distribution Hot Spot 2	Feed	Time 1	Time 2	Time 3
Control	8.02	8.08	8.31	8.42	8.50	8.55	8.35	8.48
PhotoCAT 0 kWh/m3	7.99	7.75	8.02	8.32	8.59	8.56	8.44	8.51
PhotoCAT 5 kWh/m3	8.04	7.73	8.06	8.28	8.43	8.53	8.77	8.39
PhotoCAT 80 kWh/m3	8.27	8.43	8.31	8.51	8.51	8.62	8.55	
PhotoCAT 160 kWh/m3	8.26	8.49	8.44	8.38				
Coagulation	7.11							
Enhanced Coagulation	5.67							

Table A-2

Turbidity (NTU)

					Pre-GAC			
	Salt River Water	Settled Water	Post - GAC Adsorption	Distribution Hot Spot 2	Feed	Time 1	Time 2	Time 3
Control	2.86	0.90	0.39	0.09	0.31	0.11	0.14	0.15
PhotoCAT 0 kWh/m3	0.40	0.20	0.21	0.10	0.34	0.16	0.18	0.16
PhotoCAT 5 kWh/m3	0.30	0.13	0.21	0.13	0.16	0.11	0.14	0.45
PhotoCAT 80 kWh/m3	0.44	0.23	0.20	0.11	0.12	0.10	0.08	
PhotoCAT 160 kWh/m3	0.38	0.07	0.16	0.09				
Coagulation	1.04							
Enhanced Coagulation	0.48							

Table A-3

Alkalinity (mg/L as CaCO3)

					Pre-GAC			
	Salt River Water	Settled Water	Post - GAC Adsorption	Distribution Hot Spot 2	Feed	Time 1	Time 2	Time 3
Control	112	90	194	168	128	140	138	146
PhotoCAT 0 kWh/m3	107	92	140	160	130	124	130	145
PhotoCAT 5 kWh/m3	106	74	132	150	130	132	158	128
PhotoCAT 80 kWh/m3	100	82	130	130	130	124	112	
PhotoCAT 160 kWh/m3	85	72	112	116				
Coagulation	85							
Enhanced Coagulation	12							

Table A-4

UV 254 (1/cm)

					Pre-GAC			
	Salt River Water	Settled Water	Post - GAC Adsorption	Distribution Hot Spot 2	Feed	Time 1	Time 2	Time 3
Control	0.086	0.039	0.032	0.013	0.086	0.002	0.035	0.064
PhotoCAT 0 kWh/m3	0.052	0.029	0.014	0.015	0.084	0.001	0.029	0.058
PhotoCAT 5 kWh/m3	0.025	0.019	0.009	0.014	0.042	0.001	0.018	0.029
PhotoCAT 80 kWh/m3	0.000	0.003	0.000	0.003	0.004	0.001	0.001	
PhotoCAT 160 kWh/m3	0.000	0.003	0.000	0.002				
Coagulation	0.058							
Enhanced Coagulation	0.045							

Table A-5

DOC (mg/L)

					Pre-GAC			
	Salt River Water	Settled Water	Post - GAC Adsorption	Distribution Hot Spot 2	Feed	Time 1	Time 2	Time 3
Control	4.85	3.13	2.09	3.02	3.74	0.36	2.08	3.13
PhotoCAT 0 kWh/m3	3.37	2.70	1.56	1.59	3.78	0.21	1.85	3.14
PhotoCAT 5 kWh/m3	3.38	2.51	1.56	1.91	2.99	0.41	1.50	2.30
PhotoCAT 80 kWh/m3	0.74	0.54	0.22	0.60	0.74	0.34	0.30	
PhotoCAT 160 kWh/m3	0.64	0.79	0.45	0.44				
Coagulation	5.51							
Enhanced Coagulation	3.98							

Table A-6

SUVA (L/mg-m)

					Pre-GAC			
	Salt River Water	Settled Water	Post - GAC Adsorption	Distribution Hot Spot 2	Feed	Time 1	Time 2	Time 3
Control	1.78	1.26	1.51	0.44	2.30	0.42	1.68	2.04
PhotoCAT 0 kWh/m3	1.54	1.06	0.90	0.97	2.21	0.48	1.57	1.85
PhotoCAT 5 kWh/m3	0.73	0.74	0.55	0.73	1.40	0.24	1.20	1.26
PhotoCAT 80 kWh/m3	0.00	0.61	0.00	0.50	0.54	0.29	0.33	
PhotoCAT 160 kWh/m3	0.00	0.34	0.00	0.45				
Coagulation	1.05							
Enhanced Coagulation	1.13							

Table A-7

TDN (mg/L)

					Pre-GAC			
	Salt River Water	Settled Water	Post - GAC Adsorption	Distribution Hot Spot 2	Feed	Time 1	Time 2	Time 3
Control	0.32	0.54	0.21	0.52	0.29	0.20	0.21	0.29
PhotoCAT 0 kWh/m3	0.3	0.47	0.16	0.54	0.38	0.19	0.25	0.30
PhotoCAT 5 kWh/m3	0.33	0.50	0.17	0.55	0.38	0.13	0.28	0.29
PhotoCAT 80 kWh/m3	0.43	0.56	0.16	0.81	0.36	0.20	0.33	
PhotoCAT 160 kWh/m3	0.47	0.57	0.19	0.65				
Coagulation	0.3							
Enhanced Coagulation	0.21							

APPENDIX B

ION CHROMATOGRAPHY RESULTS

Table B-1
SRP Experiment

	Chloride (mg/L)	Bromide (mg/L)	Nitrate (mg/L)	Sulfate (mg/L)
Control	228	0.025	0.141	38
PhotoCAT 0 kWh/m3	220	0.054	0.196	41
PhotoCAT 5 kWh/m3	221	0.016	0.193	41
PhotoCAT 80 kWh/m3	222	0.003	0.491	42
PhotoCAT 160 kWh/m3	223	0.000	0.781	42
Coagulation	251	0.016	0.305	38
Enhanced Coagulation	313	0.034	0.205	38

Table B-2
Settled Water Experiment

	Chloride (mg/L)	Bromide (mg/L)	Nitrate (mg/L)	Sulfate (mg/L)
Control	96	0.01	2.37	231
PhotoCAT 0 kWh/m3	117	0.00	1.95	164
PhotoCAT 5 kWh/m3	117	0.01	1.86	163
PhotoCAT 80 kWh/m3	117	0.01	2.05	163
PhotoCAT 160 kWh/m3	118	0.01	2.37	164

Table B-3
DHS 1 Experiment

	Chloride (mg/L)	Bromide (mg/L)	Nitrate (mg/L)	Sulfate (mg/L)
Control	181	0.0	0.949	42
PhotoCAT 0 kWh/m3	146	0.0	1.170	36
PhotoCAT 5 kWh/m3	152	0.0	1.235	37
PhotoCAT 80 kWh/m3	154	0.0	2.474	37
PhotoCAT 160 kWh/m3	158	0.0	1.446	38

Table B-4
DHS 2 Experiment

	Chloride (mg/L)	Bromide (mg/L)	Nitrate (mg/L)	Sulfate (mg/L)
Control	-	-	-	-
PhotoCAT 0 kWh/m3	179	0.011	18.72	120
PhotoCAT 5 kWh/m3	179	0.047	18.69	121
PhotoCAT 80 kWh/m3	164	0.041	-	39
PhotoCAT 160 kWh/m3				

Table B-5
Post-GAC Experiment

	Chloride (mg/L)	Bromide (mg/L)	Nitrate (mg/L)	Sulfate (mg/L)
Control	180	0.032	0.587	30.6
PhotoCAT 0 kWh/m3	114	0.000	0.509	22.5
PhotoCAT 5 kWh/m3	130	0.002	0.602	24.3
PhotoCAT 80 kWh/m3	120	0.000	0.712	23.1
PhotoCAT 160 kWh/m3	134	0.000	0.865	25.0

Table B-6
PRE-GAC Experiment

CHLORIDE (mg/L)

	Control	No UV - 0 kWh/m3	Low - 5 kWh/m3	Medium - 80 kWh/m3
Feed	174	166	161	115
Time 1	168	143	160	163
Time 2	118	162	158	165
Time 3	178	177	131	

NITRATE (mg/L)

	Control	No UV - 0 kWh/m3	Low - 5 kWh/m3	Medium - 80 kWh/m3
Feed	0.209	0.554	0.537	0.644
Time 1	0.653	0.668	0.640	0.633
Time 2	0.209	0.479	0.813	0.753
Time 3	0.154	0.237	0.674	

BROMIDE (mg/L)

	Control	No UV - 0 kWh/m3	Low - 5 kWh/m3	Medium - 80 kWh/m3
Feed	0.036	0.014	0.042	0.056
Time 1	0.000	0.020	0.043	0.036
Time 2	0.035	0.018	0.046	0.069
Time 3	0.036	0.024	0.001	

SULFATE (mg/L)

	Control	No UV - 0 kWh/m3	Low - 5 kWh/m3	Medium - 80 kWh/m3
Feed	39	39	30	39
Time 1	38	38	37	39
Time 2	38	38	39	40
Time 3	40	42	45	

APPENDIX C

CHLORINE DEMANDS

Table C-1
SRP Experiment

Time	Control	No UV (0 kWh/m3)	Low (5 kWh/m3)	Medium (80 kWh/m3)	High (160 kWh/m3)	Coagulation	Enhanced Coag.
0	3.5	2.5	3.6	2.5	1.8	2.1	1.5
0.25	3.4	2.2	3	2.2	1.8	2	1.5
0.50	2.9	2.1	2.7	2.1	1.8	2	1.5
0.75	2.8	1.9	2.7	2.1	1.8	2	1.4
1.00	2.8	1.9	2.6	2.1	1.7	1.7	1.3
1.25	2.7	2.1	2.5	2	1.6	1.7	1.3
1.50	2.6	1.9	2.7	1.9	1.6	1.7	1.2
1.75	1.9	1.4	1.9	2	1.6	1.6	1.2
2.00	2.5	1.8	2.4	1.9	1.6	1.6	1.1
4.00	2	2.2	1.6	1.7	1.4	1.1	0.9
8.00	1.5	1.2	1.5	1.4	1.1	0.6	0.4
24.00	0.725	0.73	0.8	1.01	0.82	0.35	0.19

Table C-2

Settled Water Experiment

Time	Control	No UV (0 kWh/m3)	Low (5 kWh/m3)	Medium (80 kWh/m3)	High (160 kWh/m3)
0	2.57	3.46	2.53	3.26	3.37
0.25	2.4	3.32	2.16	2.58	2.96
0.50	2.4	3.38	2.16	2.48	2.86
0.75	2.3	3.22	2.02	2.42	2.9
1.00	2.2	2	1.96	2.38	2.92
1.25	2.26	3.12	1.96	2.32	2.84
1.50	2.16	3.1	1.86	2.3	2.76
1.75	2.14	3.1	1.82	2.36	2.84
2.00	2.18	3.26	1.76	2.3	2.78
4.00	1.94	3.02	1.6	2.06	2.68
6.00	1.78	2.74	1.52	2.02	2.52
24.00	1.16	2.3	0.86	1.54	2.18

Table C-3
Post-GAC Adsorption Experiment

Time	Control	No UV (0 kWh/m3)	Low (5 kWh/m3)	Medium (80 kWh/m3)	High (160 kWh/m3)
0	1.54	1.2	1.31	1.23	1.09
0.25	1.42	1.2	1.23	1.16	1.05
0.50	1.35	1.18	1.16	1.11	1.06
0.75	1.31	1.18	1.14	1.13	1.07
1.00	1.31	1.13	1.08	1.04	1.05
1.25	1.27	1.14	1.07	1.07	1
1.50	1.23	1.11	1.04	1.07	1.02
1.75	1.22	1.12	1.04	1.07	0.99
2.00	1.19	1.11	1	1.02	1
4.00	1.11	1.04	0.91	1.01	0.95
6.00	1.02	0.99	0.81	0.91	0.89
24.00	0.66	0.76	0.43	0.73	0.77

Table C-4
Distribution Hot Spot Experiment

Time	No UV (0 kWh/m3)	Low (5 kWh/m3)	Medium (80 kWh/m3)	High (160 kWh/m3)
0	2.1	2.3	1.9	1.4
0.25	1.9	2.1	1.9	135
0.50	1.9	2.1	1.7	1.4
0.75	1.9	2.2	1.7	1.5
1.00	1.9	2.1	1.6	1.4
1.25	1.9	2.1	1.7	1.4
1.50	1.6	2	1.7	11.3
1.75	0.9	2.1	1.6	1.3
2.00	2	2.1	0.7	1.3
4.00	1.8	1.9	1.5	1.2
6.00	1.9	1.9	1.6	1.2
24.00	1.7	1.6	1.3	1

Table C-5
Pre-GAC
Experiment
Time 1

	Control	No UV (0 kWh/m3)	Low (5 kWh/m3)	Medium (80 kWh/m3)
0	1.12	1.12	1	1.3
0.25	1.08	1.08	0.9	1.1
0.50	1.06	1.08	0.9	1.1
0.75	1.08	1.06	0.9	1.2
1.00	1.06	1.06	0.8	1.2
1.25	1.08	1.06	0.8	1.2
1.50	1.06	1.06	0.9	1.1
1.75	1.08	1.06	0.8	1.2
2.00	1.08	1.08	0.8	1
4.00	1.02	1.04	0.8	1
6.00	1.04	1.02	0.8	1
24.00	0.96	0.94	0.8	1.1

Table C-6
Pre GAC
Experiment
Time 2

	Control	No UV (0 kWh/m3)	Low (5 kWh/m3)	Medium (80 kWh/m3)
0	1.18	1.46	1.1	1.2
0.25	1.62	1.72	0.9	1.1
0.50	1.62	1.68	1	1.2
0.75	1.58	1.68	0.7	0.9
1.00	1.54	1.68	0.6	1.1
1.25	1.56	1.62	0.7	0.9
1.50	1.54	1.64	0.7	1
1.75	1.46	1.6	0.7	0.8
2.00	1.48	1.58	0.75	0.8
4.00	1.14	1.28	0.6	0.9
6.00	1	1.12	0.5	0.9
24.00	0.6	0.74	0.4	1

Table C-7
Pre GAC
Experiment
Time 3

	Control	No UV (0 kWh/m3)	Low (5 kWh/m3)
0	1.8	1.64	2.2
0.25	2.08	2.2	2.2
0.50	2.06	2.14	2
0.75	1.98	2.12	1.9
1.00	1.92	0.08	1.8
1.25	1.92	2.1	1.7
1.50	1.84	2	1.7
1.75	1.84	1.96	1.8
2.00	1.82	1.78	1.7
4.00	1.3	1.36	1.7
6.00	1.22	1.26	1.5
24.00	0.42	0.48	0.7

121

APPENDIX D

THM FORMATIONS

Table D-1
SALT RIVER THM
RESULTS

	Bromo-dichloromethane (ug/L)			Bromoform (ug/L)			Chloroform (ug/L)			Dibromo-chloromethane (ug/L)			Total Trihalomethanes (ug/L)		
	15 min	**2 hr**	**24 hr**	**15 min**	**2 hr**	**24 hr**	**15 min**	**2 hr**	**24 hr**	**15 min**	**2 hr**	**24 hr**	**15 min**	**2 hr**	**24 hr**
Control	8	13	6	ND	ND	ND	63	17	13	67	5	3	21	35	21
No UV (0 kWh/m3)	8	10	4	ND	1	ND	7	10	7	4	6	3	19	27	14
Low (5 kWh/m3)	9	13	7	1	1	1	9	18	15	6	8	4	25	40	26
Medium (80 kWh/m3)	ND	3	1	ND	1	1	ND	1	ND	ND	2	2	ND	7	4
High (160 kWh/m3)	ND	0.91	ND	ND	ND	1	ND	ND	ND	ND	1	1	ND	2	2
Coagulation	6	5	2	ND	ND	ND	4	4	3	4	3	1	14	13	6
Enhanced Coagulation	2	2	1	ND	ND	ND	1	1	2	2	2	1	4	5	4

Table D-2
SETTLED WATER
THMS

	Bromo-dichloromethane ug/L					Bromoform ug/L					Chloroform ug/L				
	15 min	**1 hr**	**2 hr**	**6 hr**	**24 hr**	**15 min**	**1 hr**	**2 hr**	**6 hr**	**24 hr**	**15 min**	**1 hr**	**2 hr**	**6 hr**	**24 hr**
Control	4	6	7	10	16	1	2	2	2	2	3	4	5	9	21
No UV (0 kWh/m3)	9	10	11	14	19	1	1	1	1	1	14	15	15	18	31
Low (5 kWh/m3)	13	16	20	24	30	1	1	1	1	1	18	22	27	38	62
Medium (80 kWh/m3)	1	2	3	3	4	ND	ND	ND	ND	1	ND	1	2	3	3
High (160 kWh/m3)	ND	1	1	1	1	ND	ND	ND	ND	ND	ND	ND	1	1	1

	Dibromo- chloromethane ug/L					Total Trihalomethanes ug/L				
	15 min	**1 hr**	**2 hr**	**6 hr**	**24 hr**	**15 min**	**1 hr**	**2 hr**	**6 hr**	**24 hr**
Control	4	7	7	10	13	12	19	21	31	53
No UV (0 kWh/m3)	5	6	7	8	11	28	31	34	41	62
Low (5 kWh/m3)	8	9	10	12	15	39	48	58	75	109
Medium (80 kWh/m3)	ND	1	1	2	3	ND	4	6	8	11
High (160 kWh/m3)	ND	ND	N	1	1	ND	1	1	2	3

Table D-3

Post-GAC THMs

	Bromodi- chloromethane ug/L					Bromoform ug/L					Chloroform ug/L				
	15 min	**1 hr**	**2 hr**	**6 hr**	**24 hr**	**15 min**	**1 hr**	**2 hr**	**6 hr**	**24 hr**	**15 min**	**1 hr**	**2 hr**	**6 hr**	**24 hr**
Control	6	10	11	14	14	2	3	3	3	3	3	5	6	8	11
No UV (0 kWh/m3)	7	8	8	9	10	2	2	2	3	3	7	6	7	8	9
Low (5 kWh/m3)	11	14	15	19	19	2	2	2	3	3	9	11	13	18	23
Medium (80 kWh/m3)	1	1	2	2	2	ND	ND	1	1	1	ND	1	1	1	1
High (160 kWh/m3)	ND	ND	ND	ND	0.5	ND	ND	ND	ND	0.5	ND	ND	ND	ND	ND

	Dibromo- chloromethane ug/L					Total Trihalomethanes ug/L				
	15 min	**1 hr**	**2 hr**	**6 hr**	**24 hr**	**15 min**	**1 hr**	**2 hr**	**6 hr**	**24 hr**
Control										
No UV (0 kWh/m3)	8	12	13	15	15	19	29	33	40	43
Low (5 kWh/m3)	8	8	9	11	12	23	25	26	31	34
Medium (80 kWh/m3)	10	13	13	16	16	32	39	43	55	60
High (160 kWh/m3)	1	1	1	2	3	1	2	4	6	7

Table D-4
DISTRIBUTION HOT SPOT THMS

	Bromo-dichloromethane ug/L					Bromoform ug/L					Chloroform ug/L				
	15 min	**1 hr**	**2 hr**	**6 hr**	**24 hr**	**15 min**	**1 hr**	**2 hr**	**6 hr**	**24 hr**	**15 min**	**1 hr**	**2 hr**	**6 hr**	**24 hr**
Control			8					5.84					8.11		
No UV (0 kWh/m3)	11	11	9	10	11	27	26	25	23	20	7	6	6	6	8
Low (5 kWh/m3)	12	13	13	16	20	11	11	11	12	11	8	9	9	10	13
Medium (80 kWh/m3)	2	3	3	4	9	2	3	4	5	9	1	1	1	1	2
High (160 kWh/m3)	ND	1	1	1	3	ND	1	1	2	6	ND	ND	ND	ND	ND

	Dibromo-chloromethane ug/L					Total Trihalomethanes ug/L				
Control			7.72					29.6		
No UV (0 kWh/m3)	23	22	20	19	17	68	65	60	58	57
Low (5 kWh/m3)	15	17	17	21	21	46	51	50	60	65
Medium (80 kWh/m3)	3	5	6	8	16	8	12	14	19	37
High (160 kWh/m3)	1	1	2	3	8	1	3	4	7	18

Table D_5
Pre-GAC THMs

Bromodichloromethane (ug/L)

	Control					PhotoCAT 0 kWh/m3				
	15min	**1 hr**	**2 hr**	**6 hr**	**24 hr**	**15min**	**1 hr**	**2 hr**	**6 hr**	**24 hr**
Time 1	ND	ND	ND	ND	ND	ND	ND	ND	ND	ND
Time 2	6.29	8.9	10.3	13.5	19.2	5.25	7.1	8.68	11.7	16.3
Time 3	10.7	14.3	15.1	20.6	22.9	10.1	14.4	16.2	20.2	24.5

	PhotoCAT 5 kWh/m3					PhotoCAT 80 kWh/m3				
	15min	**1 hr**	**2 hr**	**6 hr**	**24 hr**	**15min**	**1 hr**	**2 hr**	**6 hr**	**24 hr**
Time 1	ND	ND	ND	ND	0.68	ND	ND	ND	ND	0.59
Time 2	4.18	6.94	7.69	11.8	18.5	ND	ND	ND	ND	1.63
Time 3	10.2	12.7	13.8	16.8	15.3	-	-	-	-	-

Bromoform (ug/L)

	Control					PhotoCAT 0 kWh/m3				
	15min	**1 hr**	**2 hr**	**6 hr**	**24 hr**	**15min**	**1 hr**	**2 hr**	**6 hr**	**24 hr**
Time 1	ND	ND	ND	0.53	ND	ND	ND	ND	ND	0.68
Time 2	1.23	2.15	2.21	2.61	3.2	1.49	2.2	2.59	2.82	3.03
Time 3	0.82	1.07	0.85	1.2	1.3	0.56	0.91	0.9	1.05	1.2

	PhotoCAT 5 kWh/m3					PhotoCAT 80 kWh/m3				
	15min	**1 hr**	**2 hr**	**6 hr**	**24 hr**	**15min**	**1 hr**	**2 hr**	**6 hr**	**24 hr**
Time 1	ND	ND	ND	ND	1.39	ND	ND	ND	ND	0.61
Time 2	1.57	3.44	4.04	5.81	7.22	ND	ND	ND	ND	1.42
Time 3	1.13	1.22	1.28	1.42	1.23	-	-	-	-	-

Chloroform (ug/L)

	Control					PhotoCAT 0 kWh/m3				
	15min	**1 hr**	**2 hr**	**6 hr**	**24 hr**	**15min**	**1 hr**	**2 hr**	**6 hr**	**24 hr**
Time 1	ND	ND	ND	ND	ND	ND	ND	ND	ND	ND
Time 2	3.48	5	6.72	7.88	18.5	2.48	3.67	3.73	5.83	14.1
Time 3	9.91	13.8	15.4	21.7	39.3	9.25	13.4	14.1	22.4	42.1

	PhotoCAT 5 kWh/m3					PhotoCAT 80 kWh/m3				
	15min	**1 hr**	**2 hr**	**6 hr**	**24 hr**	**15min**	**1 hr**	**2 hr**	**6 hr**	**24 hr**
Time 1	ND	ND	ND	ND	ND	ND	ND	ND	ND	ND
Time 2	1.9	2.92	3.32	5.26	13.1	ND	ND	ND	ND	ND
Time 3	8.07	10.6	12.1	19.5	32	-	-	-	-	-

Dibromochloromethane (ug/L)

	Control					PhotoCAT 0 kWh/m3				
	15min	**1 hr**	**2 hr**	**6 hr**	**24 hr**	**15min**	**1 hr**	**2 hr**	**6 hr**	**24 hr**
Time 1	ND	ND	ND	ND	ND	ND	ND	ND	ND	ND
Time 2	6.4	10.1	12.4	14.4	17.9	6.1	8.85	10.5	13.6	16
Time 3	7.04	9.73	9.87	12.6	13	6.21	9	9.84	12.0	13.4

	PhotoCAT 5 kWh/m3					PhotoCAT 80 kWh/m3				
	15min	**1 hr**	**2 hr**	**6 hr**	**24 hr**	**15min**	**1 hr**	**2 hr**	**6 hr**	**24 hr**
Time 1	ND	ND	ND	ND	1.65	ND	ND	ND	ND	1.09
Time 2	4.98	9.43	10.7	16.1	21.6	ND	ND	ND	0.71	2.85
Time 3	8.08	9.76	10.6	12.4	9.59	-	-	-	-	-

Total Trihalomethanes
(ug/L)

	Control					PhotoCAT 0 kWh/m3				
	15min	**1 hr**	**2 hr**	**6 hr**	**24 hr**	**15min**	**1 hr**	**2 hr**	**6 hr**	**24 hr**
Time 1	ND	ND	ND	0.53	ND	ND	ND	ND	ND	1
Time 2	17	26.2	31.6	38	59	15	22	26	34	49
Time 3	29	38.9	41.2	56	77	26	38	41	56	81

	PhotoCAT 5 kWh/m3					PhotoCAT 80 kWh/m3				
	15min	**1 hr**	**2 hr**	**6 hr**	**24 hr**	**15min**	**1 hr**	**2 hr**	**6 hr**	**24 hr**
Time 1	ND	ND	ND	ND	3.72	ND	ND	ND	ND	2
Time 2	13	23	26	39	60	ND	ND	ND	0.7	6
Time 3	28	34	38	50	58	-	-	-	-	-

APPENDIX E

HAA FORMATIONS

Table E-1
SW THAA

	Monochloroacetic Acid ug/L					Dichloroacetic Acid ug/L					Trichloroacetic Acid ug/L				
	10 min	1 hr	2 hr	6 hr	24 hr	10 min	1 hr	2 hr	6 hr	24 hr	10 min	1 hr	2 hr	6 hr	24 hr
Control	1	1	1	1	1	1	2	2	3	8	2	2	2	3	6
No UV (0 kWh/m3)	1	1	1	1	2	8	8	9	10	14	8	8	8	8	11
Low (5 kWh/m3)	2	2	2	3	4	11	13	15	18	25	10	10	11	11	13
Medium (80 kWh/m3)	1	1	1	1	1	1	1	1	1	1	1	1	1	1	1
High (160 kWh/m3)	1	1	1	1	1	1	1	1	1	1	1	1	1	1	1

	Monobromoacetic Acid ug/L					Dibromoacetic Acid ug/L					HAA5 ug/L				
	10 min	1 hr	2 hr	6 hr	24 hr	10 min	1 hr	2 hr	6 hr	24 hr	10 min	1 hr	2 hr	6 hr	24 hr
Control	ND	1	1	1	1	1	1	2	2	2	5	7	8	11	19
No UV (0 kWh/m3)	ND	1	1	1	1	1	1	1	1	2	18	19	20	22	29
Low (5 kWh/m3)	1	1	1	1	1	1	1	1	2	2	25	27	30	35	44
Medium (80 kWh/m3)	ND	ND	ND	ND	ND	<1	ND	ND	<1	<1	4	3	3	4	4
High (160 kWh/m3)	ND	ND	ND	ND	ND	ND	ND	ND	ND	ND	3	3	3	3	3

Tavle E-2

Post-GAC HAAs

	Monochloroacetic Acid ug/L					Dichloroacetic Acid ug/L					Trichloroacetic Acid ug/L				
	15 min	1 hr	2 hr	6 hr	24 hr	15 min	1 hr	2 hr	6 hr	24 hr	15 min	1 hr	2 hr	6 hr	24 hr
Control	ND	ND	ND	ND	2	3	3	4	5	8	2	2	2	3	4
No UV (0 kWh/m3)	ND	ND	ND	ND	1	5	5	6	6	8	3	3	3	4	4
Low (5 kWh/m3)	2	2	2	3	3	8	9	10	12	16	5	5	6	7	8
Medium (80 kWh/m3)	ND	ND	ND	ND	ND	1	1	1	1	2	1	1	1	1	1
High (160 kWh/m3)	ND	ND	ND	ND	ND	ND	ND	ND	ND	ND	ND	ND	ND	ND	ND

	Monobromoacetic Acid ug/L					Dibromoacetic Acid ug/L					HAA5 ug/L				
	15 min	1 hr	2 hr	6 hr	24 hr	15 min	1 hr	2 hr	6 hr	24 hr	15 min	1 hr	2 hr	6 hr	24 hr
Control	ND	ND	ND	ND	1	2	3	3	3	3	7	8	9	12	19
No UV (0 kWh/m3)	ND	ND	ND	ND	ND	2	2	2	2	3	10	10	11	12	16
Low (5 kWh/m3)	ND	ND	ND	ND	ND	2	2	2	2	2	16	18	20	24	29
Medium (80 kWh/m3)	ND	ND	ND	ND	ND	ND	ND	ND	ND	ND	2	3	3	3	3
High (160 kWh/m3)	ND	ND	ND	ND	ND	ND	ND	ND	ND	ND	ND	ND	ND	ND	ND

Table D-3
DISTRIBUTION HOT SPOT
HAA

	Monochloroacetic Acid ug/L					Dichloroacetic Acid ug/L					Trichloroacetic Acid ug/L				
	15 min	1 hr	2 hr	6 hr	24 hr	15 min	1 hr	2 hr	6 hr	24 hr	15 min	1 hr	2 hr	6 hr	24 hr
Control			ND					4					2		
No UV (0 kWh/m3)	1	1	1	1	2	11	12	12	12	13	5	5	5	5	5
Low (5 kWh/m3)	2	2	2	3	3	14	14	14	16	17	5	6	6	6	7
Medium (80 kWh/m3)	2	2	2	3	3	8	9	8	8	9	4	3	3	4	4
High (160 kWh/m3)	1	1	1	1	1	4	4	4	4	4	2	2	2	2	2

	Monobromoacetic Acid ug/L					Dibromoacetic Acid ug/L					HAA5 ug/L				
	15 min	1 hr	2 hr	6 hr	24 hr	15 min	1 hr	2 hr	6 hr	24 hr	15 min	1 hr	2 hr	6 hr	24 hr
Control			ND					3					9		
No UV (0 kWh/m3)	1.06	1	1	1	1	6	7	7	7	7	24	26	26	26	28
Low (5 kWh/m3)	ND	ND	ND	1	1	5	6	6	6	7	26	29	28	32	36
Medium (80 kWh/m3)	ND	ND	ND	ND	ND	2	2	2	2	3	16	16	16	16	19
High (160 kWh/m3)	ND	ND	ND	ND	ND	ND	ND	ND	ND	1	7	7	7	8	9

Table E-5
Pre-GAC HAAs
Monochloroacetic acid

	Control					PhotoCAT 0 kWh/m3				
	15min	1 hr	2 hr	6 hr	24 hr	15min	1 hr	2 hr	6 hr	24 hr
Time 1	-	-	-	-	-	-	-	-	-	-
Time 2	ND	ND	ND	ND	ND	ND	ND	2	ND	ND
Time 3	2	ND	ND	2.4	ND	ND	2	3	5	3

	PhotoCAT 5 kWh/m3					PhotoCAT 80 kWh/m3				
	15min	1 hr	2 hr	6 hr	24 hr	15min	1 hr	2 hr	6 hr	24 hr
Time 1	ND	ND	ND	ND	ND	ND	ND	ND	ND	ND
Time 2	ND	ND	ND	ND	1.45	ND	ND	ND	ND	ND
Time 3	ND	ND	1	2	3	-	-	-	-	-

Dichloroacetic acid

	Control					PhotoCAT 0 kWh/m3				
	15min	1 hr	2 hr	6 hr	24 hr	15min	1 hr	2 hr	6 hr	24 hr
Time 1	-	-	-	-	-	-	-	-	-	-
Time 2	6	7	7	9	16	4	6	6	7.6	13
Time 3	11	13	15	19	29	12	14	15	20	30

	PhotoCAT 5 kWh/m3					PhotoCAT 80 kWh/m3				
	15min	1 hr	2 hr	6 hr	24 hr	15min	1 hr	2 hr	6 hr	24 hr
Time 1	4	3	2	2	2	2	3	2	2	3
Time 2	2	3	3	4	7	ND	ND	ND	ND	ND
Time 3	7	9	10	13	22	-	-	-	-	-

Trichloroacetic acid

	Control					PhotoCAT 0 kWh/m3				
	15min	1 hr	2 hr	6 hr	24 hr	15min	1 hr	2 hr	6 hr	24 hr
Time 1	-	-	-	-	-	-	-	-	-	-
Time 2	2	3	3	4	6	2	3	3	4	5
Time 3	4	6	7	9	12	5	6	7	9	12

	PhotoCAT 5 kWh/m3					PhotoCAT 80 kWh/m3				
	15min	1 hr	2 hr	6 hr	24 hr	15min	1 hr	2 hr	6 hr	24 hr
Time 1	3	2	2	1	1	2	2	2	2	2
Time 2	ND	ND	ND	1	2	ND	ND	ND	ND	ND
Time 3	4	5	6	7	10	-	-	-	-	-

Monobromoacetic acid

	Control					PhotoCAT 0 kWh/m3				
	15min	1 hr	2 hr	6 hr	24 hr	15min	1 hr	2 hr	6 hr	24 hr
Time 1	-	-	-	-	-	-	-	-	-	-
Time 2	ND	ND	ND	ND	ND	ND	ND	ND	ND	ND
Time 3	ND	ND	ND	ND	ND	ND	ND	ND	ND	ND

	PhotoCAT 5 kWh/m3					PhotoCAT 80 kWh/m3				
	15min	1 hr	2 hr	6 hr	24 hr	15min	1 hr	2 hr	6 hr	24 hr
Time 1	ND	ND	ND	ND	ND	ND	ND	ND	ND	ND
Time 2	ND	ND	ND	ND	1	ND	ND	ND	ND	ND
Time 3	ND	ND	ND	ND	ND	-	-	-	-	-

Dibromoacetic acid

	Control					PhotoCAT 0 kWh/m3				
	15min	1 hr	2 hr	6 hr	24 hr	15min	1 hr	2 hr	6 hr	24 hr
Time 1	-	-	-	-	-	-	-	-	-	-
Time 2	3	4	4	5	6	3	4	4	5	6
Time 3	3	3	3	4	5	3	3	3	4	5

	PhotoCAT 5 kWh/m3					PhotoCAT 80 kWh/m3				
	15min	1 hr	2 hr	6 hr	24 hr	15min	1 hr	2 hr	6 hr	24 hr
Time 1	ND	ND	ND	ND	ND	ND	ND	ND	ND	ND
Time 2	3	4	5	6	6	ND	ND	ND	ND	ND
Time 3	2	3	3	3	4	-	-	-	-	-

D/DBP Haloacetic Acids (HAA5)

	Control					PhotoCAT 0 kWh/m3				
	15min	1 hr	2 hr	6 hr	24 hr	15min	1 hr	2 hr	6 hr	24 hr
Time 1	-	-	-	-	-	-	-	-	-	-
Time 2	11	13	13	18	28	9	12	15	16	24
Time 3	20	22	25	34	46	20	26	27	38	49

	PhotoCAT 5 kWh/m3					PhotoCAT 80 kWh/m3				
	15min	1 hr	2 hr	6 hr	24 hr	15min	1 hr	2 hr	6 hr	24 hr
Time 1	7	5	4	3	4	4	4	4	4	2
Time 2	5	7	8	11	18	ND	ND	ND	ND	ND
Time 3	14	16	20	25	38	-	-	-	-	-

APPENDIX F

SEC INTEGRATED AREA TABLES

Settled Water

	Control	No UV (0kWh/m3)	Low (5kWh/m3)	Medium (80kWh/m3)	High (160kWh/m3)
50,000-100,000	1410	1480	783	1198	1486
30,000-50,000	1459	1921	593	1652	1118
10,000-30,000	3572	2922	849	2212	1001
5000-10,000	401	603	309	406	122
1,000-5,000	958	932	592	278	195
500-1,000	178	203	194	45	32
100-500	59	78	97	51	39
TOTAL AREA =	29431				

Post-GAC

	Control	No UV (0 kWh/m3)	Low (5 kWh/m3)	Medium (80 kWh/m3)	High (160 kWh/m3)
50,000-100,000	4760	1084	3652	2100	851
30,000-50,000	2528	1004	2168	1154	827
10,000-30,000	2988	1578	1642	1298	657
5000-10,000	499	456	192	226	94
1,000-5,000	1406	712	433	119	94
500-1,000	139	104	143	24	18
100-500	47	45	49	24	17

Total Area = 33132

Distribution Hot Spot

	Control	No UV (0kWh/m3)	Low (5kWh/m3)	Medium (80kWh/m3)	High (160kWh/m3)
50,000-100,000	1546	3657	870	2989	1167
30,000-50,000	862	1003	566	2335	1502
10,000-30,000	1051	730	1629	2914	2286
5000-10,000	189	86	401	446	628
1,000-5,000	429	448	540	221	311
500-1,000	80	108	120	108	57
100-500	29	31	45	54	56
10-100	5	6	7	11	13

total area = 29536

APPENDIX G

EEM IMAGES

SETTLED WATER EEM IMAGES

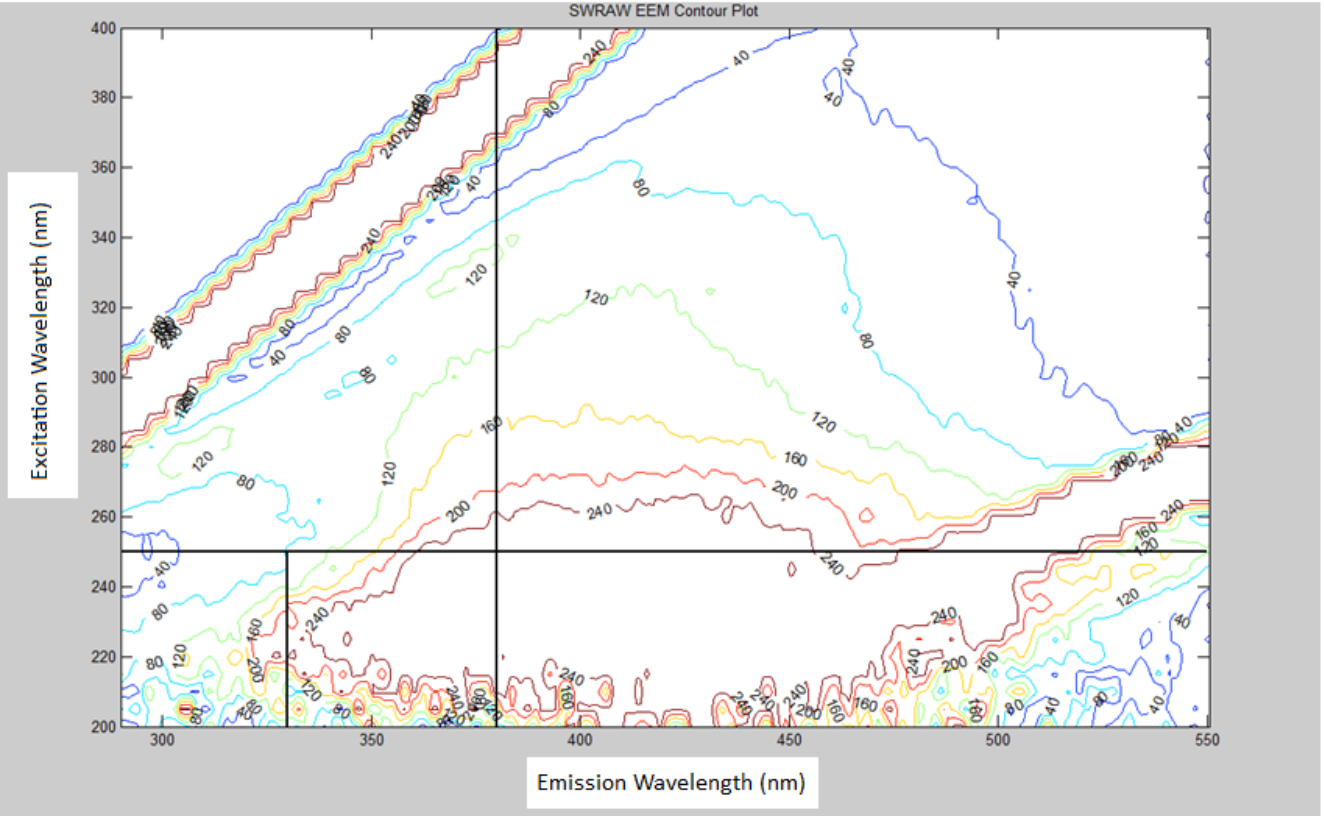

Settled water control sample with blank included

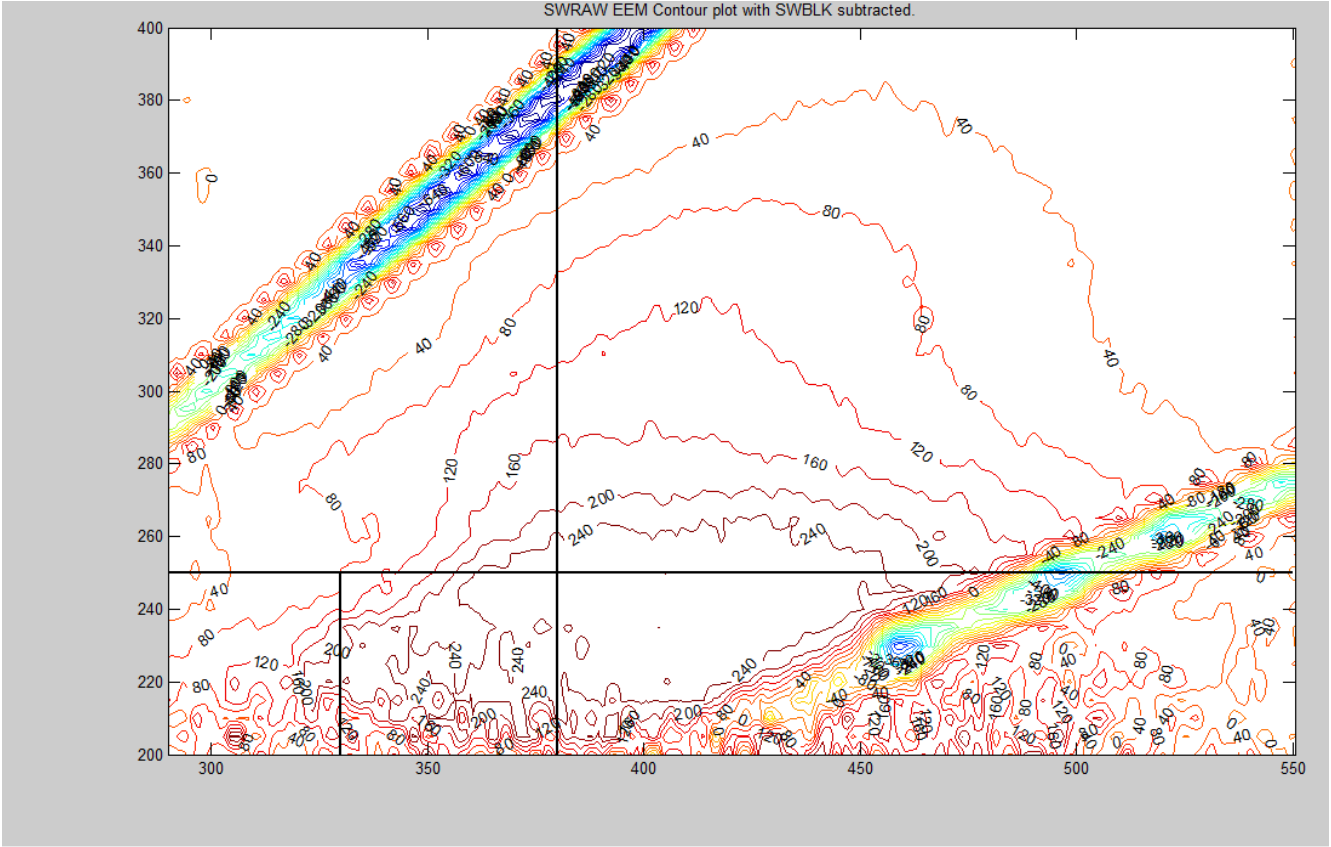

Settled water control sample with blank subtracted

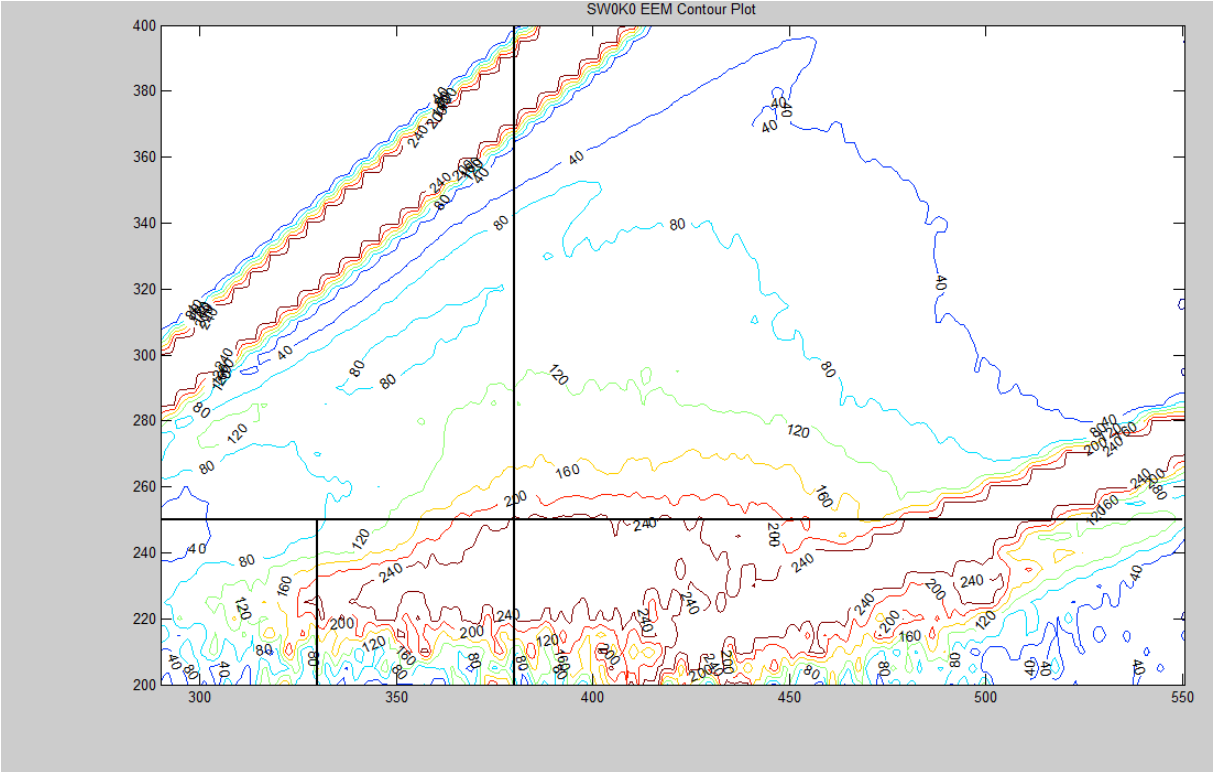

Settled water no UVsample with blank included

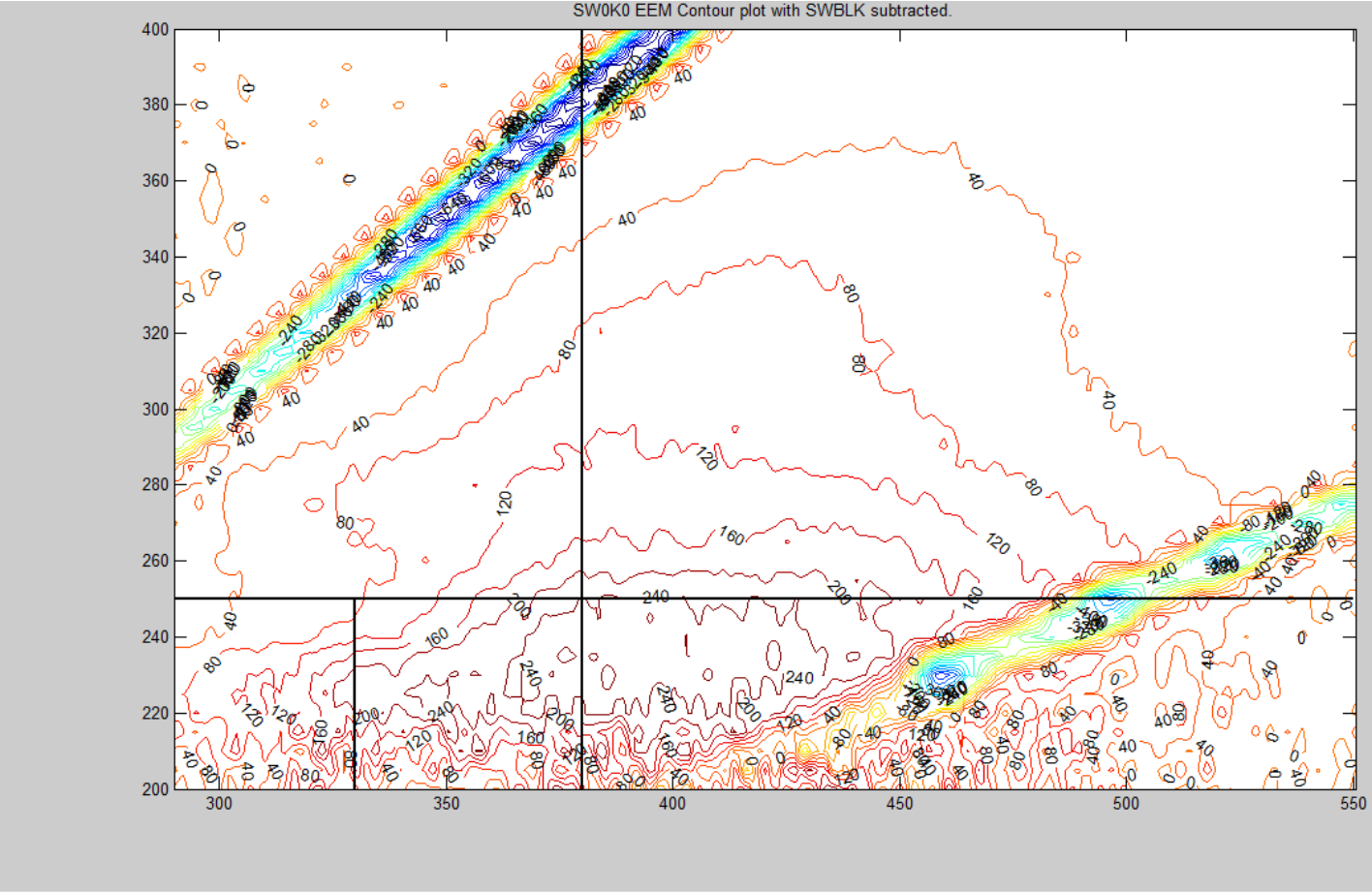

Settled water no UV sample with blank subtracted

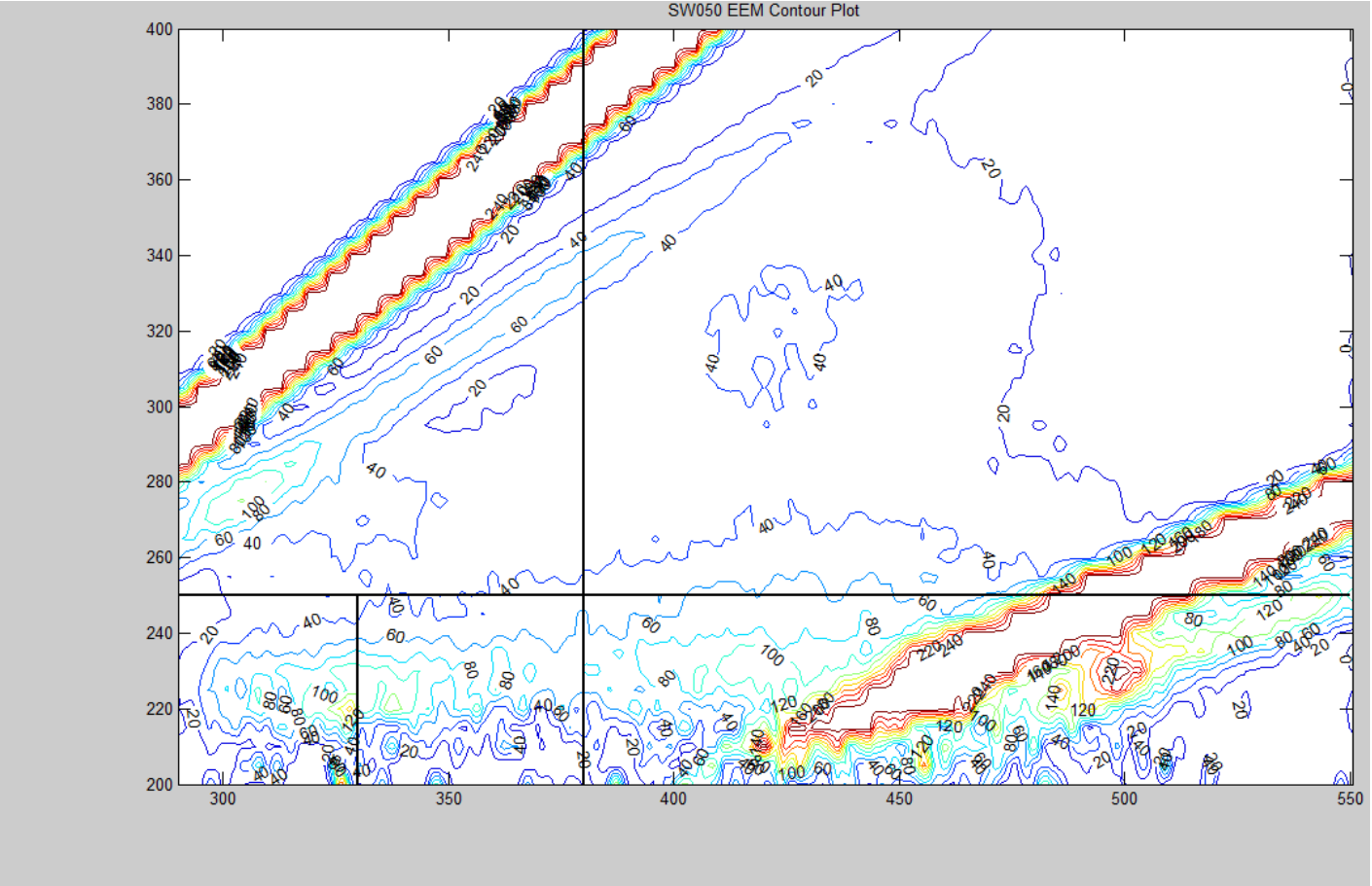

Settled water low sample with blank included

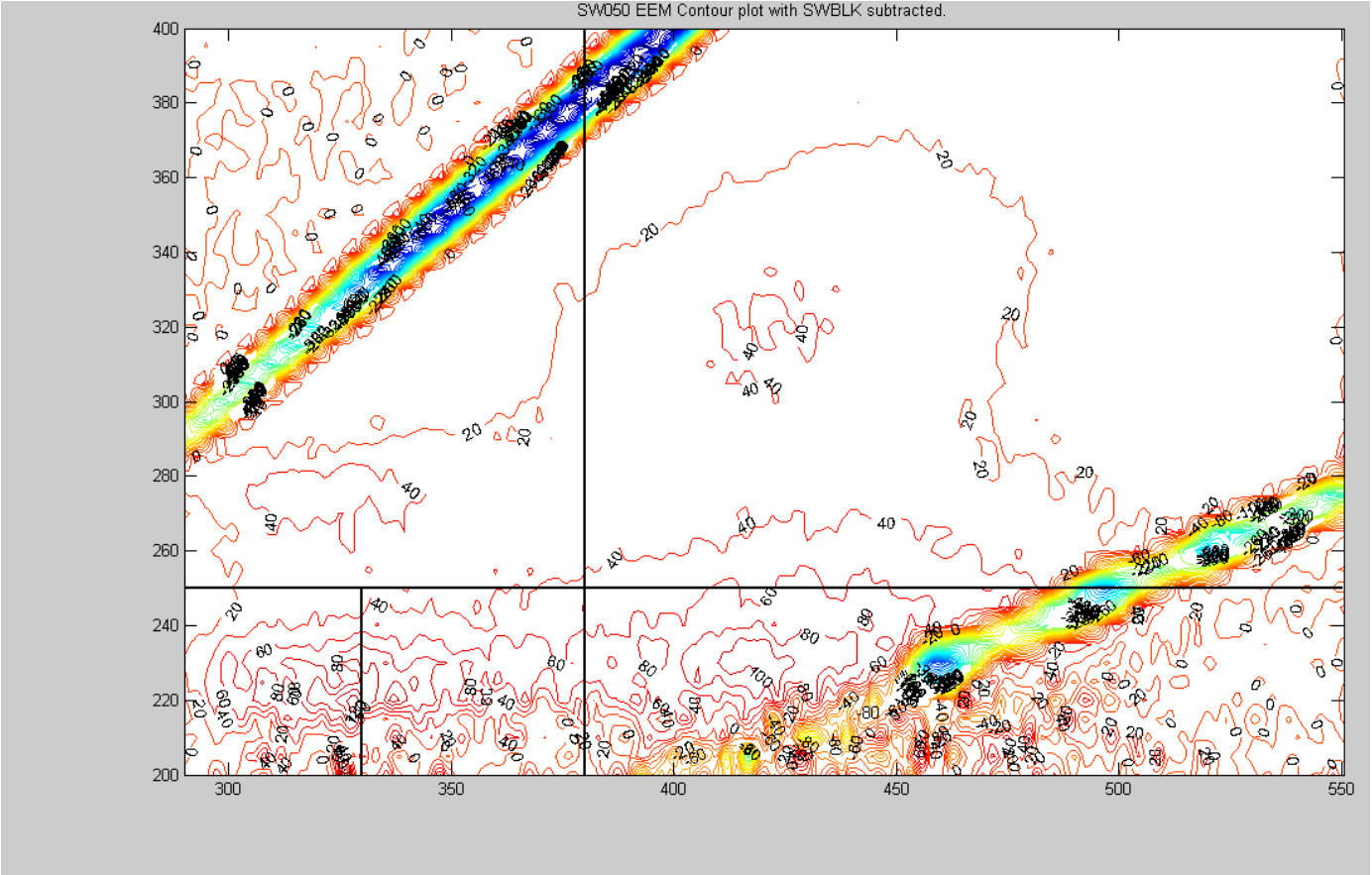

Settled water low sample with blank subtracted

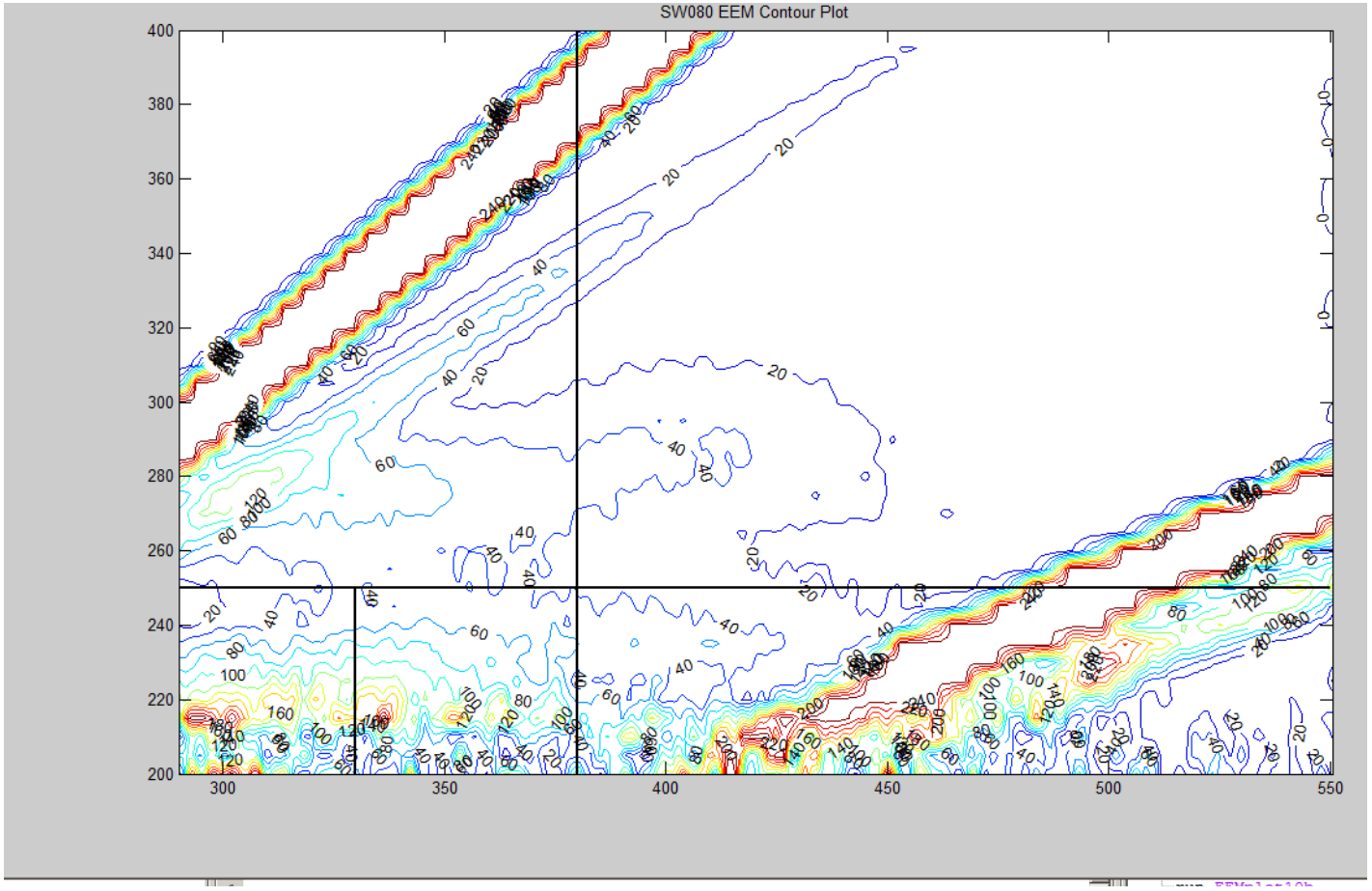

Settled water medium sample with blank included

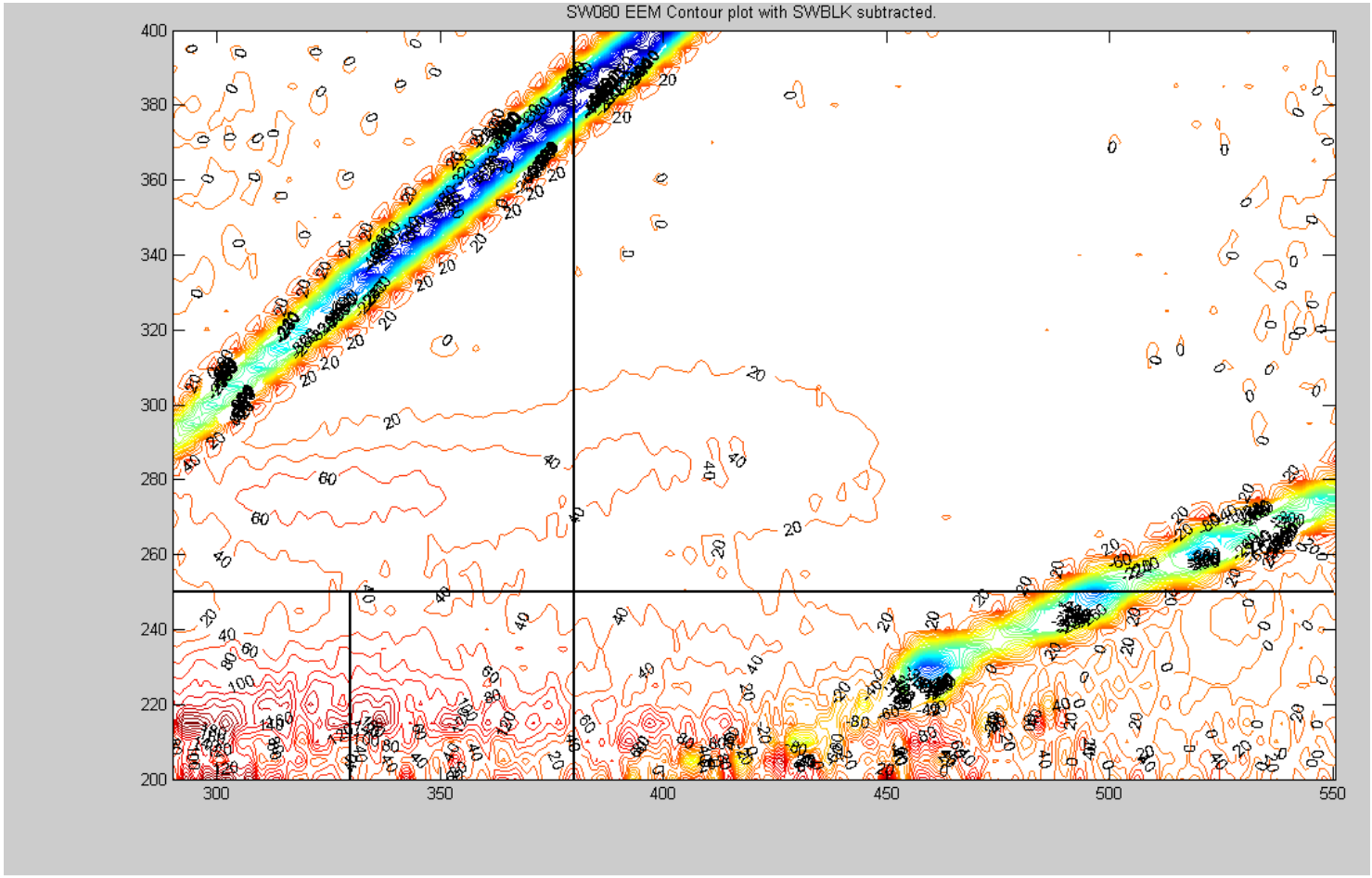

Settled water medium sample with blank subtracted

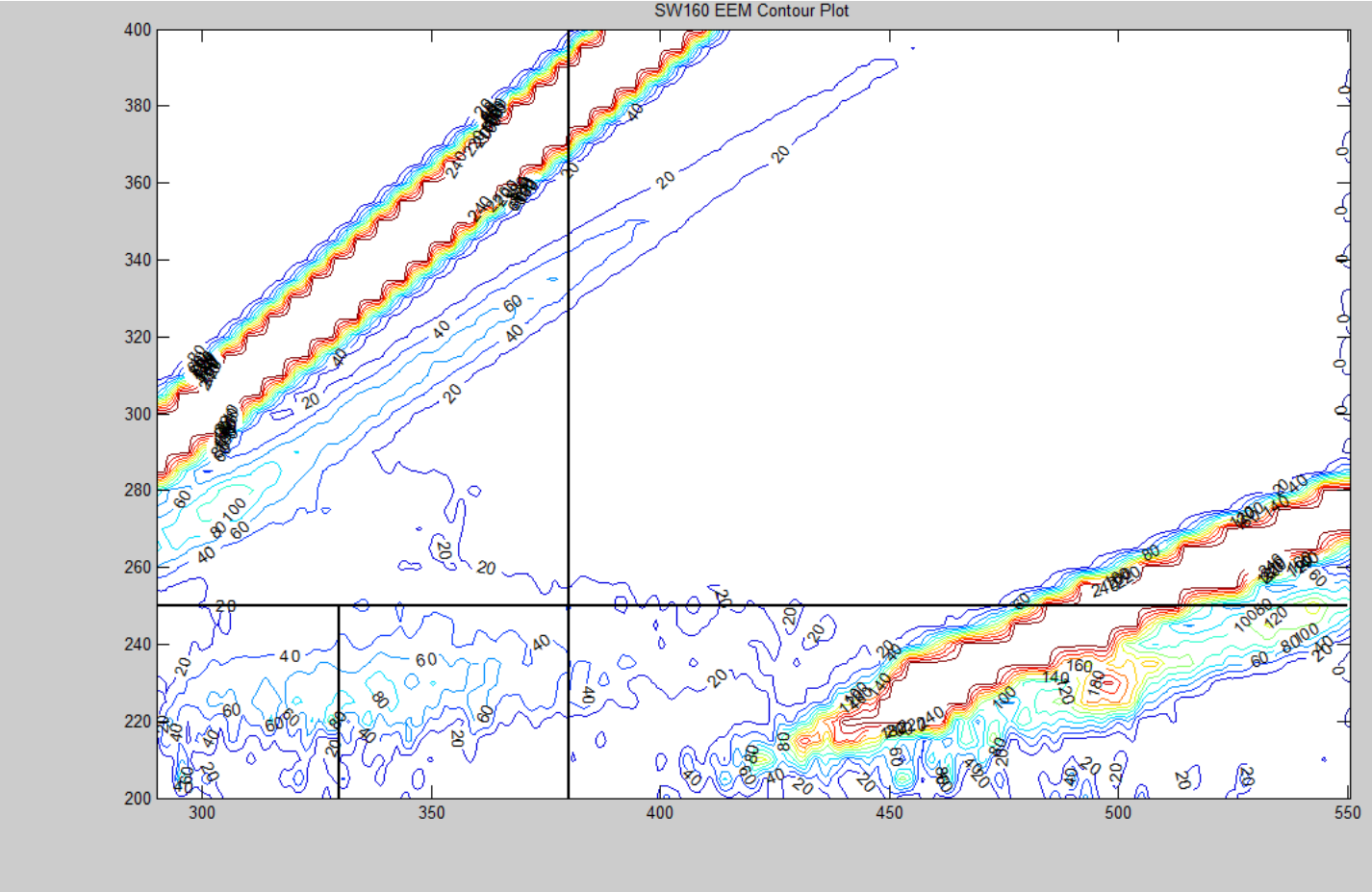

Settled water high sample with blank included

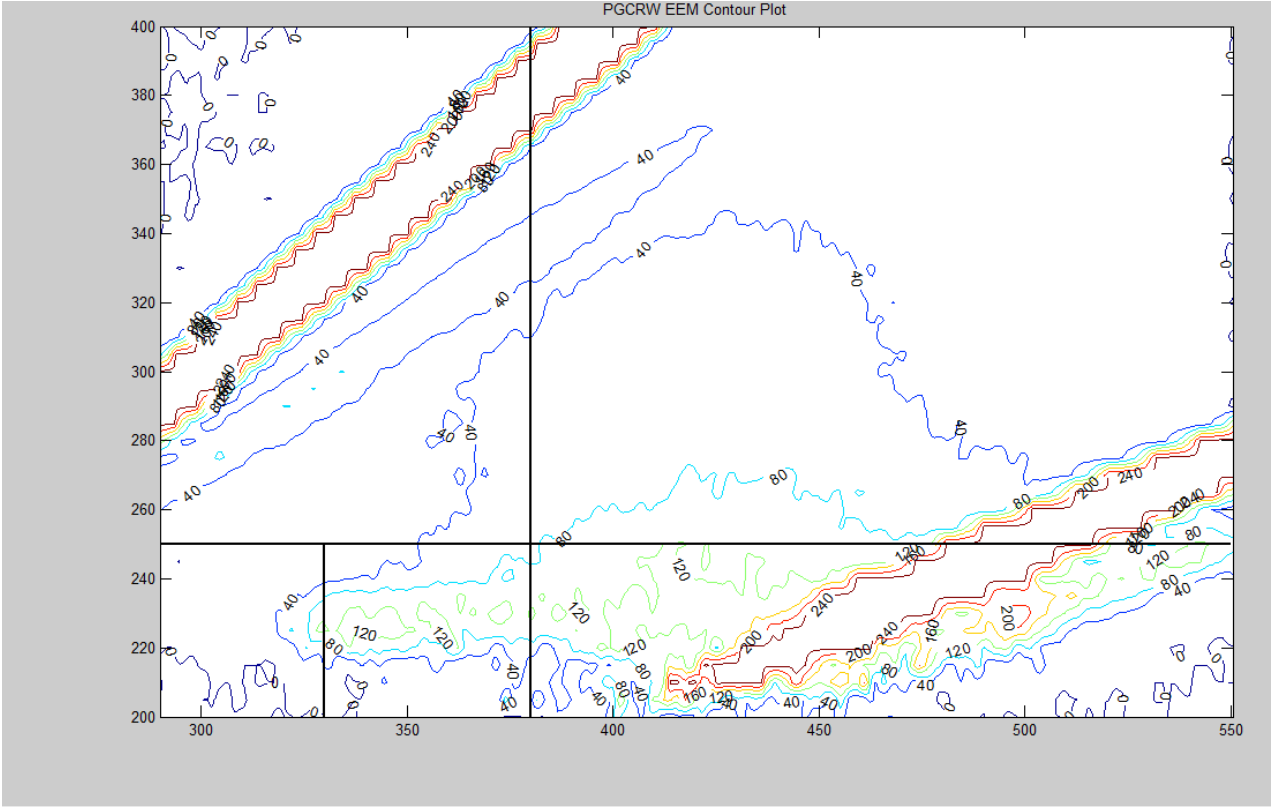

Post-GAC control sample with blank included

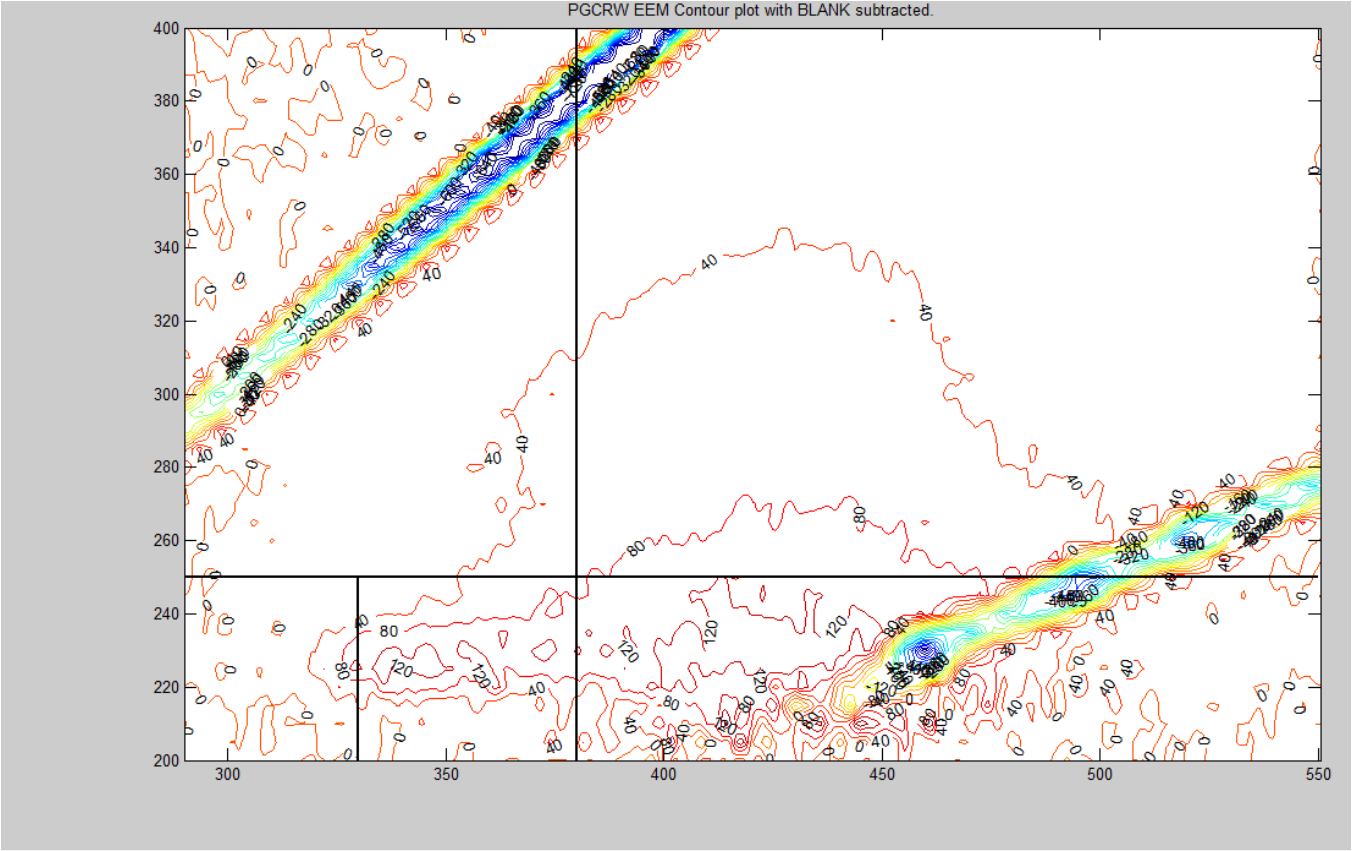

Post-GAC control sample with blank subtracted

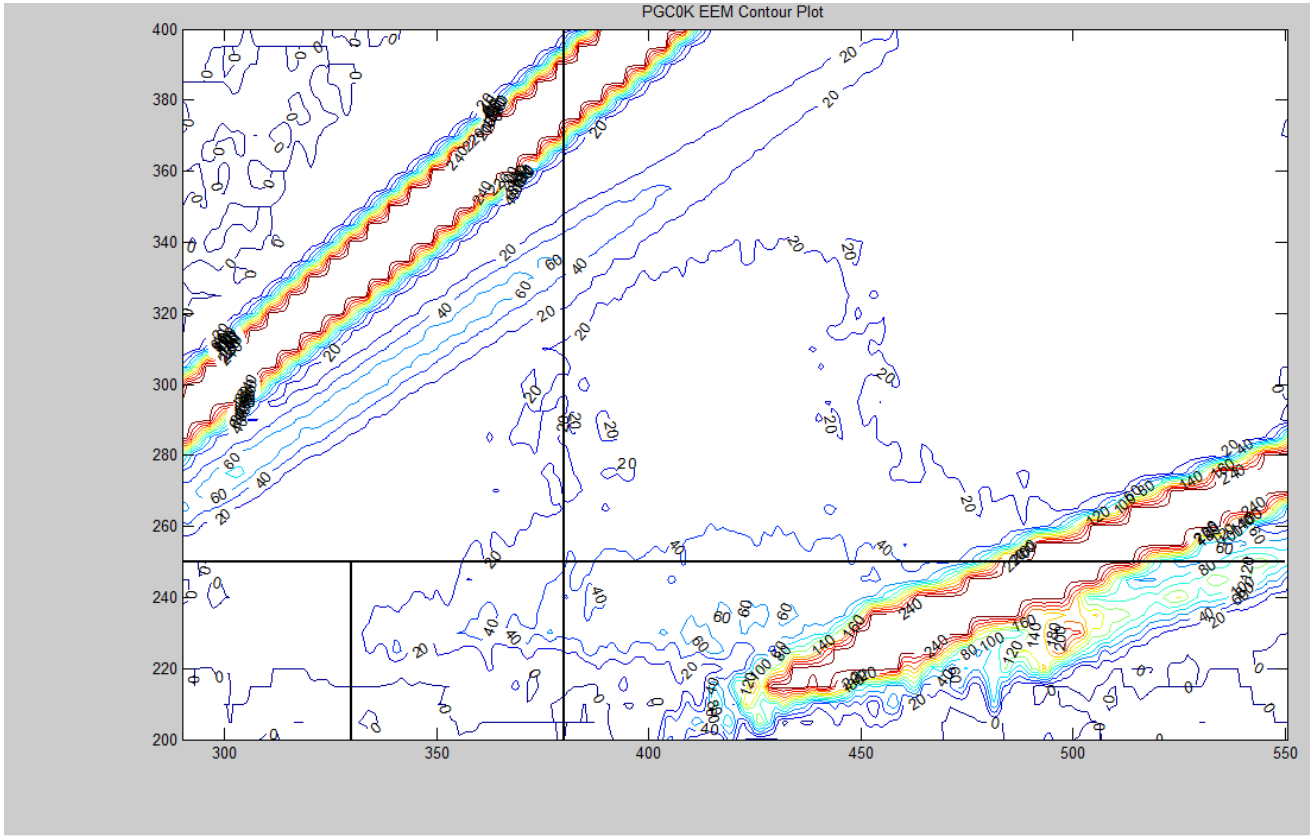

Post-GAC no UV sample with blank included

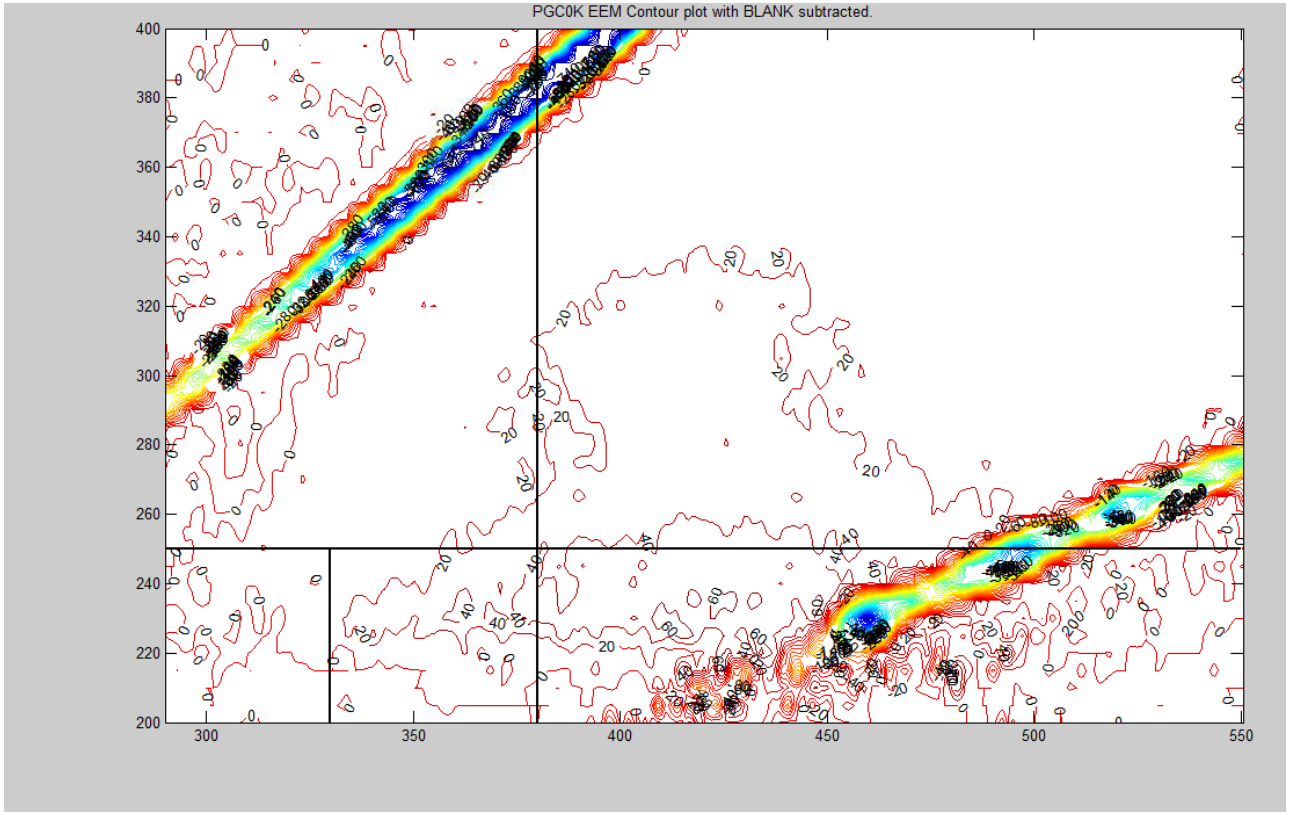

Post-GAC no UV sample with blank subtracted

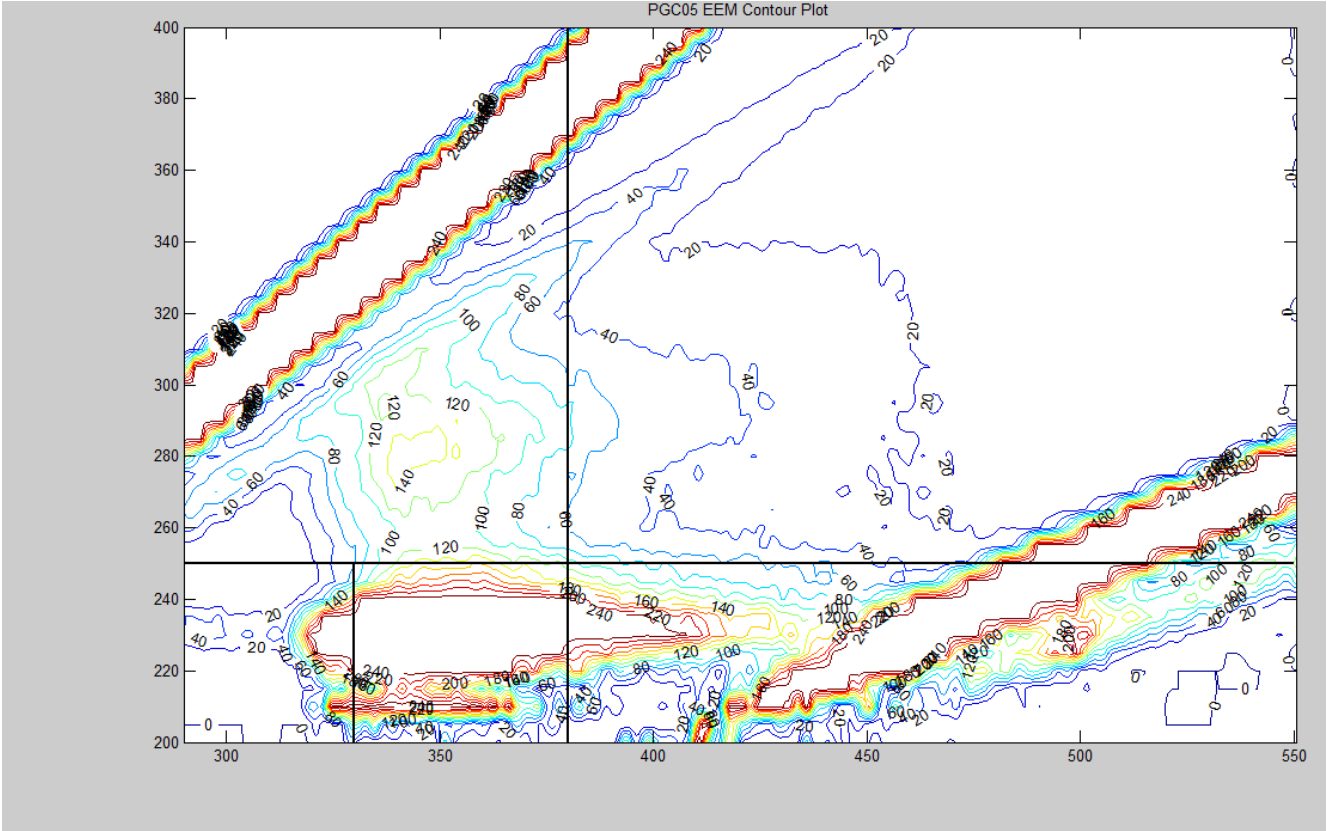

Post-GAC low sample with blank included

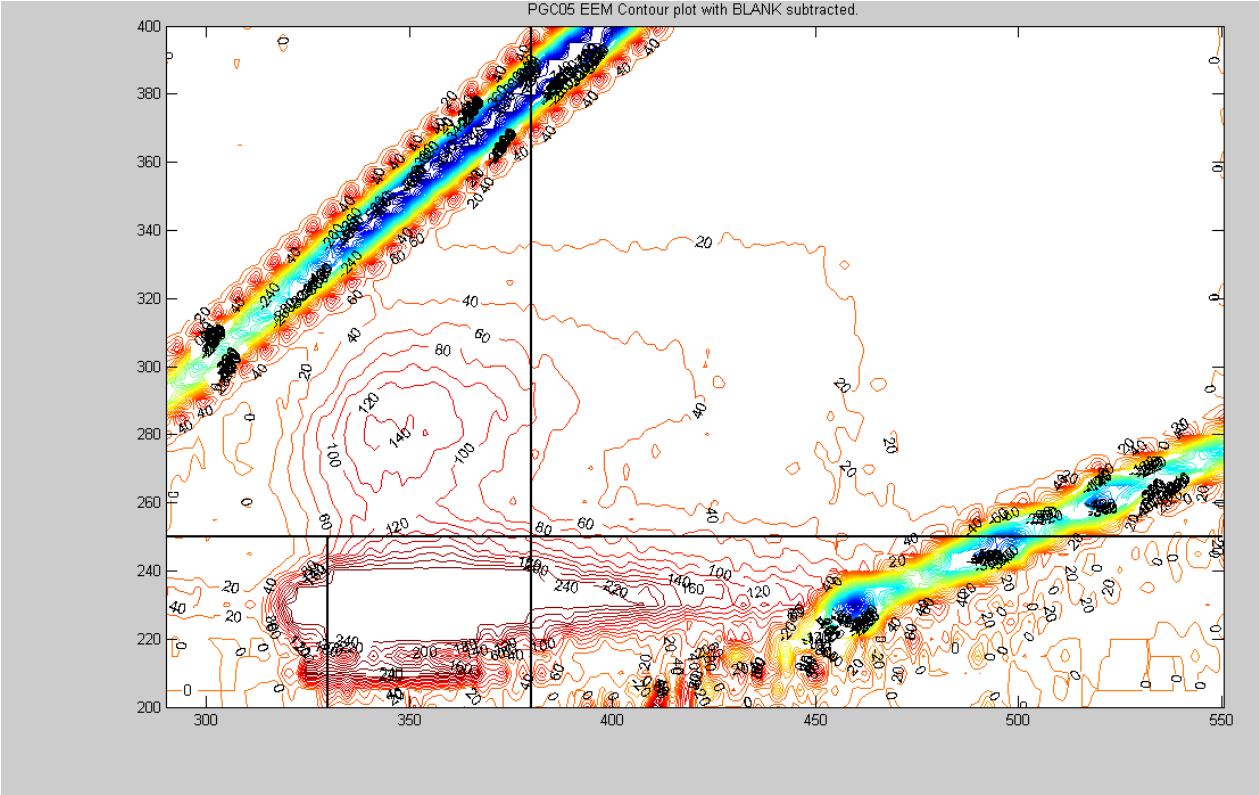

Post-GAC low sample with blank subtracted

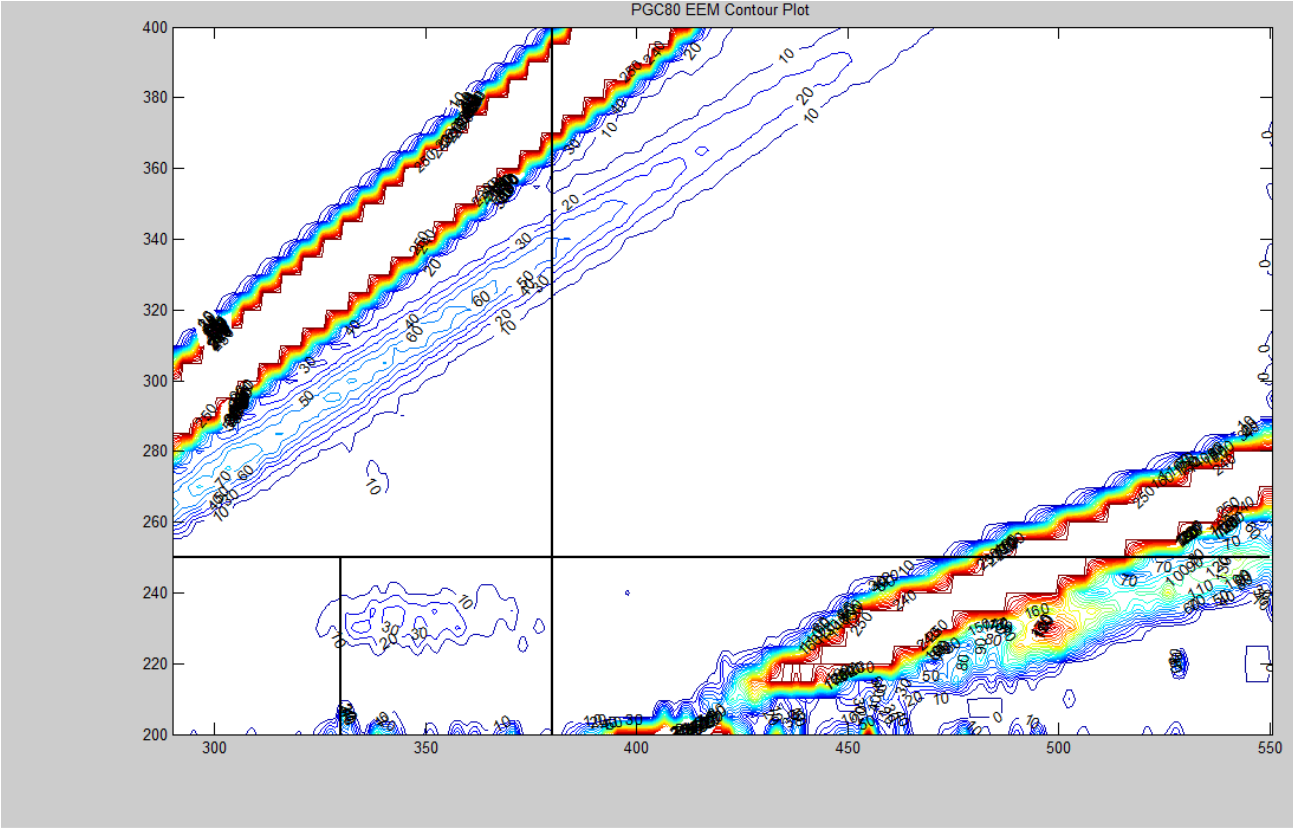

Post-GAC medium sample with blank included

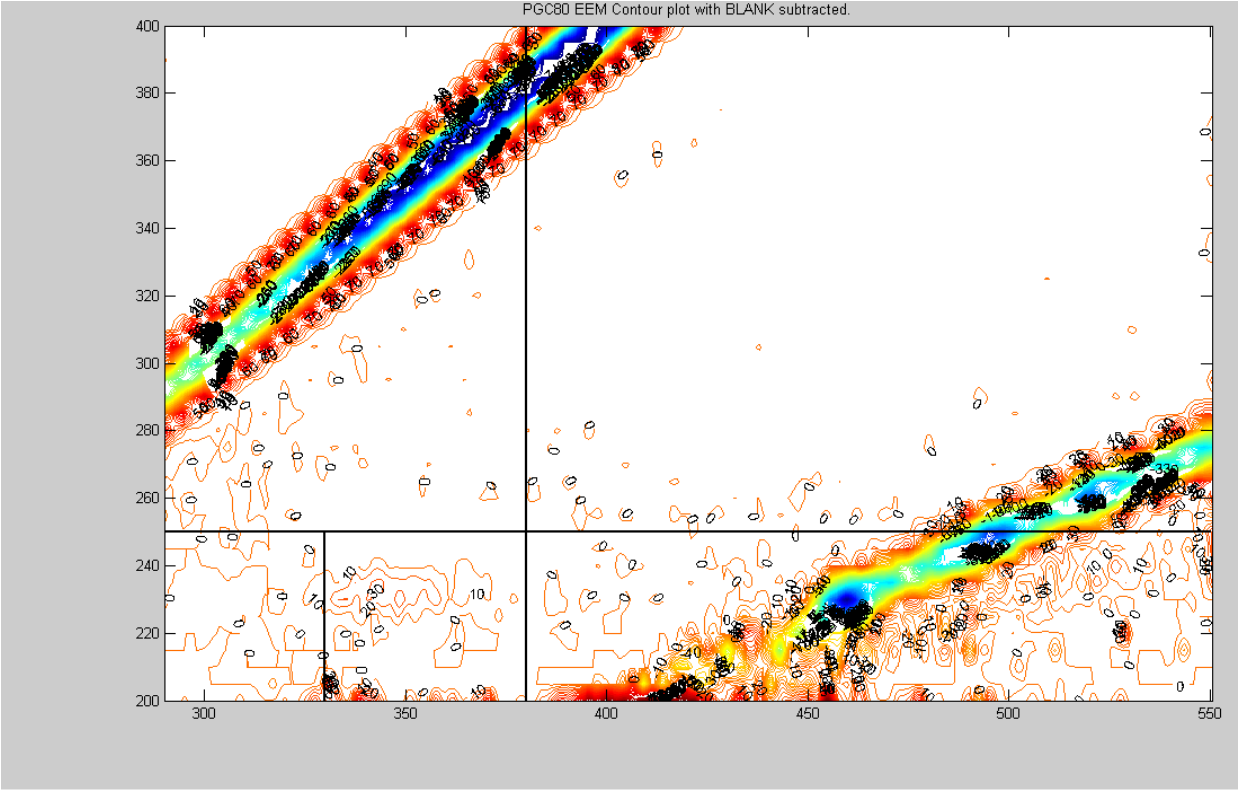

Post-GAC medium sample with blank subtracted

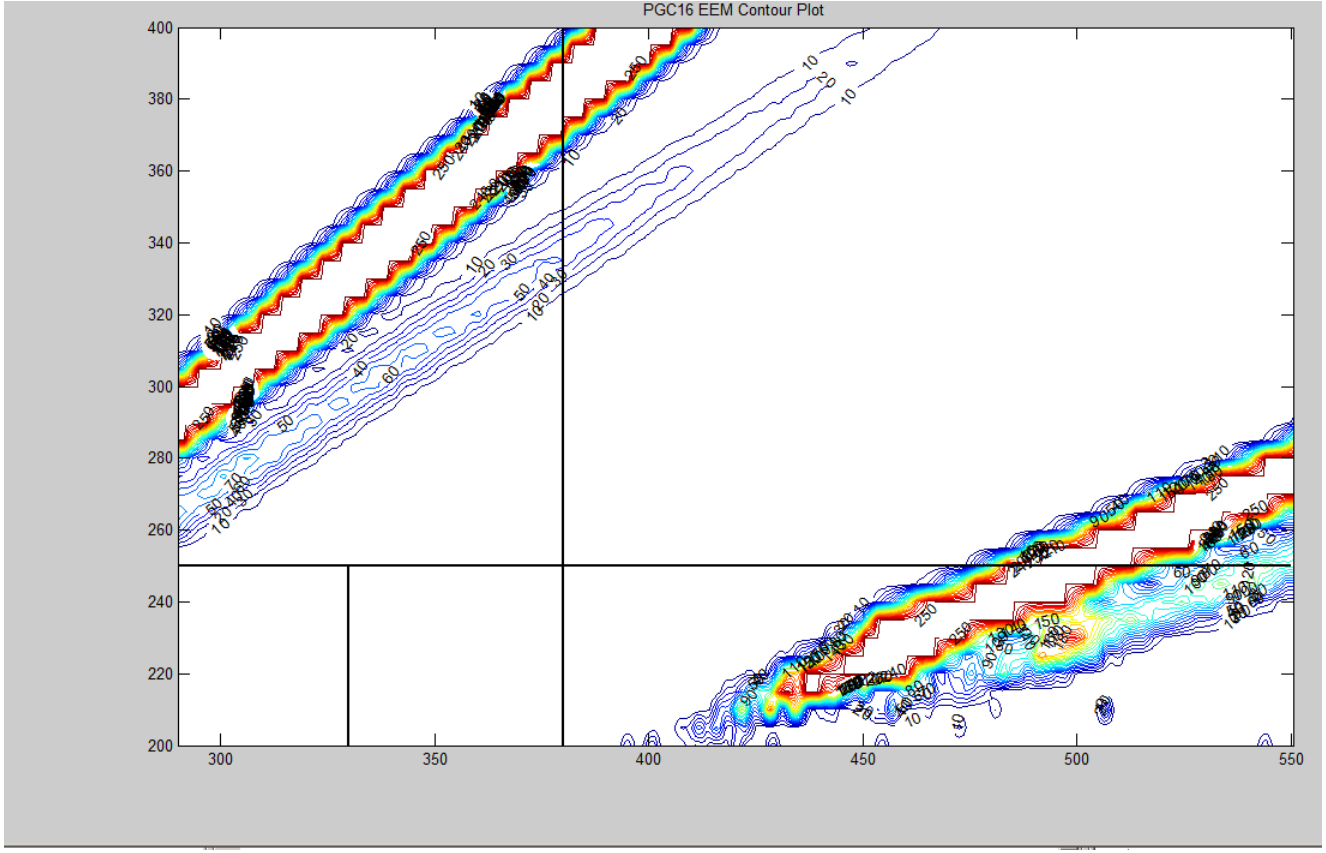

Post-GAC high sample with blank included

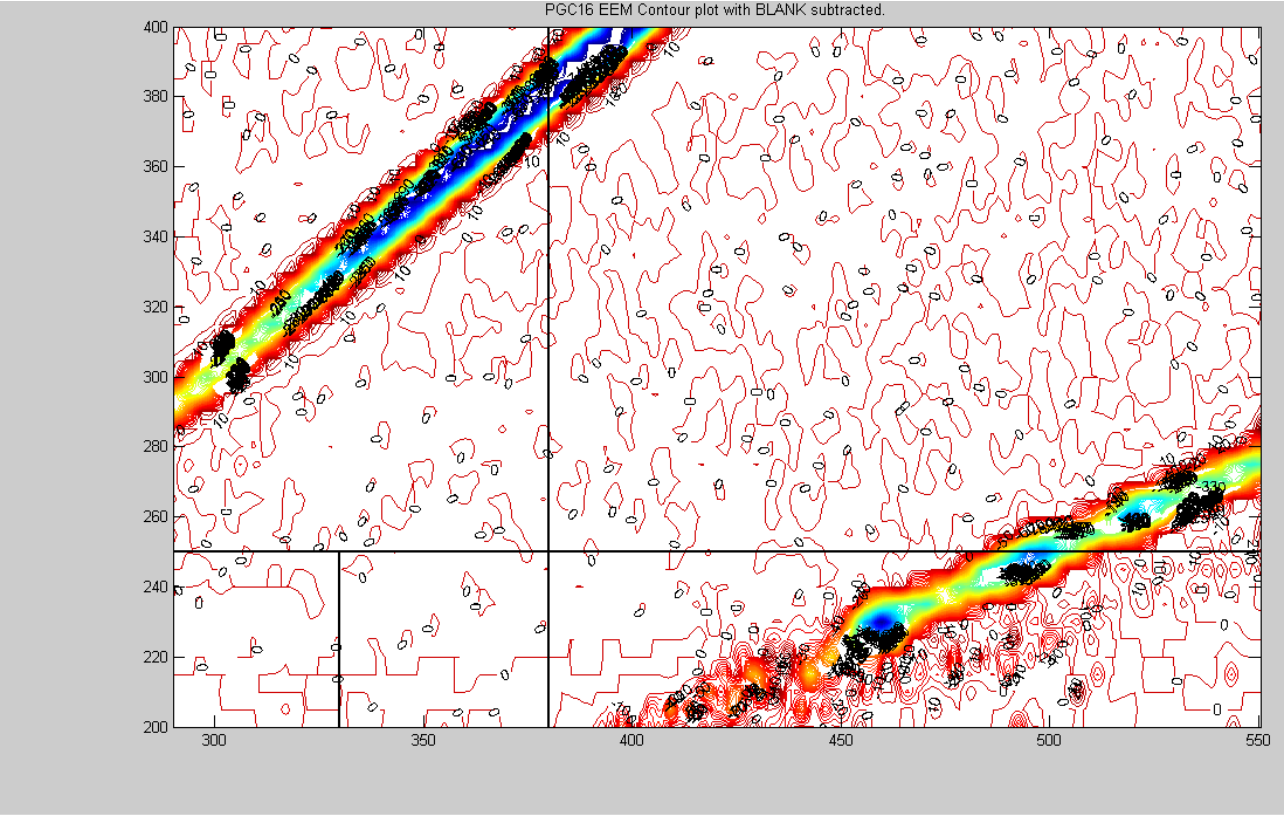

Post-GAC high sample with blank subtracted

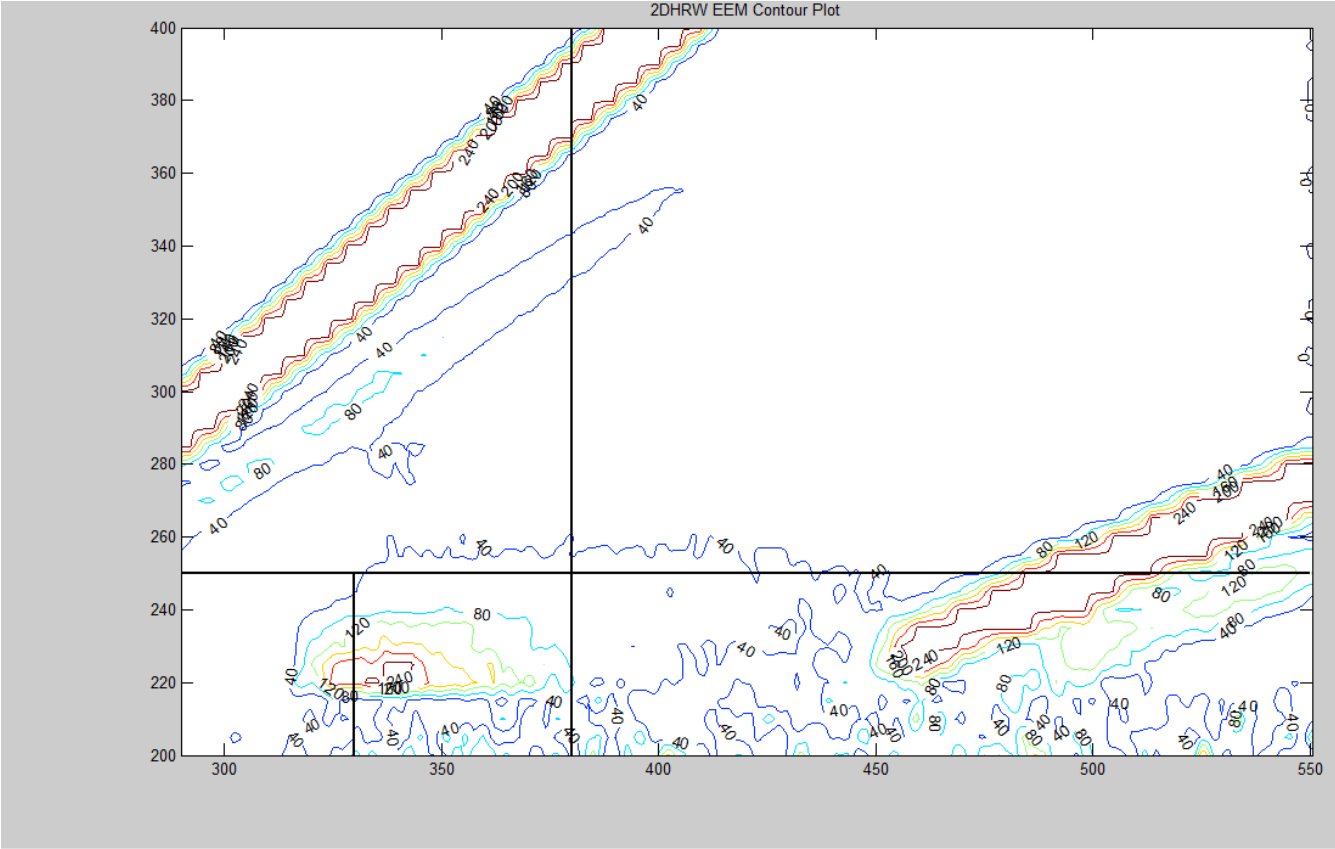

Distribution hot spot control sample with blank included

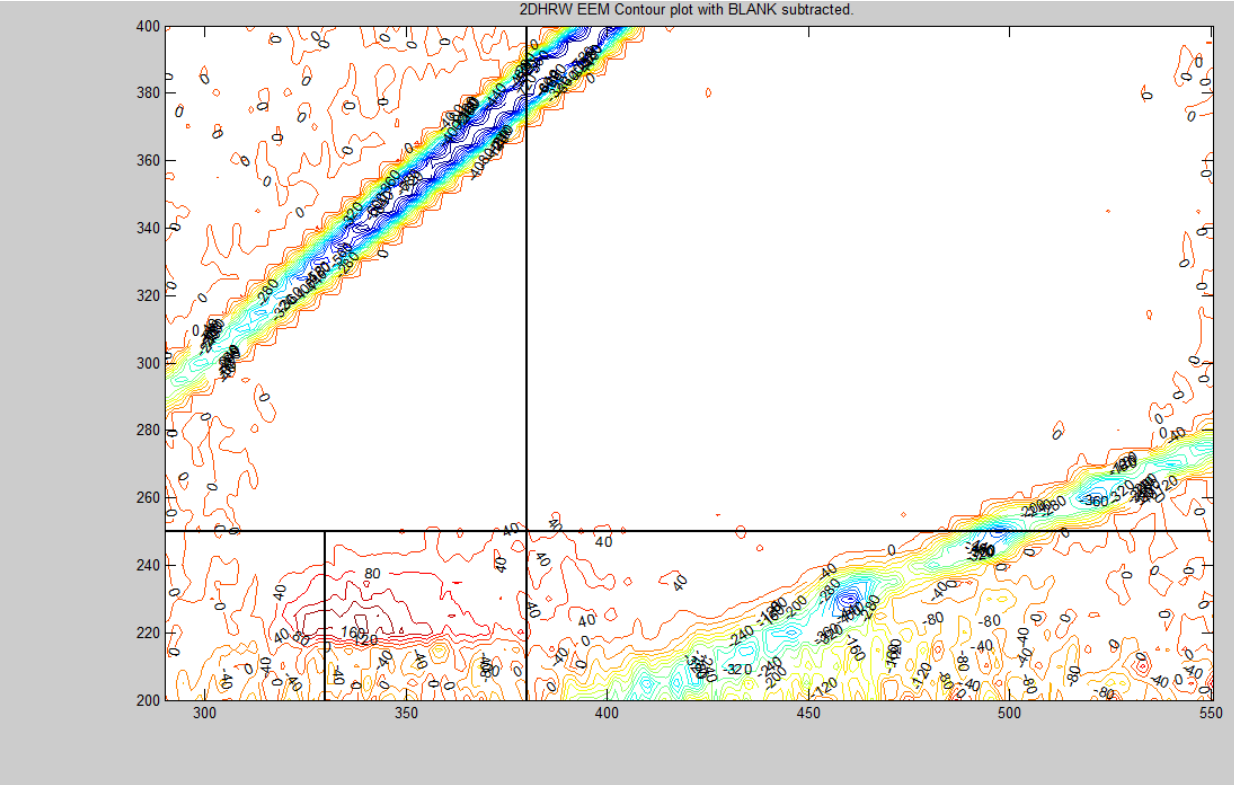

Distribution hot spot control sample with blank subtracted

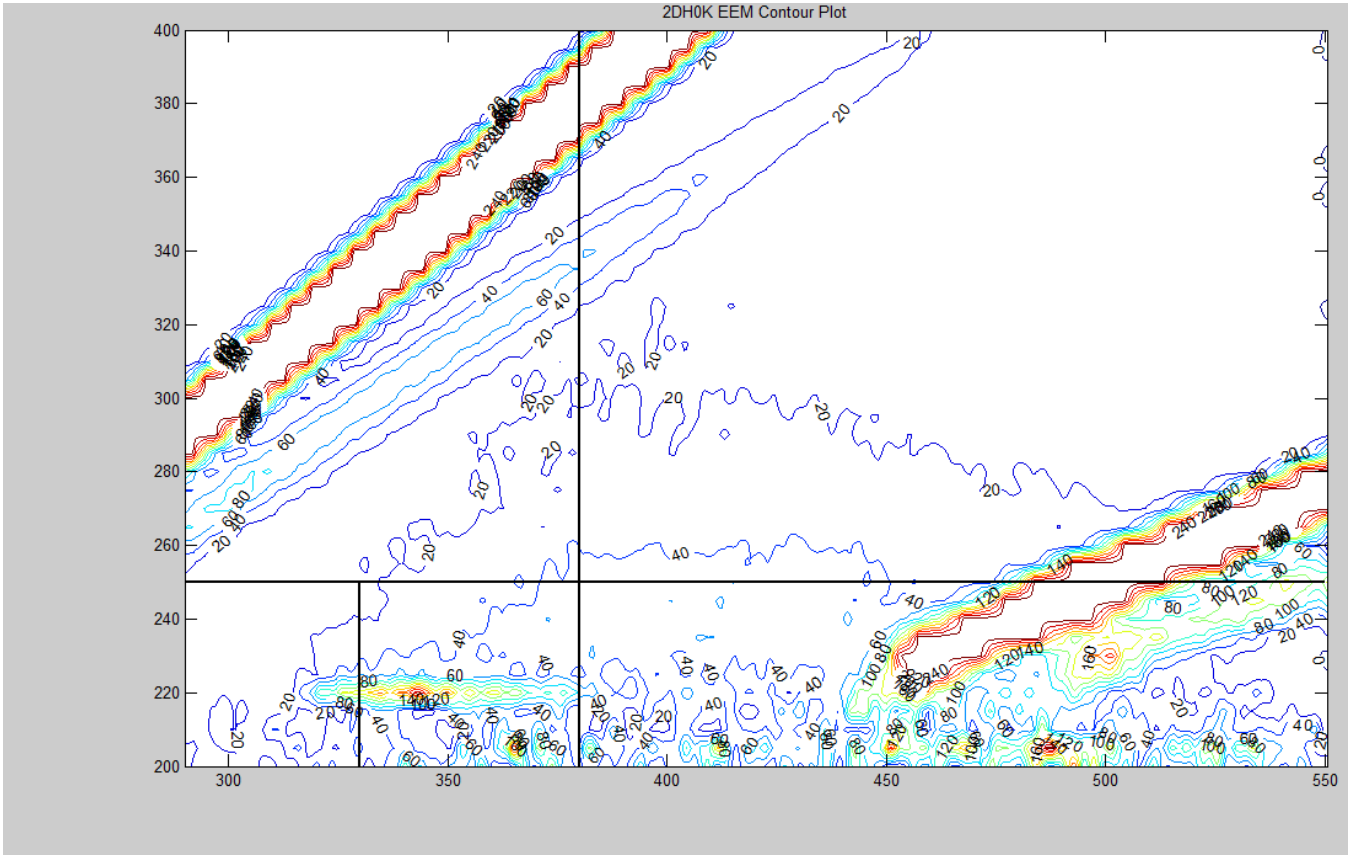

Distribution hot spot no UV sample with blank included

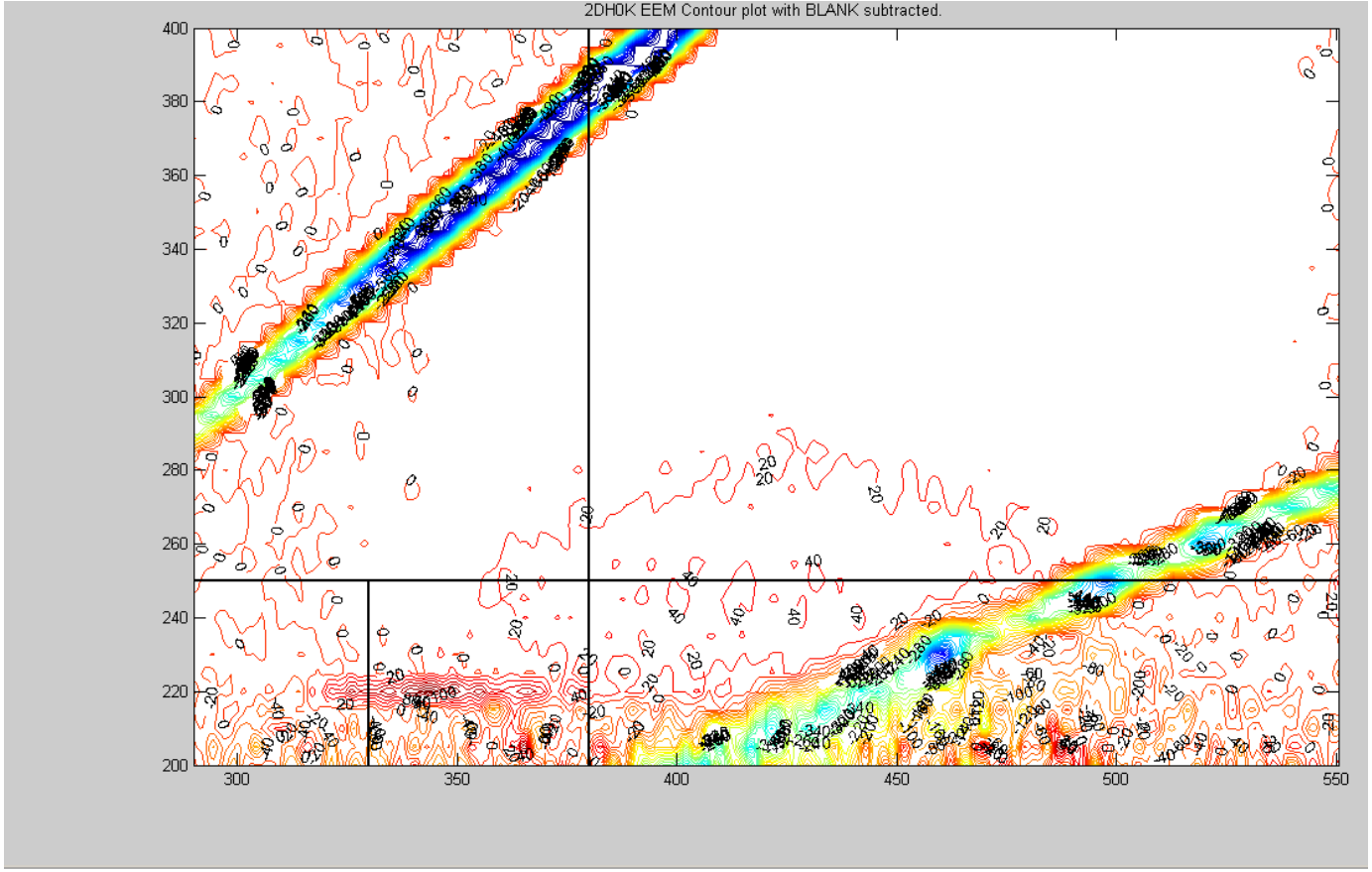

Distribution hot spot no UV sample with blank subtracted

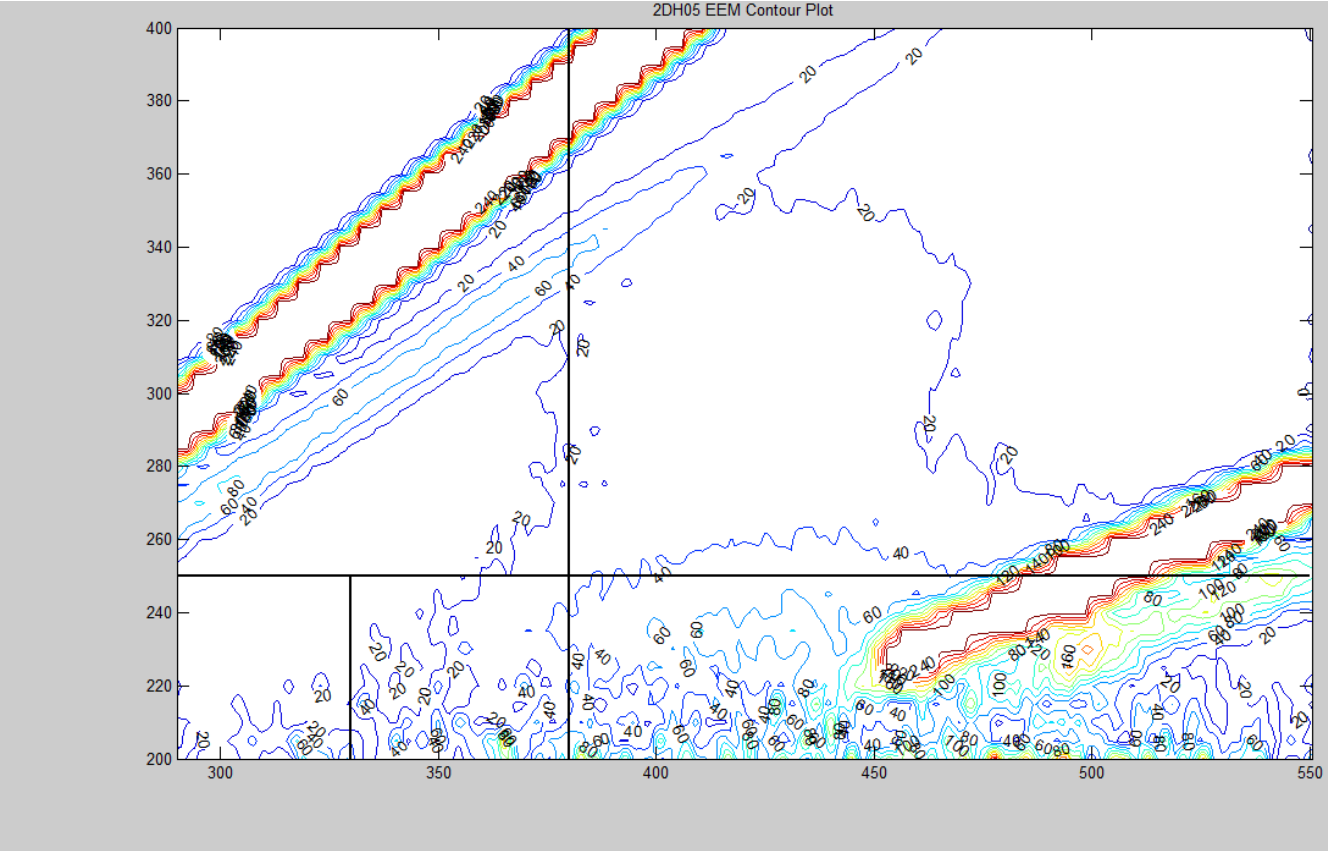

Distribution hot spot low sample with blank included

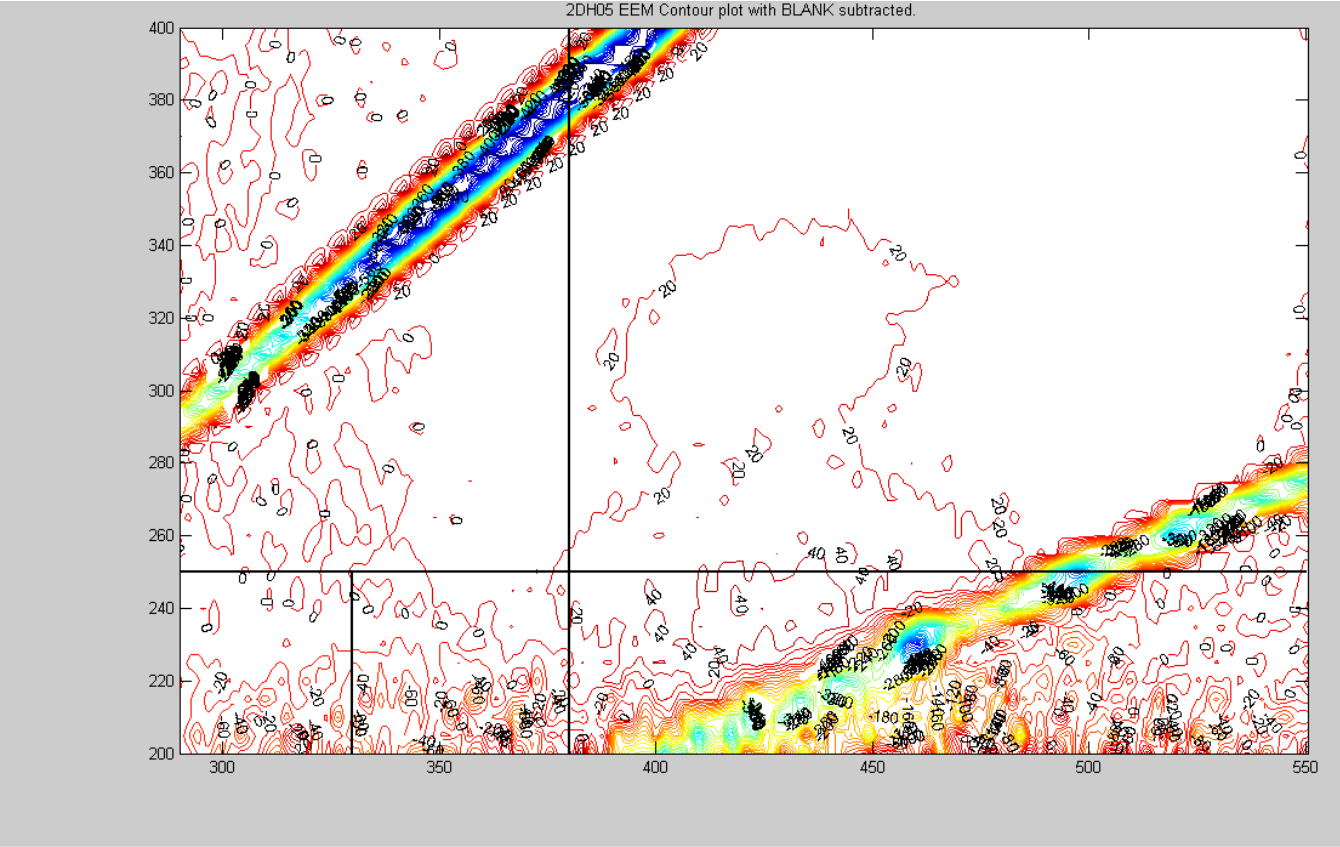

Distribution hot spot low sample with blank subtracted

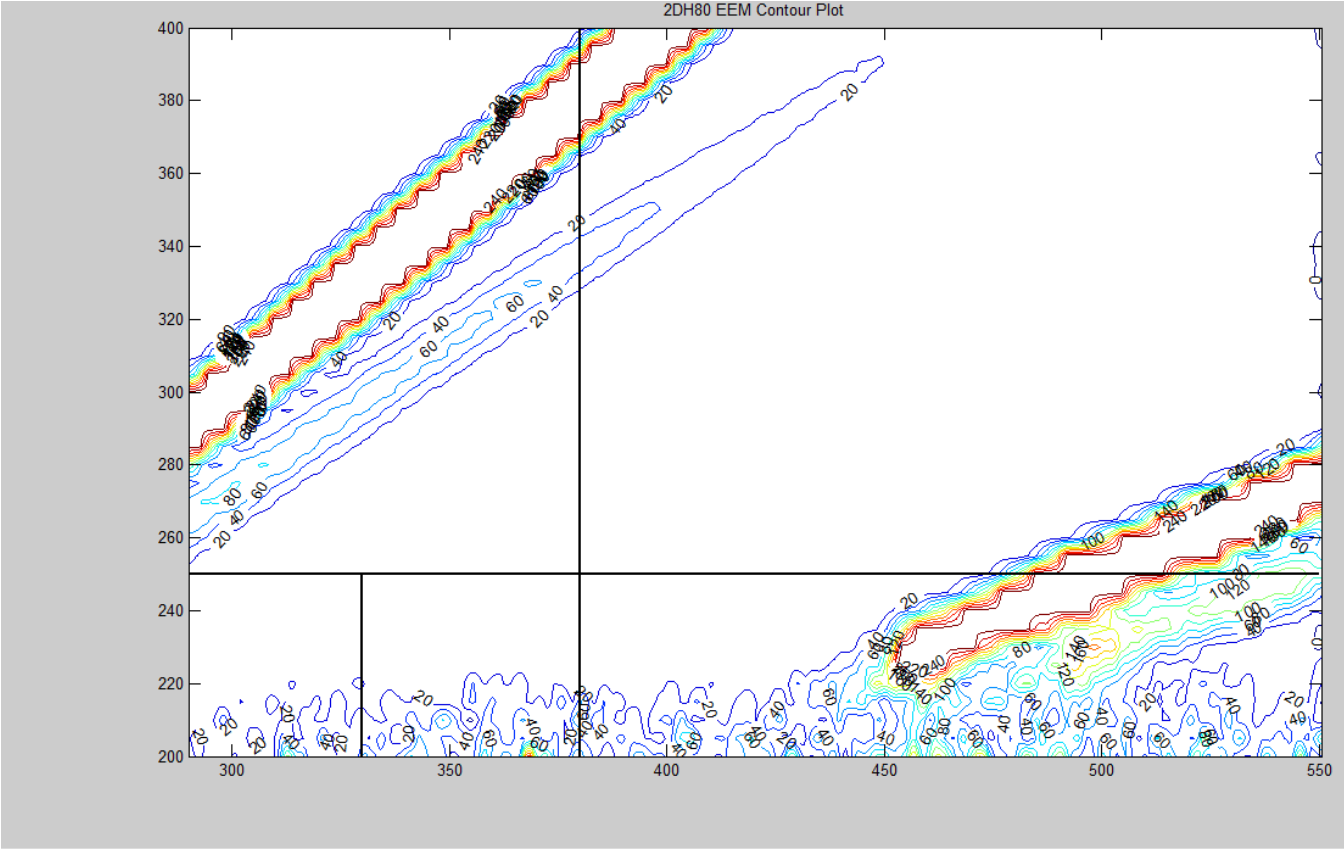

Distribution hot spot medium sample with blank included

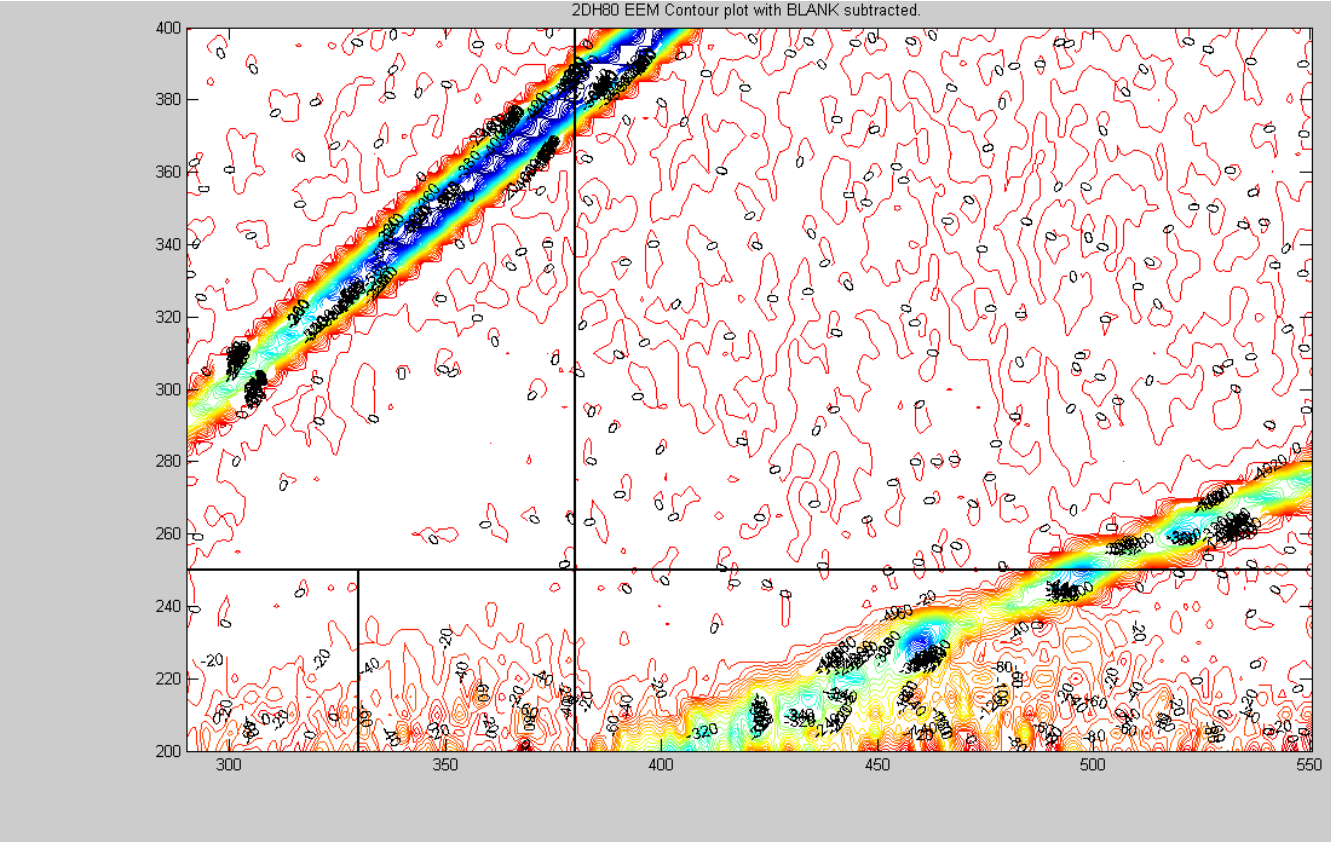

Distribution hot spot medium sample with blank subtracted

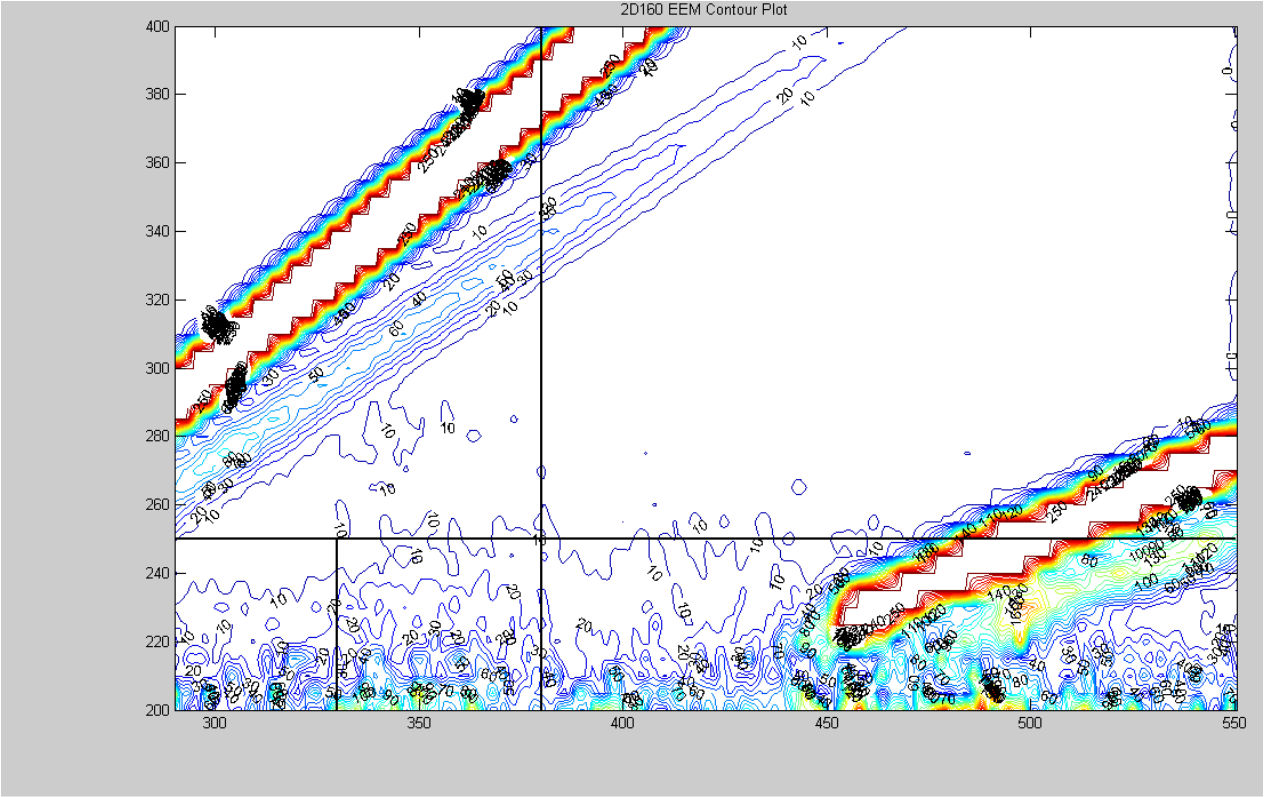

Distribution hot spot high sample with blank included

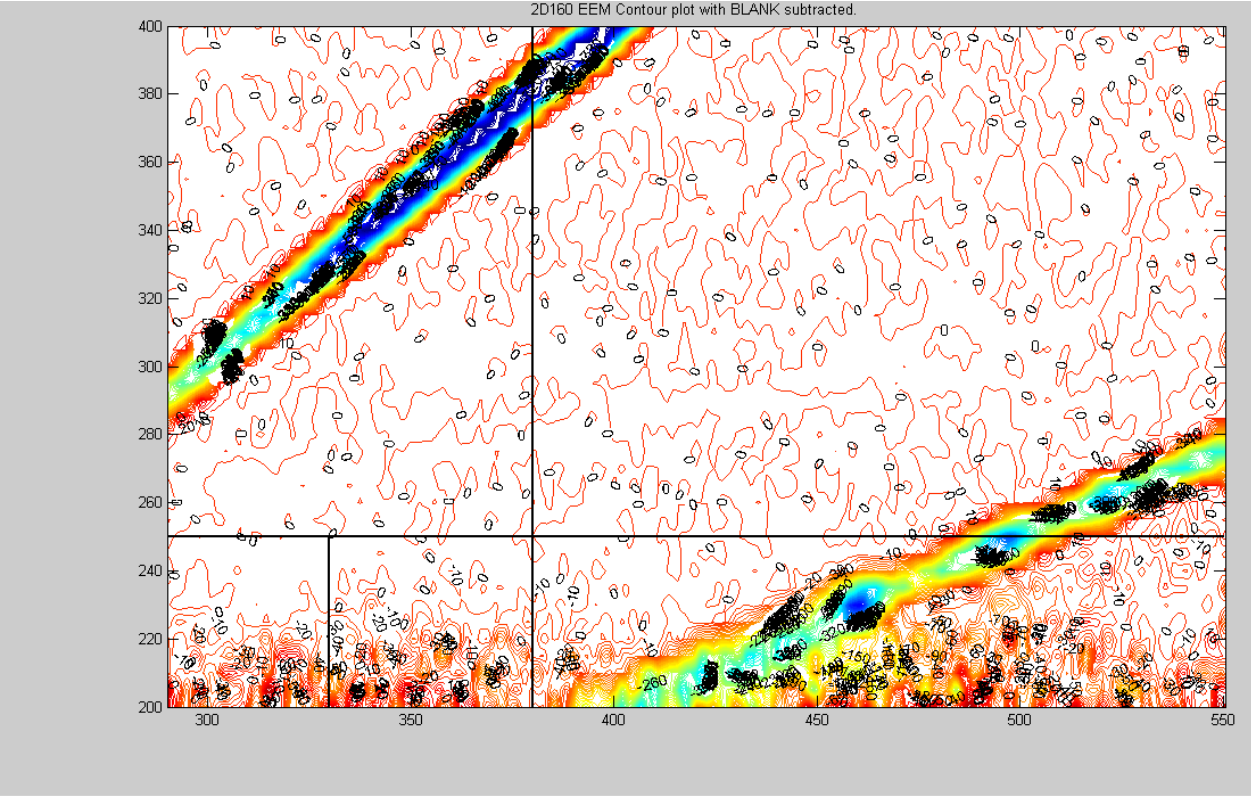

Distribution hot spot high sample with blank subtracted